EXPERIMENTAL INVESTIGATION AND OPTIMIZATION OF SUPERCHARGING AND COMPRESSION RATIO IN A BIOFUELED DI VARIABLE COMPRESSION RATIO ENGINE

Submitted in partial fulfillment of the requirements
for the award of the degree of

DOCTOR OF PHILOSOPHY

in

MECHANICAL ENGINEERING

by

Mr. GANESH SEGOJI WARKHADE
(Roll No. 715042)

Under the Supervision of

DR. A.VEERESH BABU

Associate Professor

DEPARTMENT OF MECHANICAL ENGINEERING

NATIONAL INSTITUTE OF TECHNOLOGY

WARANGAL-506 004, TELANGANA,

INDIA

March, 2019

DEDICATED

TO

MY PARENTS

NATIONAL INSTITUTE OF TECHNOLOGY-WARANGAL

CERTIFICATE

This is to certify that the thesis entitled "**Experimental investigation and optimization of influence of supercharging and compression ratio in a biofueled DI variable compression ratio engine"** being submitted by **Mr. Ganesh Segoji Warkhade** for the award of the degree of Doctor of Philosophy (Ph.D.) in Mechanical Engineering to the National Institute of Technology, Warangal, India is a record of the bonafide research work carried out by him under my supervision. The thesis has fulfilled the requirements according to the regulations of this Institute and in my opinion has reached the standards for submission. The results embodied in the thesis have not been submitted to any other University or Institute for the award of any degree or diploma.

Date:19/03/2019

Dr. A. Veeresh Babu
Associate Professor
Thesis Supervisor
Department of Mechanical Engineering,
National Institute of Technology,
Warangal.

DECLARATION

This is to certify that the work presented in the thesis entitled "**Experimental investigation and optimization of supercharging and compression ratio in a biofueled DI variable compression ratio engine"** is a bonafide work done by me under the supervision of Dr. A. Veeresh Babu and was not submitted elsewhere for award of any degree.

I declare that this written submission represents my ideas in my own words and where others 'ideas or words have not been included; I have adequately cited and referenced the original sources. I also declare that I have adhered to all principles of academic honesty and integrity and have not misrepresented or fabricated or falsified any idea/data/fact/source in my submission. I understand that any violation of the above will be a cause for disciplinary action by the institute and can also evoke penal action from the sources which have thus not been properly cited or from whom proper permission has not been taken when needed.

Date: 19/03/2019

Place: NIT Warangal

Mr. Ganesh Segoji Warkhade
Roll No. 715042

ACKNOWLEDGEMENT

First and foremost I want to thank my supervisor **Dr. A. Veeresh Babu.** It has been honor to be, I am his Ph.D. student. He cultivated seed of the research in me and inspired to apply this knowledge not only in laboratories but also in the personal life. His invaluable contributions of time and ideas provides by him during my Ph.D. stay made me wealthy in experiences, which is productive and stimulating in all aspects. The positive attitude of him at any diverse situations taught me how tackles the hurdles at any stage with joy and enthusiasm. He provided me an excellent platform to nourish and grow my professional as well as personal life.

I wish to sincerely thank university authorities, **Prof. N.V. Ramana Rao**, Director, National Institute of Technology, Warangal and other top officials who gave me an opportunity to carry out research work.

I also sincerely thank **Dr. P. Bangaru Babu**, Head, Mechanical Engineering Department, National Institute of Technology, Warangal for his continuous support towards carrying out research work.

I wish to express my sincere and whole hearted thanks and gratitude to my doctoral scrutiny committee (DSC) members **Dr. P Ravi Kumar** Professor Department of Mechanical Engineering, **Dr. G. Amba Prasada Rao** Professor Department of Mechanical Engineering, **Dr. K. Anand Kishore** Professor Chemical Engineering Department, National Institute of Technology, Warangal for their kind help, encouragement and valuable suggestions for successful completion of research work.

I express my heartfelt thanks and gratitude to **Dr. Shirish Sonavane**, Professor Department of Chemical Engineering, and research scholars working under him, for allowing to utilize the laboratory.

I would like to extend my thanks to all the faculty members in Department of Mechanical Engineering for their valuable suggestions and encouragement.

I am also thankful to all the supporting and technical staff of Department of Mechanical Engineering who has directly or indirectly helped during the course of my work.

I am thankful to all my fellow research scholars, labmates and Marathi group of scholar friends.

Last but not the least, I would like to thank my parents and wife and sons, who are surely the happiest to see me complete this endeavor. To them, I owe all my accomplishments.

GANESH SEGOJI WARKHADE

Abstract

The present work deals with three issues related to direct injection compression ignition engine. The *first concern*, the heavy utilization of fossil fuel in industrial and transportation sector leads to higher environmental pollution and depletion of its natural sources. Hence, there is need to search for new and sustainable resources of fuel. The *second concern*, the conventional CI engine work on fixed compression ratio and optimized for petro-diesel as fuel. The conventional engine at full load has a higher combustion pressure problem. The reduction of the compression ratio can minimize this problem. Moreover; it ought to be sufficiently high pressure at starting and at part load operation for better combustion, excellent reliability, longer engine life, and low emission. For utilization of the alternative source of fuel to replace the conventional petro-diesel fuel; the engine must be modified and optimized to suit the physical and chemical properties of the alternative fuel. The *third concern* is the stringent emission regulation norms imposed periodically and effective conversion of fuel's chemical energy into useful mechanical work to get more and more power from the same size of engine and quantity of fuel.

The present work addressed these concerns by performing experimental investigations of biodiesel-fueled single cylinder DICI engine with varying the percentage engine load, compression ratio, and inlet boost pressure. After reviewing the available literature, the non-edible linseed vegetable oil selected for the biodiesel production. This oil highly unsaturated and has more percentage of linolenic acid. Hence two-stage transesterification is used to convert the raw oil into biodiesel. In the **first stage** of the investigation, the biodiesel prepared from non-edible linseed oil (LB100) blended with petro-diesel (PD) on the volume basis and tested in compression ignition engine at different CR and load to replace the petro-diesel. The obtained result compared with baseline fuel PD operated at rated compression ratio 17.5:1. The result shows the higher value of cylinder combustion pressure; cumulative heat release, combustion duration, and combustion mean gas temperature and lower ignition delay for biodiesel and its blends compared to PD. On an average the ignition delay increases by 30% and 3.3% at CR 14:1 and 16:1 respectively, and declining by 28.3% at CR 18:1 for LB blends. At CR 16, the maximum BTE improvement observed was 26.73% for LB30. The maximum gain in BSFC for LB10 was 3 -12% higher. The EGT increases with load, biodiesel contents and

decreases with CRs. The emission of CO, HC, and CO_2 reduced with an increase in CRs except penalty in the discharge of NOx by a maximum of 30.8% for LB30 at CR18. Thus higher blends, i.e., LB20 and LB30 can also be used as an alternative fuel in a partially modified diesel engine, i.e., at CR 18.

The **second stage** considered the optimization of working parameters of unmodified compression ignition engine powered with the linseed methyl ester biodiesel and its blends as an alternative fuel. The objective accomplished by choosing three levels for each input parameters. Taguchi's L9 orthogonal array with Taguchi based grey relational analysis (TGRA) was utilized to get the optimum combination of input parameters. The optimum combination of input parameters by TGRA observed to be fuel mix B10, CR 18, and load 100%. The S/N ratio analysis of grey relational grade (GRG) shows the fuel B10, CR 16, and load 100% optimal input factor level. This optimal level further confirmed by analytical hierarchy analysis (AHP) and TOPSIS method. The analysis of variance for contribution for GRG demonstrates the most influential affecting variable is the load of 52.82% contribution followed by CR 28.38%, and fuel 10.52%. The confirmatory results demonstrate the improvement by 56.1%. Overall, the present study provides a necessary framework to enhance further research in this area.

Based on the results of stage-I. The biodiesel blends LB10, LB20, and LB30 shows performance in agreement with standard petro-diesel. Therefore, in the **third stage**, the experimental setup is modified for supercharged condition (forced induction) for further investigations. The present work carried out with above said three biodiesel blends and petro-diesel (PD). The operating input parameters were 4 different CRs (14, 16, 17.5, 18) and 3 boosting pressure (g) (0.5, 1, 1.5 kPa) including the natural aspiration (NA) of the engine. The output characteristics measured for all tested fuels and compared with baseline fuel (PD) at standard operating condition (CR 17.5 at NA). The output parameters considered for projected downsizing are performance and combustion characteristics. From the investigations, found that the supercharger improves the engine performance by 10-15%. The boosting improves both phases of combustions namely premixed and diffusion. The exhaust gas temperature decreases with increase in boost pressure and CR for all tested fuels. The exact engine downsizing in terms of increase in specific power and decrease in specific weight are discussed in detail.

Table of Contents

List of Figures

List of Tables

Abbreviations and Nomenclature

CI	Compression Ignition
DICI	Direct Injection Compression Ignition
VCR	Variable Compression Ratio
SI	Spark Ignition
CA	Crank Angle
VGT	Variable Geometry Turbocharger
TDC	Top Dead Center
BDC	Bottom Dead Center
r	Geometrical Compression Ratio
V_d	Swept Volume
V_c	Geometrical Clearance Volume
V_a	Actual Volume Of Air
P_e	Residual Exhaust Gas Pressure
P_i	Intake Manifold Pressure
P_a.	Atmospheric Pressure
P_k	Pressure At The End Of The Suction Stroke
r_k	Actual Compression Ratio
V_r	Actual Clearance Volume
η_v	Volumetric Efficiency
ϕ	Fuel-Air Equivalence Ratio
HC	Hydrocarbons
CO	Carbon Monoxide
NOx	Nitrogen/Nitric Oxide
CO_2	Carbon Dioxide
PM	Particulate Matters
AHP	Analytical Hierarchy Process

TGRA	Taguchi’s Grey Relational Analysis
TOPSIS	Technique For Order Preference By Similarity To An Ideal Solution
CR	Compression Ratio
WFO	Waste Fish Oil
LTC	Low Temperature Combustion
BSFC	Brake Specific Fuel Consumption
BTE	Brake Thermal Efficiency
BP	Boost Pressure
EGT	Exhaust Gas Temperature
PD	Petro-diesel
LB	Linseed Biodiesel
RSM	Response Surface Methodology
IT	Injection Timing
IP	Injection Pressure
ANOVA	Analysis Of Variance
DOE	Design Of Experiment's
S/N	Signal To Noise Ratio
FFA	Free Fatty Acids
CP	Combustion Pressure
RPR	Rate Of Pressure Rise
NHR	Net Heat Release
CHR	Cumulative Heat Release
ID	Ignition Delay
CD	Combustion Duration
MGT	Mean Gas Temperature
HSU	Hartridge Smoke Unit
GRG	Grey Relational Grade

MCDM	Multicriteria Decision Making
p_i	Performance Index

Chapter 1

Introduction

In the late 18th century, the two pioneers, Dr. Rudolf diesel along with Akroyd-Stuart invented first compression ignition engine. Later on, in 1892, Dr. Rudolf diesel filed a patent for the compression ignition based engine. Since then, over the years, diesel engines have had a lot of design and development improvement and became the backbone for all modern transportation facilities and was considered the primary source of transportation in world war II (Heywood, J. B., 1988).

Compression ignition (*CI*) engines are superior in many aspects namely lower fuel consumption, emissions of carbon monoxide (*CO)*, unburned hydrocarbon (*HC*), and higher performance characteristics compared to spark ignition engine. Besides this, *CI* engines have high fuel efficiency (40% - 50%), thermal efficiency, reliability and excellent power, hence used widely for medium and heavy-duty commercial, as well as public transport application (Chang, D.Y. Z. *et al.*, 1996). However, these desirable features of *CI* engine have increased the number of vehicles on roads and prime movers in the industrial application has created other issues such as increased amount of greenhouse gases, price volatility, and diminishing sources of conventional fossil fuel. The shrinking source of fossil fuel and strict emission regulations for the transport vehicles. These issues have forced the researcher to look for new technology development as well as modifying the existing engines for efficient use of fuel (Kruiswyk, R. W.,2012; Mohd, A. *et al.*, 2014). Simultaneously look for the option of different alternative fuel to meet the demands as well as replace the conventional fossil diesel fuel shortly.The cconventional CI engine works on fixed compression ratio and at full load has a higher combustion pressure problem. The low compression ratio can minimize this problem.Also, it should be sufficiently high pressure at starting and at part load operation for better combustion, excellent reliability, and longer engine life, low emission (Watson, N.,J.M. S.,1982).Therefore, there must be a practical way to vary compression ratio continuously during the engine operation for meeting the actual load and speed requirement. The engine operates on variable compression ratio (*CR*) improve the engine performance, efficiency, and exhaust

emissions. The engine effectiveness and work output dependent upon the compression ratio under which the engine operates as shown in the Fig. 1.1. Indicated and thermal efficiency increases with compression ratio while mechanical efficiency decreases (Roberts, M., 2002).

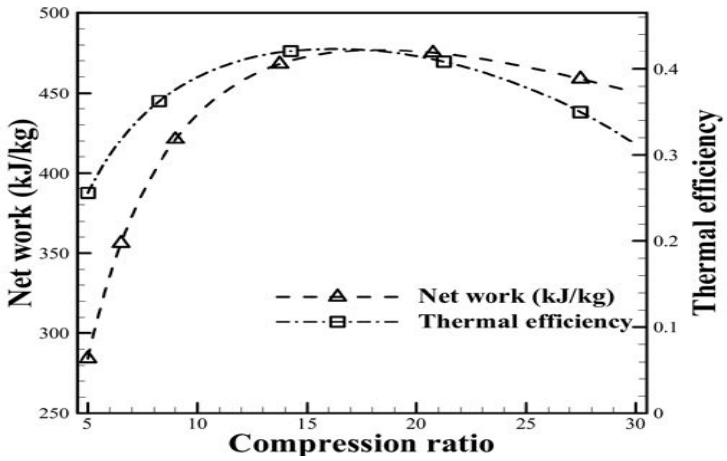

Fig.1.1 Effect of compression ratio on network and thermal efficiency (Mahmood Mousavi, S. *et al.*,2013)

Also with increasing of *CR*, the fuel consumption decreases. Hence, the variable compression ratio engine useful for facing the twin problems of automobile transportation related to emission and fuel crisis. For reducing engine-out emissions, mainly the NO_x.The fuel properties controlled, particularly the fuel cetane number. If the cetane number is more, it burns with short ignition delay as a result low combustion temperature and reduces the NO_x emissions (Venkateswarlu, K. *et al.*, 2012). Lower cetane number fuel burns at comparatively higher ignition delay and resting time of fuel in the combustion chamber is more, thus burns at higher temperature causes higher NO_x. Therefore, any fuel, which has natural higher cetane number, can take advantage of lower emission with variable compression ratio enabled engine as shown in Fig.1.2.

The amount of injected fuel burns during the combustion stroke decides the quantity of power developed by the engine. The burning of the amount of injected fuel primarily depends on the mass of oxygen (air) present in the combustion chamber. The total energy released due to combustion of fuel, only 37-43% energy use in the form brake power and remaining energy wasted through rejected heat(convection, radiation) and in cooling water (Stobart, R. and R. Weerasinghe, 2006; Kruiswyk, R. W., 2008).

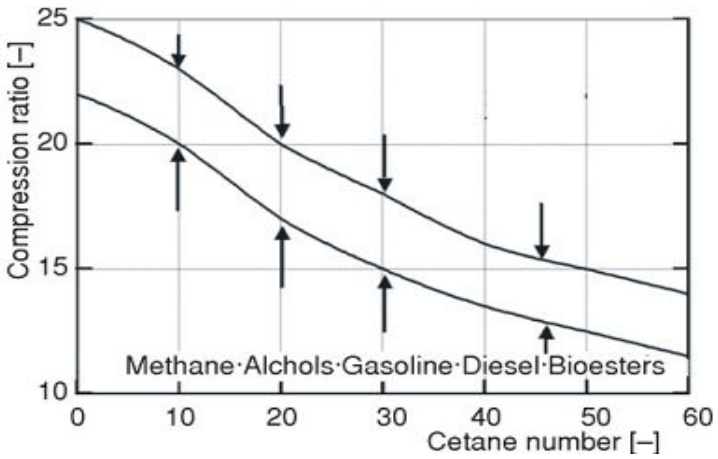

Fig.1.2 Fuels for diesel engines and compression ratio (Pešić, Radivoje, Davinić, Aleksandar, Veinović, S., 2005)

Naturally aspirated engine has the volumetric efficiency about 80% to 90% (Heywood, J. B.,1988) and this can even exceed the 100 %using turbocharger which forces more air into a cylinder as shown in Fig. 1.3. As a result, engine injects more fuel, this extra quantity of air and fuel increases the brake power of the engine per stroke.

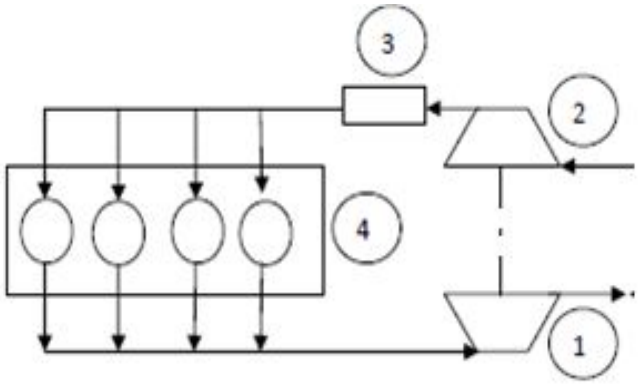

1. Turbine, 2.Compressor, 3. Intercooler, 4. Engine

Fig. 1.3 Turbocharging system in CI engine (Fu, J. *et al.*, 2014)

It improves the engine performance by way of enhanced efficiency, power output, high power to weight ratio and reduction of engine weight, NOx, and PM emissions. The Variable geometry (VGT), wastegate, and twin turbo are principle sorts of a turbocharging framework by which, it acceptsextra air.The passenger vehicles prefer VGT and commercial vehicles to others (wastegate, twin turbo). The turbocharger forces the air (boost pressure) at the inlet is proportional to the square of the speed of compressor (Hugh Maclnnes,1976). The combining of the turbocharger to the CI

engine can improve the engine brake power by 15-25% depending upon the types of engine. There are two primary methods of boosting (forced induction) the engines, i.e., turbocharging and supercharging have their own some pro and cons. For boosting the engine with turbocharger, firstly, it should have the sufficient amount of volume flow rate of exhaust gas to overcome the inertia and to rotate the turbine of the turbocharger. Additionally, there is a time lag between the demand for power and supply of boost pressure by the turbocharger, known as turbo lag. Whereas, in mechanical superchargers, there is no turbo lag, but it consumes the around 9-10% of engine power for running it.

The biofuels produced from the vegetable oil has been viewed as promising option and sustainable power source to use in the internal combustion engine. The biofuels processed from the biomass, vegetable oils and animal fats can be used efficiently in the CI engines. Biofuels are carbon neutral considering the complete cycle of CO_2, so utilization of vegetable-based biofuels seen as beneficial for the environmental pollution reduction point of view. Moreover, this move can give a boost to the agriculture sector, if produced at mass scale. Hence, to encourage the agriculture sector, and to ease the fuel shortage, and burden on the economy, India had proposed for blending the 20% biodiesel and alcohol in transportation fuel by 2017 under the national biofuels policy (Energy, M. of N. & R., 2017).The biodiesel produced from the vegetable oil has many excellent features such as around 11-12% higher oxygen content and higher cetane number, and at the same time,it has approximately 11% less energy content than the fossil diesel fuel due to the presence of oxygen molecule. Moreover, the higher density and viscosity of biodiesel have the combustion difficulties at partial and full load, affects the power output of the engine. The issues like environmental concern, alternative source of energy and scope of improvement in biodiesel combustion due to the forced induction of air are the driving force for researching in this area. These work explores the potential of reduction of the size of the engine and consequently the reduction of harmful emissions and an increased performance parameter.Even the small improvement is a big deal for overall advantage in all issues concern.

1.1 Background

This section construed in brief the concept of engine downsizing, the basic operation of 4-stroke compression ignition engine with naturally aspirated and supercharged condition, the process of combustion and the mechanism of pollutant formation. It also discusses the different techniques for changing the compression ratio, types of superchargers for engine downsizing and classification of sources of biodiesel based vegetable oil.

1.1.1 The concept of engine downsizing

The idea of the downsizing of engine refers to the either more enhanced power from the same size of the engine or same power and reduced emissions from the smaller engine as presented in the Fig. 1.4. It is the result of car manufacturer's attempt to provide more efficient vehicles that emit fewer emissions. This concept of engine downsizing either uses the same swept volume of the engine for higher power and torque with reduced emissions from the engine or smaller engine swept volume for the same power and torque with reduced emissions of the original engine. The downsized engine consumes the less fuel and saves the manufacturing cost as well (Smith, A., 2008; Merker, G. P. *et al.*, 2011).

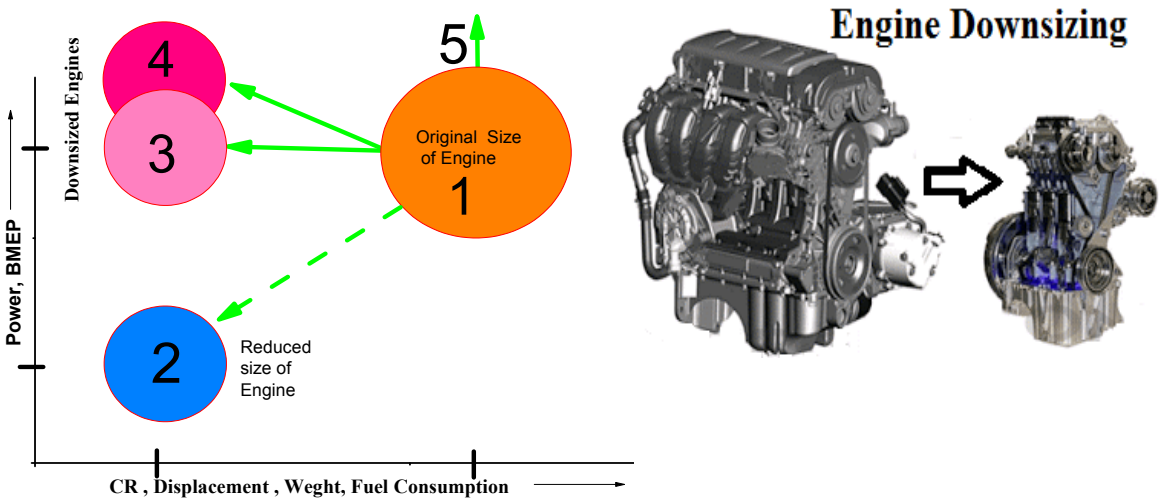

Fig. 1.4 Concept of engine downsizing

1.1.2 Operation of naturally aspirated and supercharged CI engine

The 4–stroke compression ignition *(CI)* engine completes the working cycle in two revolutions of the crankshaft. The total duration of the cycle regarding crank angle is 720^0CA. In these two revolutions, the piston moves between two extreme left and a

right end of the cylinder known as the top dead center (*TDC*) and bottom dead center (*BDC*) respectively. The movement of the piston from *TDC* to *BDC* is known as stroke, and each cycle of compression ignition engine completes by such 4 strokes. In each cycle, the following processes take place for the smooth operation of the engine. Intake and compression of air, injection of fuel at the end of compression (normally - 23^0CA *bTDC*), mixing, atomization, ignition of prepared charge, combustion, expansion, and exhaust of burnt gases as shown in Fig.1.5.

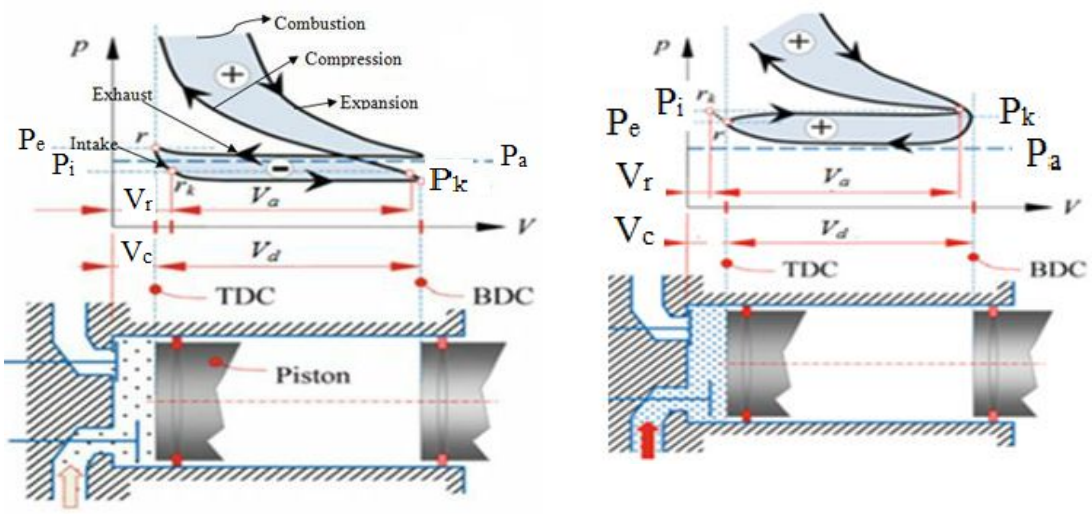

Naturally aspirated *CI* engine Supercharged/turbocharged *CI* engine

Fig. 1.5 Operation principle of naturally aspirated and supercharged CI engine

(Pehan, B. K. • M. K. • S., 2013)

After inducting the air during the suction stroke (intake), the air is compressed to a compression ratio (r) corresponding to the clearance volume at the end of compression stroke varying from 14:1 to 25:1 (Bauer, H., 2004). The compression ratio r is given as

$$r = \frac{V_d + V_c}{V_c}$$

Where V_d is the swept volume or piston displacement volume, i.e., the volume occupied between *TDC* and *BDC*, V_c is the clearance volume at the end of compression stroke between the top of piston and piston head.

The actual volume of air inducted V_a during the suction stroke is less than the swept volume of engine V_d in case of the naturally aspirated engine. The pressure of residual exhaust gases P_e is higher than the intake manifold pressure P_i. The pressure in the cylinder P_k at the end of the suction stroke is less than the atmospheric pressure P_a.

Due to this, the actual compression ratio r_k is less than the geometrical compression ratio r and the actual clearance volume V_r is more than the geometrical compression clearance volume V_c. Whereas, in case of the supercharged/ turbocharged engine the intake manifold pressure P_i is higher than P_a. This high-pressure induction of inlet air further compresses the residual gases in the cylinder and actual clearance volume V_r is less and more amount of fresh air introduced in the cylinder and has a higher volumetric efficiency (η_v) and maybe even more than 1.

$$\eta_v = \frac{V_a}{V_d}$$

1.1.3 Forced induction

In a naturally aspirated engine, the difference between atmospheric pressure and in-cylinder vacuum pressure decides the amount of fresh air inhaled into the engine cylinder and further reduced by the system of induction and cylinder head. Forced induction system can overcome this limitation and deficiencies of the naturally aspirated engine. The forced induction system pushes the more amount of air at a higher pressure than atmospheric air at the inlet. The brake power of the engine is the function of boost pressure at the inlet. It is observed that increase of intake air pressure by 0.42 – 0.55 bar enhances the power by the 30-40%. Forced induction system can be either turbocharging or supercharging based on the type, capacity, and application of the engine.

The turbocharger extracts the energy of the exhaust gas through its component exhaust gas turbine and utilizes this energy for to overcome the friction and for boosting the inlet air as well using the compressor coupled at common shaft as given in the Fig. 1.6.

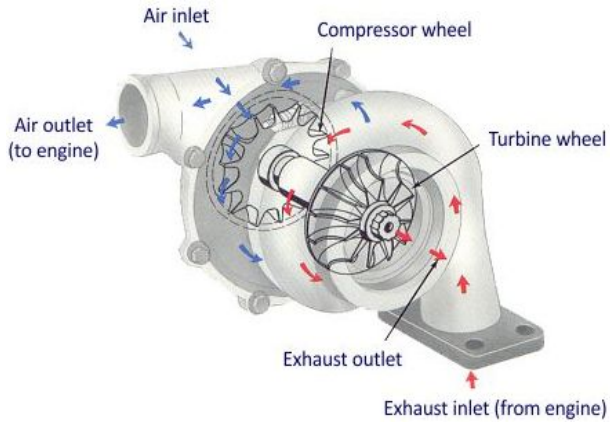

Fig. 1.6 Turbocharger component details and working principle (Schwitzer, 1991)

The mechanically, electrically or hydraulically driven compressors, blowers used to increase the boost pressure of air at the inlet of the engine known as superchargers. The superchargers are mainly classified on the way of action on the air to increase the boost pressure. The Fig. 1.7 depicts the working principles of the supercharger and the Fig. 1.8 presents the classifications of superchargers.

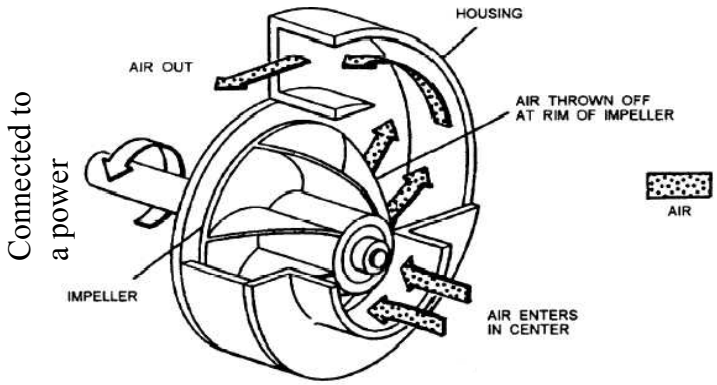

Fig. 1.7 Centrifugal blower type supercharger (Carsguide, 2018)

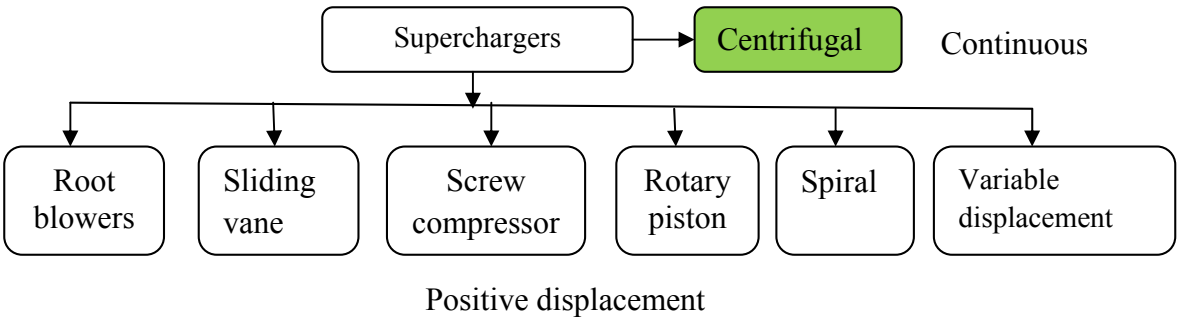

Fig. 1.8 Classification of superchargers

1.1.4 Combustion process

The fuel injects into the combustion chamber during the compression stroke chamber approximately -23^0 CA before *TDC.* The liquid fuel injected into the hot and compressed air breaks up into fine droplets and vaporizes, forming a combustible air-fuel mixture. As the air pressure and temperature are above fuel's ignition point, initial ignition of fuel takes place after a short delay. The termignition delay refers to the duration between the start of injection and start of ignition. The ignition delay period follows the combustion in diesel engine, progresses in two phases. In the initial phase, a portion of total fuel injected, which is initially mixes with air within the

flammability limits, gets rapidly combusted. This phase of combustion terms as the premixed phase of combustion. The Fig.1.9 depicts the premixed phase is rapid and realizes the high peaks of heat release over the small period of combustion (Zhen, D. *et al.*, 2013). Heat-release history in this combustion phase is a strongly dependent on ignition delay period, which in turn depends on some factors such as evaporation and mixing process, air-fuel ratio, fuel quality, and local temperatures. In-cylinder pressure rises rapidly with increase in the premixed phase of combustion, as shown in Fig.1.9.

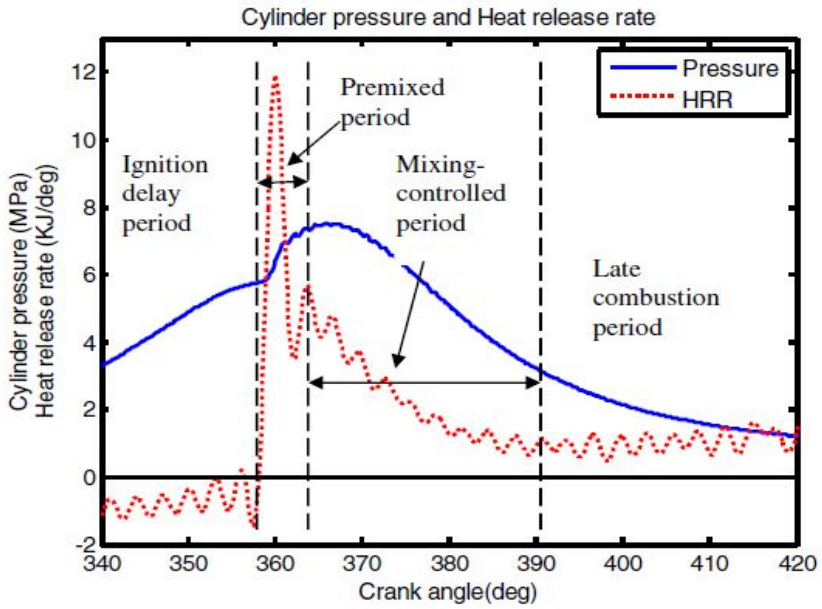

Fig. 1.9 Stages of combustion with cylinder pressure and heat release rate (Zhen, D. *et al.*, 2013)

The remaining fuel mixes with burnt gases and is burnt in slightly a slow in diffusion phase of combustion. The figure shows that diffusion phase of combustion is further categorizedinto stages 2 and 3 viz. mixing-control combustion and late combustion. The combustion rate in this phase is comparatively slow due to the controlled mixing of partially burnt gases and air. During stage2, remaining fuel partially oxidizes in the presence of high in-cylinder temperatures and reducing oxygen availability. This phase of combustion promotes soot formation, particularly in fuel-rich areas. During period 3, final oxidation of partially oxidized fuel and remaining fuel takes place. The chemical reaction rates decrease significantly in this phase due to the start of the expansion stroke and degradation in oxygen availability.

1.1.5 Emission formation mechanism and legislation to control

The Fig. 1.10 presents the emission formation in the compression ignition engine as the function of fuel-air equivalence ratio. The entire region of fuel spray divides into three distinct regions based on the variation of fuel-air equivalence ratio ϕ from inner central core to the radially outward surface of spray. The first central core region, where the fuel-air equivalence ratio is richer than the flammable rich fuel-air equivalence ratio, i.e., $\phi > \phi_R$ and the second enveloping region's ϕ value lies between rich and lean flammability limits, $\phi_L < \phi < \phi_R$. The third outer most regions are too lean to burn, i.e., less than the minimum lean flammability limits, i.e.,$\phi_L > \phi > 0$.

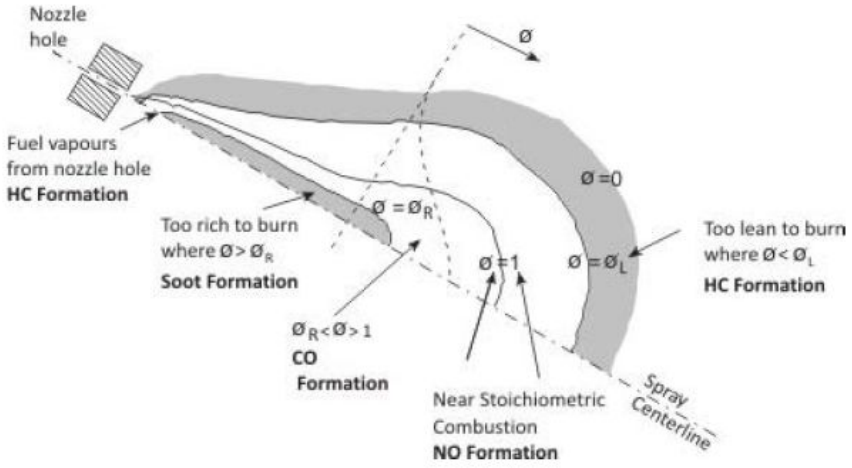

Fig. 1.10 Fuel spray with ϕ variation and emission formation (Pundir, B. P., 2010)

As the fuel injected into the combustion chamber, after ignition delay, few fuel particles reach the flammable limits, and it occurs where the value of ϕ is stoichiometric or close to it. At this region, fuel burns with high temperature and contribute the maximum *NO* formation. The *CO* forms in the region of ϕ, where it is rich and flammable and soot forms at the central core where the fuel only vaporize but lacking the oxygen and temperature to reach the flammable limit. At the outer surface, the mixture is too lean to start combustion and leads to the formation of Unburned HC. Similarly, the fuel in the nozzle sac volume and crevices may get vaporized at the end of combustion and does not burn owe to the *HC* emissions. The compression ignition engines have many useful features as compared to spark ignition engine. However, the few constituents of emission from these engines are prone to cause health and environmental problems particularly emissions of nitrogen oxide (*NOx*), carbon dioxide (CO_2), and particulate matters (*PM*). Hence the most of the countries

started to implement the legislation to curb the emissions of a toxic constituent from the engine (European Commision, 2010; the United States Environmental Protection Agency, 2016).The European Union norms EURO started in 1992 as presented in Fig. 1.11, India also implemented the norms of Bharat stage-II equivalent to EURO-I norms in the year of 2000. After that further stages of regulation such as Bharat stages-II, III, and IV.

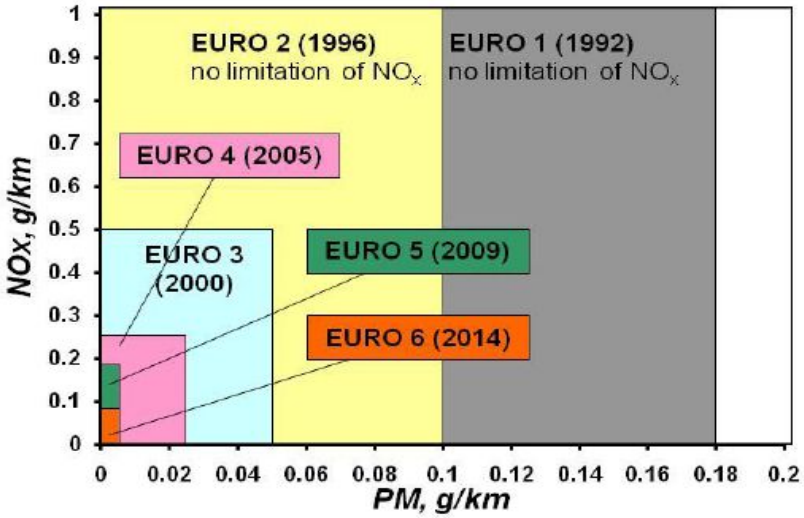

Fig. 1.11 EURO norms for diesel engine (European Commision, 2010)

1.1.6 Variable compression ratio engine

The automotive manufacturer's primary concern is to cope up with stricter emission norms and variability of high fuel price due to getting a shortage of it worldwide. This challenge addressed with appropriate technology for maintaining high thermal efficiency and fuel economy at lower emissions. The concept of variable compression ratio engine could scale down this challenge up to some extent. There are various methods available for changing the compression ratio. However, this concept of changing the compression ratio in running condition not yet been successfully implemented. Authors (Shaik, A. *et al.*, 2007) have reviewed the various methods for achieving the variable compression ratio (*VCR*) in an internal combustion engine. There are six different ways to get the *VCR*, 1) Variation of combustion chamber volume using a secondary piston or valve, 2) connecting rod geometry modification, 3) Moving the cylinder head, 4) Moving the crankshaft axis, 5) Variation of piston deck height and 6) Moving the crankpins.

1.1.7 Sources of biodiesel production

The various renewable fuels preferred as a blending constituent with fossil fuel to meet the fuel demand like ethanol and biogas for SI engine partially. The fuel processed from the straight vegetable oils known as biodiesel use in the compression ignition engine due to their comparable physical and chemical properties. The biodiesels are carbon neutral as presented by the cycle of carbon dioxide in the Fig.1.12. The source of biodiesel productions is different oil feedstocks. These may be edible or nonedible available throughout the world like linseed, soybean, rapeseed, sunflower, safflower, Karanja, jatropha, neem (Raheman, H. and S. V. Ghadge, 2008; Jindal, S. *et al.*, 2010; Dhar, A. *et al.*, 2012; Krishnan, P. N. and D. Vasudevan, 2015).

These different available sources of feedstock divide into three main categories (generations), and forth one is the artificial technique of biodiesel production by capturing the CO_2 from the environment. The basis of these three main generations of biofuels is on the way of biodiesel production, cleanliness, and their impact on the environment.

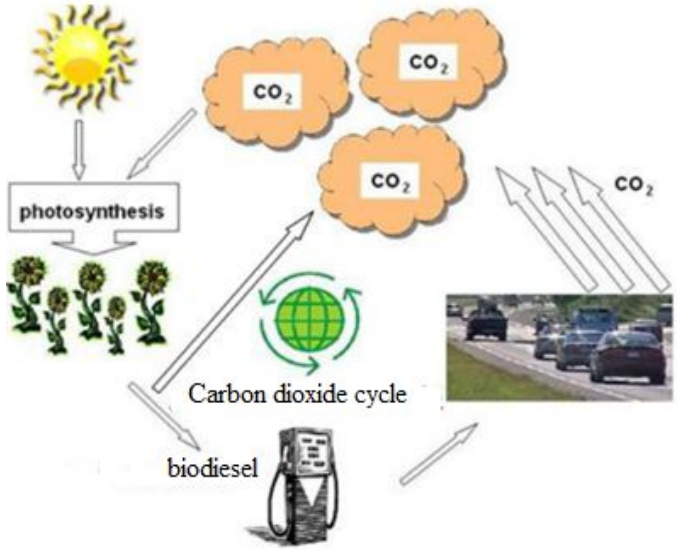

Fig.1.12 The cycle of carbon dioxide from vegetable feedstock

- **I-generation**: These biofuels derived from the edible feedstock such as sugarcane, soybean, rapeseed oil, sunflower oil. The biochemical methods like esterification, transesterification, fermentation, and hydrolysis used to produce the

biodiesel/biofuels. These affect the food security of the nation; hence there is always the debate about food vs. energy.

- **II-generation**: The nonedible feedstock used for the production of biodiesel and these vegetables does not affect the food bearing crops. These may be agriculture waste, forestry or organic residues. The other plant-based oil mainly includes Karanja, jatropha, need, mahua, linseed, palm, and Pongamia.
- **III-generation**: These are the algae and microbes based biofuels. These are fastest growing species as compared to all other options of biodiesel production sources and also do not need any fertile land and can grow in any unused land.
- **IV-generation**: This is an extension of 3rd generation in which algae and microbes are genetically modified to grow faster by capturing the more CO_2 from the environment. The initially this method of biofuels production would be costly but in the long run would be an economically viable option.

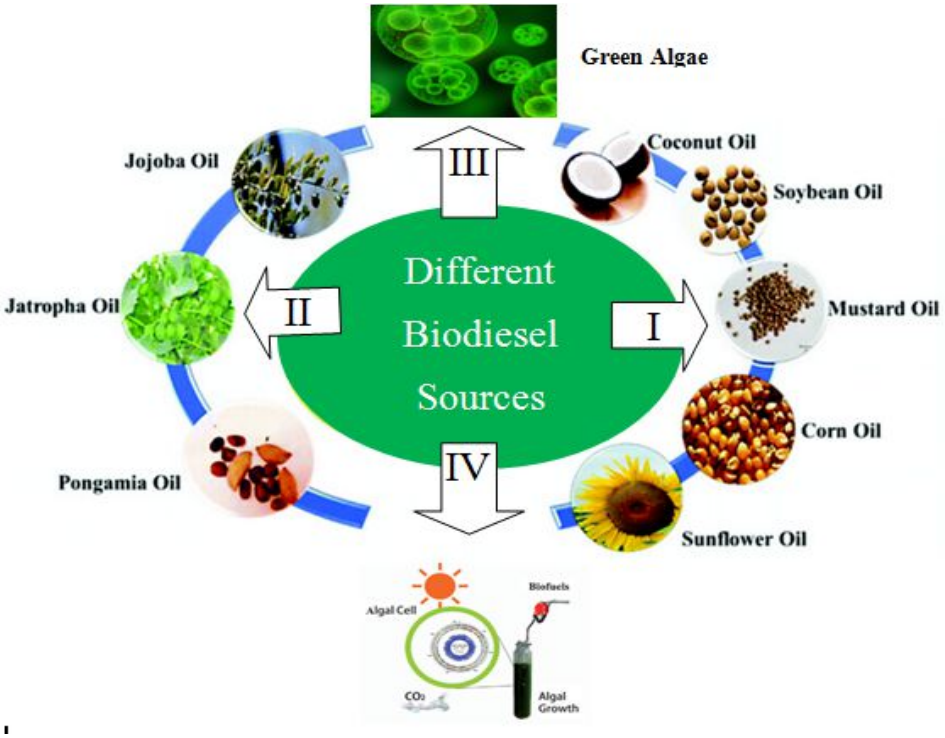

Fig. 1.13 Different sources of feedstock for biodiesel production

1.2 Present Work

The energy is the indispensable part of all walks of life, and therefore the demand has been rising every year across the globe and consequently, the fuel prices are rising (Briggs, I. *et al.*, 2013). Additionally, this has raised many issues simultaneously

which needs to be addressed and of course many researchers, manufacturers are working in this direction. The *first concern* is the dwindling of limited sources of fossil fuel. The estimate indicates that the out of total world's energy demand, 37% met by the crude oil alone (Dorian, J. P. *et al.*, 2006; Asif, M. and T. Muneer, 2007; Kjärstad, J. and F. Johnsson, 2009; Kegl, T., 2012).The projected total reserve of oil sources has 2 trillion barrels and already consumed around 900 billion barrels (Bentley, R. W., 2002).The *second concern* lies in the requirement of the vast amount of fossil fuel (diesel) due to a large number of diesel vehicles consuming around 81% energy share of the transport sector. Hence it is an immediate need to search for cost-effective and viable alternative source of fuel. Conversely it is also true; nonetheless, if we could succeed in developing the alternative source of fuel, the massive consumption of diesel fuel all over the world, the problem still be there but somewhat lesser extent. Therefore, every effort to reduce the diesel fuel consumption and to devise an alternative fuel counts a lot. The *third concern* is the stringent emission regulation norms imposed periodically and effective conversion of fuel's chemical energy into useful mechanical work to get more and more power from the same quantity of fuel and engine (Watson, N., J. M. S., 1982).

All these issues are tried to address here by experimentally varying the compression ratio in a laboratory-based single cylinder compression ignition engine. At each different compression ratio, the engine loading condition has changed along the different forced induction conditions. At all these different engine input parameters, the performance output characteristics calculated and analyzed for both the baseline fuel as well as alternative biodiesel fuel blends. Based on the obtained experimental results, the engine downsizing parameters has calculated and quantified concerning percentage improvement over naturally aspirated engine operating condition.

1.3 Thesis structure

In Chapter 1 under Introduction presents the motivation for the present work and general theory of variable compression ratio along with forced induction engine, sources of biodiesel. The earlier researchers who have contributed to the biofueled engine downsizing using the forced inductions may be turbocharged based or supercharged based and different optimization techniques used for biofueled compression engines described under Literature review. The gaps in the literature and

scope for the present work spotted in Chapter 2. Chapter 3 details the fuel preparation and methodology adopted in developing the basic experimental setup and experimentations of *VCR* diesel engine. Detailed results and discussions (stage-I) of preliminary experimental work of naturally aspirated biodiesel blends fueled engine. Chapter 4 elaborates the performance optimization using the different techniques such as analytical hierarchy process (*AHP*), Taguchi's grey relational analysis (*TGRA*), and technique for order preference by similarity to an ideal solution (*TOPSIS*) presented in the same chapter. The basic experimental setup modified for the supercharged condition. The outcome of downsized *VCR* engine demonstrated in the form of different graphs illustrating the variation in parameters chosen and discussed thoroughly under the heading results and discussion (stage-II) as Chapter 5. The broad and specific conclusions drawn from the present study are listed out as conclusions.

Chapter 2
Literature Review

Globally many research organizations, universities, and institutes are trying their level best for replacing the fossil fuel with a viable, sustainable, and cost-effective alternative fuels in the vehicles. Further, to cope up with ever-increasing stricter emission regulation norms. To achieve this, and fulfill up to some extent or more, various techniques and methodology have been devising such as forced induction, variable compression ratio, exhaust gas recirculation, and new types of alternative fuels and in-cylinder combustion technologies are being tried simultaneously. This chapter reviewed exhaustive and detailed works of literature for biodiesel, and its blends fueled in variable compression ratio diesel engine and effects of forced induction techniques with particular emphasis on a mechanically supercharged biodiesel-fueled diesel engine. The literature has been reviewed and cited here for the effect of these input engine operation parameters on combustion, performance and emission characteristics and engine downsizing parameters as well.

2.1 Compression Ratio and Injection Pressure

The many of the literature reported on an experimental study of variation of *CR* and very few also studied simulation models to account for the effect of *CR* on engine performance.

Nagai, T. and M. Kawakami (1989) carried out numerical experiments on a high-medium speed and small-medium size diesel engine using a two-dimensional combustion simulation model. The authors observed that varying *CR* from 13 to 15 has resulted only in a marginal increase of *NO* emissions with a significant reduction in *BSFC*. With an increase in *CR*, ignition lag was observed to shorten generating smoother combustion, consequently effectuating lower combustion noise.

The engine operation was stable with waste fish oil (WFO) biodiesel and higher in-cylinder pressure and shorter duration of heat release rate than diesel. Also, the gross thermal efficiency was 2.92% more, and 1.1% lowered combustion loss for WFO

biodiesel. The emissions of CO_2 and NO_x was slightly more and *HC*, *CO* reduced significantly for biodiesel (Alam, M. *et al.*, 2004).

Experiments carried out by variation of *CR* by changing stroke length revealed that mean in-cylinder pressures increased around 8% with an increase in *CR*. Regarding emissions, increase in *CR* has observed to increase emissions of oxides of nitrogen because of increase in in-cylinder temperatures attained by the gas mixtures (Yamin, J. A. A. and M. H. Dado, 2004).

Reduced diffusion phase and enhanced premixed phase has been observed with reduced CR, as reported by Laguitton, O. *et al.* (2007) in his experimental study on a DI diesel engine. The authors observed that a similar effect produced by reducing *CR* as by retarding injection timing.

Mendez, S. and B. Thirouard (2009) carried out experiments on both multi-cylinder and single cylinder engines incorporating common rail direct injection for implementing pilot and split injections. In contrast to other literary works, the authors opted for lower compression ratios of 14:1, 15:1 and 16:1 along with high EGR rates to achieve low temperature combustion (LTC) thermodynamic conditions. Authors reported that multiple injections over a single combustion event under such LTC conditions had a significant improvement in tackling the trade-offs associated with combustion noise, emissions, and *BSFC* rates. The maximum heat release rate was reported to reduce with double injections with a reduction in unburned species at low load conditions.

MacMillan, D. *et al.* (2009) investigated the effect of variation of compression ratio on heat release rate and performance of the engine. CR variation was achieved by changing volume of piston bowl, leaving bore and stroke unaltered. The authors observed an increase in indicative performance of the engine at reduced compression ratios at low load operation. This improvement reasoned with the reduced blowby and heat transfer losses, increased the net heat release. Increase in compression ratio was reported to generate a useful amount of work as it extended the limits for advanced injection timings.

Many works in the literature reported a combination of variation of *CR* with other in-cylinder techniques for further improvement in engine emissions and performance.

Raheman, H. and S. V Ghadge (2008) studied the effect of variation in *CR*, injection timing and engine load on a Ricardo EG engine using biodiesel and its blends with high-speed diesel fuel. The authors observed a decrease in engine performance with an increase in the percentage of biodiesel blend above 20% compared to the conventional engine performance. They reported that the high *CRs* in conjunction with advanced injection timings could compensate for this loss of engine performance.

Venkanna, B.K. *et al.* (2009) reported about the raw honge oil blends with diesel fuel at various injections opening pressure. The 20% blend has almost similar combustion, performance and emission parameters compared to standard diesel fuel. However, for blends, 30% and 50%, performance and emission parameters found to be more reduced and premixed heat release rate was quite improved for blend 30% at higher injection opening pressure.

Puhan, S. *et al.* (2009) investigated the effect of injection pressure on the performance characteristics of linseed methyl ester biodiesel-fueled single cylinder compression ignition engine. They reported at optimum injection pressure 240 bar, the *BTE* is almost equal and emissions of *HC,CO*, and smoke is lower with slightly increased NO_x for linseed biodiesel than diesel. At higher injection pressure noted the reduced ignition delay and higher peak in-cylinder combustion pressure at full load for linseed biodiesel compared to diesel. The combustion duration found similar irrespective of injection pressure and recommended the injection pressure of 240 bars for linseed biodiesel for better performance of the engine.

The comparative combustion analysis was done using the Karanja, jatropha, and polanga (Calophyllum inophyllum) oil biodiesel. The reported peak pressure for polanga biodiesel is better as compared to other fuel discussed since it has 6.61 bar higher pressure than the diesel fuel. The ignition delays of neat biodiesel Karanja, jatropha, and polanga varied between 6.30- 4.50, 5.90 - 4.20, and 5.70- 4.20 respectively. These ignition delays were lower than the diesel and were increasing with the load (Sahoo, P. K. and L. M. Das, 2009).

Zhu, Y. *et al.* (2010) developed a numerical simulation model using GT-power to predict gas flow and heat transfer inside the cylinder using DI-jet combustion model to predict combustion rate and associated emissions from a diesel engine. It showed

that at an engine speed of 2200 rpm, full load and no *EGR* conditions, increasing the *CR* from 16.2 to 18.2 had improved *BSFC* by 3.4 %, with a significant increase in *NOx* emissions by 14.3 %. However, decreasing *CR* from 16.2 to 14.2 has decreased *NOx* emissions by 13.8 % and has increased BSFC by 4.5 %. The authors concluded that with an increase in *CR*, thermal efficiency could improve without an increase in *NOx* by maintaining the correct *EGR* and *VGT* position.

Jindal, S. *et al.* (2010) work studies the effect of combining increasing *CRs* (16:1, 17:1 and 18:1) with variation in fuel injection pressures on engine emissions and performance. Neat jatropha methyl ether (JME) used as a fuel, and the results compared to diesel fuel. The authors reported that the combination of these parameters has resulted in the enhanced performance of the engine in connection with *BTE* and *BSFC*. The high injection pressure of 250 bar when used at higher *CR* of 18:1, *BTE* and *BSFC* increased by almost 9 % and 10 % respectively. It was also observed by the authors that high *CRs* have increased hydrocarbon (*HC*) emissions and exhaust temperature of the gases while showing a significant reduction in smoke and *CO* emissions. The authors opined that to yield better performance and emissions in biodiesel-fuelled engines, high *IP* is should have been utilized as a part of conjunction with increased *CRs*.

Gumus, M.(2010) experimented with using the methyl ester of hazelnut kernel oil to investigate the combustion and heat release characteristics. He noted the pressure-time diagram of biodiesel was similar to the diesel fuel. The start of combustion is advanced, ignition delay and cumulative heat release rate reduced and combustion duration increased with increasing the fraction of biodiesel in the blends. These lowered combustion and heat release characteristics improved by increasing the compression ratio (18:1 to 20:1) and injection pressure (20 and 24 MPa). The brake thermal efficiency was lower, and brake specific fuel consumption (*BSFC*) was higher for biodiesel fuel when compared with diesel fuels.

Gandure, J. and C. Ketlogetswe (2011) conducted a comparative study on a variable compression engine fuelled with petrodiesel fuels and native marula seed oil. The authors observed that, at 80 % load, the performance of engine fuelled with marula seed oil is very close to petrodiesel fuel. Also at a *CR* of 16:1, the optimum

performance obtained regarding brake power and engine torque for both the fuels as mentioned above.

Experimental studies on the variation of *CR* mostly involved the use of biodiesels, biofuels, and their blends. Muralidharan, K and D. Vasudevan (2011) studied the combustion, performance and emission characteristics of a single cylinder, variable compression ratio (*VCR*), and multi-fuelled engine with waste cooking oil methyl ester and its blends with conventional diesel fuel. The *CRs* varied from 18:1 to 22:1. The authors observed that at higher *CRs,* usage of waste cooking oil methyl ether blend with 40 % by volume basis had shown an increased delay in fuel ignition. They observed a significant improvement in performance as well as emissions when compared to standard diesel fuel especially at full load conditions.

Jindal, S.(2011) performed the experimental work to investigate the effect of compression ratios (16, 17, 18) and injection pressures (150, 200, 250) simultaneously. He observed the *BTE* improved by 5.45% using the pure Karanja biodiesel with an increase in *CR* from 16:1 to 18:1. The emissions of *NOx, HC*, smoke opacity, and *EGT* were less at all available combinations of injection pressure and CR as compared to diesel fuel. The noted maximum performance improvement in BTE 8.2% and *BSFC* 2.92% at IP 250 bar and *CR* 18. The similar results observed by Mohanraj T and Kumar KMM (Mohanraj, T. and K. M. M. Kumar, 2013), except EGT, was decreasing with increasing in CR using esterified tamanu oil.

The average improvement in brake thermal efficiency was around 7%, and brake specific fuel consumption reduced 15-20% by varying the compression ratio 14:1 to 18:1 using the Karanja biodiesel and its blends. Authors observed the reduction in emissions and exhaust gas temperature with increase in compression ratio except for NOx, which also increases with biodiesel fuel blends. The operating parameters of the engine also optimized using the genetic algorithm and reported the load 6 kg, compression ratio 18, injection pressure 247 bar, and biodiesel blend B95 are an optimal combination of engine input operating parameters (Amarnath, H. K. and P. Prabhakaran, 2012).

The *BSFC* and *BTE* were higher for all blends of neem oil methyl ester (biodiesel) than the diesel. Except for *NOx,* the emission *HC, CO* of all blends of neem oil biodiesel were lower and started of combustion was advanced for a higher fraction of

biodiesel blend and a little bit delayed for lower blends (up to B20) as compared to diesel. Heat release rate was similar, and combustion duration was shorter than diesel. Hence authors have suggested that lower blends of biodiesel, i.e., up to B20 biodiesel blends can be used efficiently in an unmodified engine (Dhar, A. *et al.*, 2012).

Jindal, S. and B. L. Salvi (2012) have performed the experimental optimization of fuel blends for improvement in performance using the linseed methyl ester biodiesel. It is investigated that the biodiesel blend LB10 found optimal, which shows the growth of *BSFC* by 4-6%, indicated thermal efficiency by 10-12%, and other characteristics viz. mass fraction burned, brake mean effective pressure, and rate of pressure rise is comparable with diesel. The emission of *HC, CO*, and smoke opacity reduced and *NOx,* CO_2 increased a little bit.

El-Kassaby, M. and M. A. Nemit-Allah (2013) conducted experiments using waste cooking oil blending ratios at varying compression ratios. The authors observed that as the *CR* increased, engine torque increased for all the blends. *BSFC* decreased with increasing *CR*. However, *BSFC* increased with increasing percentage of blends. As *CR* increased from 14 to 18, the reported CO_2 emissions increased by 14.28 %, 52 % decreased *HC*, 36.84 % increased *NOx* emissions. 13.95 % decreased the ignition delay for an increase in the *CR* from 14 to 18.

Experimental work carried out by Debnath, B. K. *et al.*(2013) on diesel engine fuelled with palm oil methyl ester (POME) studied the effects of VCR and injection timings on exergy and energy potential of POME. Energy analysis includes shaft power; energy input corresponding to fuel injected the output of cooling water and exhaust emission. The POME fueled engine could recover up to 26 % of the fuel input. Rest is flown through exhaust gases, cooling water and unaccounted heat losses. With an increase in *CR* and at the same brake power or shaft power, the reported amount of fuel injected decreases. Also, increase in *CR* also resulted in increased cooling water temperature and a decrease in exhaust energy flow rate.

Experiments were carried out by Nagaraja, S. *et al.*(2013) on a single cylinder diesel engine using preheated palm oil blends of diesel at a temperature of 900C. The performance and emission characteristics of these fuel blends compared with that of neat diesel fuel under increasing *CRs* of 16 to 20. At highest *CR* of 20, mechanical efficiency and brake power of 20 % volume blend have shown an increase by 14 %

and 6 % respectively when compared with standard diesel operation. The emission of *HC* and *CO* reduces with increase in *CRs*.

Amarnath, H. K. *et al.*(2014) studied the comparative experimental analysis using the Karanja and Jatropha methyl ester with diesel fuel in a variable compression ratio diesel engine. Authors argued that at full load and higher compression ratio the performance of biodiesel's are similar to the diesel fuel. As the compression ratio increased from 14 to 18, the average improvement in the brake thermal efficiencies (BTE) of diesel fuel, jatropha, and Karanja methyl ester were noted 6.34, 5.31 and 1.42% respectively. At all engine loading conditions and compression ratios (CRs), the emission of biodiesels is lower than the diesel fuel except NOx.

The combustion characteristics studied using the waste cooking oil (WCO) biodiesel and observed the advanced start of injection, combustion, and reduced ignition delay. Furthermore, Author also reported that the maximum heat release rate and rate of pressure rise in cylinder slightly reduced and combustion durations was longer using WCO biodiesel as compared to diesel fuel. On addition of 5 and 10% of biodiesel fraction in the diesel fuel, 4% increment noted in BSFC and 2% reduction in BTE. These additions of biodiesel reduced the smoke opacity, HC and almost no effect on the emission of CO and slightly increased in the emission of NOx (8.7%) and CO_2 (Can, Ö., 2014).

The reported improvement in BTE was 8.51% as the CR varied from 16.5:1 to 17.5:1 and reduction of HC and CO with a penalty on NOx emission for WCO methyl ester as compared to diesel (Hirkude, J. and A. S. Padalkar, 2014).

Hariram, V. and R. Vagesh Shangar (2015) conducted experimental analysis on a DI diesel engine with varying CRs from 16 to 18 and its effect on performance, combustion and emission were studied. The authors observed that for an increase in CR from 16 to 18, BSFC decreased by 30 % and BTE improved by 13 %. At 100 % load, peak pressure was reported to increase by 21 %; delay period decreased by 9 %. The authors' opined that CR of 18 was considered to be useful yielding high BTE and less BSFC compared to the lower CRs.

Combustion characteristics of neat castor biodiesel and its blends for compression ratio varying from 15 to 18 investigated and found that maximum cylinder pressure

was more for B50 and maximum heat release rate for B100 at compression ratio 18. Whereas, better results obtained for mass fraction burned for compression ratio 15 and 18. With increasing compression ratio, net heat release rate decreases and mean gas temperature, cylinder pressure increase for all fuel blends (Singh, B and S. K. Shukla, 2016).

Krishnan, P. N. and D. Vasudevan (2015) performed the experimental study using the methyl ester of tamanu oil blends with diesel fuel. The maximum thermal efficiency of blend B40 was 5.2% higher than diesel fuel as 41.75%. The BSFC and EGT of all blend decrease with increases in loads. The mechanical efficiency of blends shows the increments with loads, and at full load, the maximum mechanical efficiency for B20 and B40 was 93.77% and 87.62 % respectively.

Channapattana, S.V. *et al.*(2015) experimented with the Honne biodiesel. The thermal performance of biodiesel at IP 240 bar and full load found to agree with diesel fuel. The emissions of *HC, CO* reported minimum for at higher CR 18 and IP 240 bar. The emission of *NOx* was more with an increase in IP and fraction of biodiesel in the blends. The blend B20 has better thermal performance but higher emission level when compared with other blends. The EGT increases with increase in IP for all fuels due to improvement in combustion. The EGT for biodiesel blends is observed lower as compared to diesel fuel, and it increases by 12% for variation of IP from 180- 240 bar.

Babu, A. R. *et al.* (2016) studied the simultaneous effect of different IPs (190, 210,230 bar) and *CRs* (16.5 and 19) using the methyl ester of palm stearin blend of 40. The reported reduction in the emission of smoke opacity, *CO*, and *HC* was 1.66%, 8.66%, and 27.36% respectively at *CR* 16.5, 210 bar as compared baseline fuel operated at rated condition (*CR* 16.5, *IP* 190 bar). Moreover, at *CR* 19, IP 210 bar, the reductions in the emission of *CO, HC*, and smoke opacity are 6.8%, 23.58%, and 3.5% respectively. The emission of *NOx* increased by 8.42 % and 13.13% at these above two operating conditions as compared to baseline fuel petrodiesel at the rated condition of operation.

Kommana, S. *et al.*(2016) used the two biodiesels (Palm kernel oil (PKO) methyl ester and Eucalyptus oil (EuO) methyl ester) mixed them in volume percentage and carried out the experimental work at variable *CRs* such as 14-19 and IPs from 180 – 220 bar. At effective CR 19 and IP 220 bar, the blend B15 showed the better emission

and combustion parameters as compared to diesel fuels. The emission of HC, CO, and smoke was reduced by 42.99%, 41.09%, and 37.05% respectively whereas NOx emission increased by 9.02%.

Ananthakumar, S. *et al.*(2017) carried out the investigation in single cylinder CI engine for blends of waste plastic oil, diethyl ether, and diesel fuel with varying the CRs. The blends prepared by taking the proportion of 2.5, 7.5 and 12.5% of waste plastic oil and DEE with diesel fuel and *CR* varied from 12 to 20. The BSFC was higher and BTE lower for all tested blends when compared with diesel fuel. The emission of HC and smoke was approximately similar to the diesel for tested blends. The emission of CO_2 was less, and *CO* was higher for waste plastic oil and higher *NOx* due to higher amount net heat release and combustion temperature when compared with diesel fuel.

Pali, H. S. and N. Kumar (2017) experimented with using the Sal methyl ester (SME) biodiesel in a single cylinder compression ignition engine. They reported that for the SME, BTE was higher and BSFC was similar to the diesel fuel. Using the SME biodiesel, the engine operation was smoother and observed the increase in combustion heat release, *NOx*, and emissions of *HC; CO*, smoke opacity was lower as compared to baseline diesel fuel.

Datta, A. and B. K. Mandal (2017) reported the effect of variable compression ratio on engine output characteristics. The brake thermal efficiency decreased by 7.9% and increases with compression ratio from 16:1–18:1 for all blends of the methyl ester of neat palm stearin oil as compared to diesel fuel. With the increase of biodiesel fraction and compression ratio, both exhaust gas temperature, and brake specific fuel consumption increases. The heat release rate of biodiesel and its blends are less than the PD. The ignition delay decreases with increment in compression ratio. The results reported the reduction of exhaust gas emissions except slight penalty on the emissions of *NOx* and CO_2.

Pankaj D. and R. Gupta (2018) investigated the effect of Jatropha biodiesel and turpentine oil blends on performance and emission characteristics with variable compression ratio. Authors reported the dual biofuels blend could be better alternative fuel. Also noted 2.17% improvement in brake thermal efficiency and emission of *HC,*

CO, NOx, and smoke opacity decreased by 17.5%, 13.04%,4.21% and 30.8% respectively.

2.2 Forced Induction

The forced induction is the most important technique to increase the volumetric efficiency of the engine. Increased mass of fresh air inducted at higher pressure in the same volume of engine cylinder improves the combustion efficiency of fuel due to increased turbulence and swirl ratio of charge air results the lesser amount of specific engine exhaust emissions. The forced induction reduces the ignition delay, and consequently, the pre-mixed phase of combustion lessens and improvement in the diffusion phase of combustion. Sometimes, due to the better mixing and presence of more amounts of oxygen molecules present in the inducted air promotes both phases of combustion due to the more oxidation of *HC, CO*, and soot.

The effect of forced induction studied by the number of researchers using the techniques either turbocharging or supercharging with fuel as petrodiesel or different blends of biodiesel with various types of engines. The literature review has been presented based on the forced induction methods.

2.2.1 Effect of Turbocharging

In this system the energy of exhaust gases used for rotating the turbine coupled on a common shaft with the compressor of the turbocharger. In this section, all the literature discussed and included which used the turbocharger for the investigation purpose.

Saito, T. *et al.* (1984) experimented to investigate intercooling effect of the methanol of a turbocharged diesel engine on its performance and emission characteristics. The methanol was injected into the intake manifold to mix with the hot compressed air from the turbocharger. The methanol injection was limited to a ratio of 0.2 (ratio of methanol to air) to avoid the knocking due to rapid combustion and incomplete evaporation of fuel. The injection timing retarded from 6^0 - 0^0CA bTDC to reduce the *NOx* emission. The experimental results reported that the intercooling of methanol was recommended at high load owing to reduction of smoke and *NOx* emission.

However, it is avoided at lower load due to resulting the lower thermal efficiency and increase of total HC.

Rychter, T. J. *et al.*(1992) evaluated the concept of varying compression ratio (CR) using a thermodynamic simulation model of a turbocharged diesel engine. It observed that with an increase in *CR* to 20 at 75 % load operating condition, there was a reduction in fuel consumption. It also reported about 2 % reduction in ignition delay with an approximately 6dB reduction in combustion noise.

Ryan, T. W., and S. M. Shahed (1994) work deliver the outcome of usage of high injection pressures coupled with increased intake pressures on a heavy-duty diesel engine combustion characteristics. Authors reported that with a combination of high injection pressures and intake pressures, ignition delay reduced with ignition occurring very close to the nozzle. Reduction in the effect of either of the operating parameter increased ignition delay leading to ignition location occurring far from the nozzle.

Peterson, C. L. *et al.* (1995) reported the findings of a turbocharged diesel engine fueled with ethyl ester of waste hydrogenated soybean oil. Authors argued that with the biodiesel-powered engine, the engine power and smoke opacity was reduced by 4.8% and 71% respectively as compared to petrodiesel. The maximum torque reduced by 6% and 3.2% in 1700 and 1300 rpm, respectively. The exhaust emissions of HC, *CO,* and *NOx* were scaled down by 54%, 46%, and 14.7% respectively, whereas the emission of CO_2 increased by 0.57% and PM by 14 %.

Peterson, C. L. *et al.* (1996) carried out on field case study with neat Rapeseed ethyl ester biodiesel-fueled turbocharged truck traveled the total distance of 14,069 km. The modified engine of the vehicle for biodiesel fuel injection supply only. During the entire journey, the engine ran satisfactorily and noted the reduction of *HC, CO, NOx* as 55.6%, 50.6%, 11.8% respectively, whereas an increase of CO_2 (1.1%) and PM (10.3%).

The experimental study carried out by Wu, J. *et al.*(2006) for investigating the combustion and emission characteristics of the turbocharged diesel engine fueled with dimethyl ether (DME). The brake power and torque were higher and BSFC lower for DME at low and medium speeds when compared to diesel fuel. The combustion

characteristics such as cylinder pressure, the rate of pressure rise, and combustion noise found to be lesser for DME than diesel fuel. Also, the combustion duration and emission of NOx is less than the diesel fuel, 41.6% reduced the emission of NOx for DME.

Lee, S. and R. D. Reitz (2007) estimated the characteristics of stoichiometric diesel combustion to improve engine emissions and ISFC. The analysis has shown that BP and IP have a significant effect on ISFC. For example, increasing the boost pressure from 110kPa to140kPa has reduced ISFC by 11.5g/kW-hr while keeping the other operating parameters constant. It also indicated that soot emissions increased with engine load and retarded injection timings and the other operating parameters such as boost pressures, swirl ratio, inlet air temperature were found to be insignificant.

Colban, W. F. *et al.*(2007) work investigates the effect of intake pressures (from 1.0 bar to2.0 bar) on two imposed low temperature combustion (LTC) strategies on a diesel engine operating at light duty with a single cylinder. One LTC strategy achieved by advancing the injection timing with high rates of EGR and the other at retarded injection timings with moderate levels of EGR. Authors reported that intake pressure at unusually high load increased specific fuel consumption (ISFC) and efficiency of combustion. In concern with emissions, soot emissions were observed to decrease with increased intake pressures specifically at high concentrations of oxygen and increased at reduced oxygen levels. The authors opined that further NOx reduction was achieved with increased charge intake, though oxygen concentration in the chamber is more influential for NO_x formation.

Canakci, M.(2007) reported the experimental work of turbocharged diesel engine using the soybean biodiesel and diesel No. 1 & 2. They found a marginal reduction of *HC, CO, PM*, and around 11.2% of higher NO_x with using the biodiesel as compared to diesel No. 2. The BSFC of biodiesel was 13.8% higher, and for diesel No. 1 the BSFC and NOx were reduced by 16.1% and 1.2% respectively compared with diesel No. 2. Author opined that the biodiesel must be blended with diesel No. 1 instead of No. 2 for reducing the NO_x.

Karabektas, M. (2009) investigated the performance and emission characteristics of rapeseed methyl ester biodiesel and diesel fuel using naturally aspirated and turbocharged diesel engine at different engine speeds. The turbocharger of 0.7 bar

boost pressure capacity was installed with the engine, and the test was conducted with the variation of speed between 1200 to 2400 rpm in the steps of 200 rpm at full load condition. The authors noted the brake power and torque of diesel fuel were higher than biodiesel in both naturally aspirated and turbocharged condition. However, the improvement in brake power and torque was observed more in case of biodiesel than diesel fuel in the turbocharged condition as compared to naturally aspirated. Further improvement is noted in *BSFC* and *BTE* of both the fuel in the turbocharged engine. The emission of *NOx* was higher for biodiesel than diesel fuel in both the operating conditions and *CO* was reduced significantly in turbocharged operating condition for biodiesel. The overall improvement in performance and emission for biodiesel was more as compared to diesel fuel at the turbocharged operating condition.

Moscherosch, B. W. *et al.*(2010) reported the results of soy methyl ester biodiesel-fueled turbocharged diesel engine on combustion, performance, and emission parameters. The testing was done using petrodiesel as base fuel and neat biodiesel and it 20% blends, i.e. (20% biodiesel, 80% petrodiesel). With the use of biodiesel the emission of NOx reduced by 16% and carbonaceous soot matter emissions by 22% and 62% for B20 and B100 respectively. However, the BSFC increased by 15% as compared to petrodiesel.

Rakopoulos, C. D. *et al.* (2010) worked on turbocharged diesel engine using the fuels such as petrodiesel, biodiesel and n-butanol blends with petrodiesel. This test was conducted for investigating the effect of fuel blends and transient operating conditions on the emissions of *NOx* and smoke opacity. The turbocharger lag was found to be a most crucial parameter for the emission. The authors reported the peak value of *NOx* increased by 52% and 35% for both fuel blends. However, smoke opacity reduced by 40 % and 73% respectively for both biodiesel as well as n-butanol blends.

Tan, P. *et al.* (2012) assessed the regulated and unregulated emissions of a turbocharged diesel engine using the different blends of jatropha biodiesel. The emission of *NOx*, smoke increases and *HC* decreases with the fraction of biodiesel in the blends. The *CO* was higher at low loads. The most of the unregulated emissions reduce with load and increases with biodiesel in the blends such as formaldehyde, acetaldehyde, and acetone. The emission of toluene decreases with increase in load and biodiesel fraction in the blends.

Thangaraja, J. *et al.*(2012) experimented the Jatropha methyl ester biodiesel-methanol blend fueled turbocharged diesel engine to investigate the effect on NO_x emission and performance characteristics. The experimental results of J90M10 (biodiesel 90% and methanol 10%) blend and neat biodiesel J100 compared. Authors reported that at full load operation the emission of NO_x and smoke for blend was found to be reduced by 28% and 56% respectively similarly the reduction of peak pressure and *BTE* was 2% and 0.5% respectively as compared to neat biodiesel J100.

Wu, Q. *et al.* (2013) reported the effect of a microemulsion of water with biodiesel of turbocharged diesel engine on performance, combustion, and emission characteristics. The micro-emulsified biodiesel was prepared by using the 5.6% and10% water. The obtained results showed that the micro-emulsified biodiesel has significantly increased the peak cylinder combustion pressure and peak heat release rate with longer ignition delay and shortened combustion duration. The neat biodiesel-fueled engine has reduced the emission of *HC, CO*, and smoke except for 9% higher NO_x as compared to diesel fuel. Nevertheless, the micro-emulsified biodiesel marginally reduced the emission of smoke and NO_x except the higher amount of *HC* and *CO* emission at low and medium loads. Hence, the authors have recommended the use of the micro-emulsified biodiesel for improving the combustion and emission parameters simultaneously.

Maina, P. (2014) explored the combustion and emission characteristics of jatropha curcus oil, and its methyl ester fueled turbocharged diesel engine. The author reported with the turbocharging improvement in the combustion and emission characteristics. He noted BSFC was higher and out power for jatropha curcus oil and its methyl ester biodiesel were lesser as compared to diesel fuel. The emission of smoke and CO_2 was lower as compared to baseline fuel diesel.

An experimental study was carried by Gonca, G. *et al.* (2015) of combined Miller cycle and turbocharging for the reduction of *NOx* and improving the power in a single cylinder four stroke diesel engine. With supercharging of 1.1bar and 1.2bar and with two different versions of Miller cycles which provide 5^0CAand 10^0 CA retardation compared to standard condition have increased efficiency by 5.1%and 6.3% respectively. *NO* decreased by 27%.

Krishnan, S. R. *et al.*(2016) conducted experiments on a single cylinder research dual-fuel engine (diesel ignited-propane), to study the effects of different boost pressures from 1.1bar to 1.8 bar. At a constant injection timing and fuel injection pressure, inlet pressure increment has resulted in a reduction of ignition delay of the mixture. The authors observed that rate of heat release curves exhibited more of single-stage burning although with varying combustion rates and with different maximum peak measures. It was also observed that increasing inlet pressures increased fuel conversion efficiency of the engine. Regarding emissions, indicative specific *HC* and *NOx* emissions decreased.

Abedin, M. J. *et al.* (2016) experimented with turbocharged diesel engine by varying the speed at full load using the Alexandrian laurel (Calophyllum inophyllum) biodiesel (ALB) and its blends (10%, 20%) with diesel fuel. The results of ALB compared with baseline fuel and a B5 blend of 5% palm biodiesel. The BSFC of all tested fuel blends were 6-20% higher than the diesel fuel. Authors observed by using the ALB, ignition delay, the combustion peak pressure, net heat release, and combustion duration were less and mass fraction burned was more when compared to diesel fuel. Similarly, all the blends have significantly reduced the emission of HC. The emission of *CO* and *NOx* for ALB was noted 2.5% and 3% higher than the diesel fuel.

Silitonga, A. S. *et al.*(2017) conducted the experimental work using the jatropha biodiesel to investigate and validate the data of combustion, performance and emission characteristics using the kernel-based extreme learning machine (KELM) model developed by Matlab language. Authors opined that experimental data confirms the predicted data by the KELM model within the range of percentage error of 0.1259–2.3838.

Lijiang, W. *et al.* (2018) performed the experimental work to investigate the effect on combustion process and *NOx* emission using the four different blends of waste cooking oil biodiesel on turbocharged marine diesel engine. The work was conducted on two rpm of engine 1050 and 1500 rpm. The observed peak heat release rate decreases with increase in biodiesel blends and engine speed. The maximum reduction of peak of heat release rate noted for 1050 and 1500 rpm as 11.04% and 19.86% respectively.

2.2.2 Effect of Supercharging

Zhang, L. *et al.*(1994) analyzed the effect of supercharging on combustion process on an optically accessed diesel engine. The authors concluded that peak heat release rate value decreased with increased boost pressure with the decreased premixed rate of combustion and increased the diffusion rate of combustion promoting NOx formation. It was further opined that soot formation during mixed-controlled phase could be reduced by a significant amount with increasing oxygen availability.

Tanin, K. V. et al. (1999) conducted a test on Caterpillar 3400 series engine with increasing boost pressures from 0% to approximately 85 %. The authors had shown a substantial reduction in BSFC levels up to 55% when all the other crucial parameters such as engine speed, the load were kept constant. The authors opined that increasing intake pressures beyond 55% was found to be less beneficial. It was also reported that soot emissions decreased with increase in boost pressures.

Amba Prasad Rao, G. and P. R. Mohan (2003) studied the effect of supercharging (0.2,0.3, 0.4 bar (g)) pressure on the performance of a direct injection diesel engine using untreated cottonseed oil as fuel under different injection pressures (IPs) 180, 210 and 240 bar. Authors reported that no effect of IP on engine performance but the supercharging pressure of 0.4 bar (g) improves the BSFC by 15% at recommended IP compared to the naturally operated condition of the engine.

Aoyagi, Y. *et al.* (2004) conducted experiments on a DI diesel engine incorporated with the common rail fuel injector system. Increased supercharging of intake air reduced ignition lag due to an increase in motoring pressure. This observed to bring in an entire diffusion mode of combustion. The authors opined that high boost pressures in combination with high injection pressures resulted in enhanced heat release rates (HRRs) and shortened duration of combustion. A reduction in soot emissions was also observed with increase in oxygen content of the cylinder resulting in lowered net soot production.

Benajes, J. *et al.*(2004) investigated the effects of boost pressures (BP) and injection pressures (IP) on a single cylinder diesel engine equipped with a standard rail injection system on *NOx*, soot, and brake specific fuel consumption. The authors observed that as intake pressures increased, physical and chemical delay of the

mixture to be combusted decreased with the intensive mixing of fuel and air. Around 50% reduced combustion duration. In concern with emissions, NOx emissions increased marginally as a result of high heat release rates. The authors concluded that due to better mixing of air and fuel oxidation of soot formed has been promoted reducing soot emissions. Faster combustion rates were observed to be infused with increased charge densities with a reduction in brake specific fuel consumption (BSFC).

Aoyagi, Y. *et al.* (2006) conducted the experimental work on a single cylinder heavy-duty diesel engine to reduce the exhaust emissions. The effect on engine performance and emission was investigated by using the high boost pressure and EGR rate. The engine was equipped with an external supercharger and EGR system. The authors observed at a high boost pressure of 500 kPa and EGR rate of 50%, the emission of NOx was reduced significantly without any noticeable change in the emission of PM.
To increase the volumetric efficiency of hydrogen-fuel port fuel injections in spark ignition engine Verhelst, S. *et al.* (2009)carried out experimental study on a single cylinder hydrogen engine fitted with supercharging and EGR. The authors observed a decrease in the tailpipe NOx emissions along with an increase in engine efficiency using a combination of supercharging, EGR and a three-way-catalyst (TWC).

Jayashankara, B. and V. Ganesan (2010) investigated the effects of injection timing and in-take pressures on the performance and emissions of a diesel engine with single cylinder and direct injection. A CFD model was used for this purpose, and intake pressures were varied from 1.01 bar to 1.71 bar. Authors opined that with an increase in intake pressures, in-cylinder peak pressure increases and in-cylinder temperatures, and the peak value of heat release rate reduced with an increase in overall heat release with a reduction in ignition delay. Regarding emissions, with increased cumulative heat release, in-cylinder temperatures elevated, increasing *NOx* emissions and reduced soot emissions were observed because of improved oxidation capabilities of the charge inducted into the engine.

Jagadish, D. et al.(2011) investigated the effect of supercharging (50 kPa) on performance characteristics of ethanol-diesel blends fueled engine with using the palm stearin methyl ester as an additive. They reported the improvement in BSFC, *BTE, EGT*, and in various emission characteristics such as *HC, CO,* NO_x, and smoke

opacity. Authors reported the increment in output brake power, torque, and brake thermal efficiency of biodiesel-ethanol blends as compared to the naturally aspirated engine. Furthermore, the reduction of *BSFC* and *NOx* with the slightly higher amount of emission of *HC, CO*.

Ishikawa, N. (2012) compared the performance and emission characteristics of 3 L capacity diesel engine using the mechanical supercharger and turbocharger under steady-state operating condition. For the same operating condition, mechanical supercharger has the higher boost pressure which facilitates the use of a higher amount of EGR results in the lower *NOx* emission. The time required to attain for steady state boost pressure condition is shortened, and suddenly the fuel flow increased for a mechanical supercharger in transient operating condition. Furthermore, the emission of *NOx* reduced by 50% and fuel consumption penalty was 5.5% for the mechanical supercharger.

The effect of cottonseed oil and diesel fuel blend (B20) has been analyzed by Joshi, D. *et al.*(2014) using supercharged single cylinder diesel engine's performance characteristics. They observed an increase in BTE and decrease in smoke and emissions of blend B20 using supercharged engine compared to diesel fuel. The mechanical efficiency was improved by 10-20% at supercharged pressure 3 bar.

Yoshimoto,Y.(2016) carried out an experimental study using root blower type supercharger on single cylinder diesel engine. The boosting pressures were varied from 100 kPa to 140 kPa. The biodiesels used are rapeseed oil, soybean oil, and coconut oil methyl esters. Also, the blend of coconut oil methyl ester and 1-butanol was mixed in the ratio 60:40.It is reported that for all tested fuels, the emission of *CO* and smoke has scaled down considerably and brake thermal efficiency improved notably as compared to diesel fuel

Kolakoti, A. and B. V. A. Rao (2017) evaluated the effect of palm methyl ester with an additive as coconut methyl ester in a supercharged single cylinder diesel engine. The obtained results are compared with diesel fuel. The 3% of coconut methyl ester in the palm methyl ester showed the significant reduction in the emissions. At full load operation, the noted reduction is in the emission of *CO*, smoke, *NOx*, and CO_2 were 0%, 37.6 *HSU*, 44 ppm, and 1.54% respectively.

Talibi, M. *et al.* (2017) carried out the experimental investigations using the combined combustion of H_2 and diesel in a diesel engine by varying the input parameters such as engine load, EGR, and inlet boost pressures. They found that by using the EGR and boost pressure, the emission of NO_x, PM, and CO_2 reduces due to combined combustion. At a low and medium level of supercharged pressure, with an increase of H_2 in the intake increases the NO_x and reduces the number of particulate matters.

2.3 Effect of Intake Air Temperature

Solbrig, C. E. and T. A. Litzinger (1990) executed experiments on a direct injection diesel engine which is optically accessible. Intake temperature of the charge was varied along with swirl ratio to study their effect on engine combustion, emission and performance characteristics. From the investigations, with an increase in intake temperature, the authors observed a reduction in ignition lag, premixed peak rate and overall fraction burnt in premixed phase. The authors reported that NOx emissions increased with increase in charge temperature.

Nagai, T. and M. Kawakami (1989) carried out simulating calculations using emptying and filling processes, two-zone combustion model and extended Zeldovich reaction mechanisms to understand the combustion and NO formation of a single cylinder diesel engine at various operating conditions. It was reported by the authors that different charge temperature from 20^0 C to 40^0C, the variation in NO formation was found to be uniformly increasing. This was attributed to the increase in charge temperature before burning to lead to higher in-cylinder temperatures prompting the formation of NO emissions.

A multizone model of high-speed direct injection diesel engine was developed by Bazari, Z. and B. A. French (1993) to study and tackle the trade-offs associated with its performance and emissions. Variation of performance and emissions were observed at three various charge temperatures and three various load conditions while keeping the other parameters unchanged. The authors reported lowering of NOx emissions with reduced charge temperatures, especially at high loads. A marginal reduction was also observed in soot emissions and BSFC with charge cooling. The authors concluded that charge cooling is advantageous in both emissions and performance point of view.

Alam, M. *et al.*(2006) conducted experiments on a six-cylinder, turbocharged, water cooled engine operated at a wide range of inlet temperatures. The authors found that increasing the inlet temperature decreased the air flow rate and affected air-fuel ratio during combustion. Also, a decrease in ignition delay was found with increasing inlet temperatures increasing the exhaust gas temperatures. The authors observed an increment in NOx emission given to the increased in-cylinder temperatures before combustion.

2.4 Optimization Techniques for Biodiesel Blends

The all existing transport and industrial diesel engines are designed and optimized, considering fuel as petroleum diesel. Therefore, operating parameters must be optimized to use the biodiesel as fuel in the unmodified engine to reduce the design and modification cost. Many researchers have studied the optimization of compression ignition engine using different biodiesel/diesel fuel blend. The various techniques used for optimization of engine parameters. These are response surface methodology (RSM) (Amarnath and Prabhakaran, 2012; Datta Bharadwaz et al.,2016; Ravikumar, 2013; Win et al. , 2005; Yusri et al. , 2017), Taguchi approach (N. Logothetis, 1988; Wilson , 2012; H. W. Wu and Wu, 2013), Taguchi-grey relational analysis method (GTM) (Gul et al.,2016; Jadhav and Tandale, 2016; H. W. Wu and Wu, 2012),GTM-TOPSIS method (Gnanasekaran Sakthivel et al., 2014), genetic algorithm and artificial neural network (Alonso et al., 2007). These techniques are helpful for reliability and accuracy to get the result in a minimum number of experiments and cost. Parameter optimization of Karanja biodiesel/diesel fuelled engine carried out using nonlinear regression and reported the optimized factor of fuel blend B13 and IT at 24 ^{0}bTDC (Maheshwari, Balaji, and Ramesh, 2011). Thermodynamic and Taguchi model used to analyze the Jatropha biodiesel fed engine. The maximum engine performance for biodiesel found at optimized engine design and performance parameters (Ganapathy, Murugesan, and Gakkhar, 2009).
The algorithm based on particle swarm optimization (PSO) used to investigate the diesel engine parameters for improving the fuel efficiency and decreasing the engine out emissions (D. Wu and Gao, 2016).

The optimization of performance and emission parameters carried out in a single cylinder diesel engine of power 5.2 kW fuelled with Karanja biodiesel. The input

parameters were compression ratio, fuel fraction, injection timing (IT), injection pressure (IP), and load with output parameters fuel consumption, emission, and brake power. The input parameters were taken at 4-level and Taguchi-GRA approach used with orthogonal array L_{16} for getting optimum settings. Authors reported the compression ratio 17.7, brake power 3.64 kW, biodiesel blend B20, IT 27 ^{0} bTDC, and IP 230 bar optimum operating parameters of the engine (Sivaramakrishnan Kaliamoorthy, R. P., 2013).Fish oil biodiesel blends and a load on the engine was varied at six and five levels respectively. The optimization of various performance, combustion and emission parameters has been done using fish oil biodiesel. The Taguchi-fuzzy approach used to optimize the parameters, and ANOVA is used to get the effect of each working parameter on output parameters (Sakthivel, G. and M. Ilangkumaran, 2017). An experimental study is carried out in a dual fuel mode of CNG-diesel and optimizations of IP, load, and energy shared by CNG (CES) have been done to reduce the brake specific fuel consumption, emission of net hydrocarbon (NHC) and particulate matter (PM). Using grey-Taguchi approach, they reported the optimal input parameters as load 4 kg, IP 540 bar, and CES of 15% (Roy, S. *et al.*, 2014). Zhan-Yi Wu et al. Wu, Z. Y. *et al.* (2014) investigated the combustion and emission features at optimal operating condition using Taguchi approach. They noted the biodiesel fuel blend B10, liquid petroleum gas (LPG) 40%, EGR ratio 20%, and load 60% as the optimal operating parameter for reducing the emission of smoke by 52% and NOx 31%.

The design of experiment's (DOE) Taguchi method used for the analysis purpose of the biodiesel-fueled engine. This method proposed by the Dr. Genichi Taguchi *et al.*(1989) for optimization of the parameter, which provides the information about the best control parameters in the least number of experiments. The accuracy and reliability of Taguchi method solely depend upon the way the factors and their values have been chosen. In Taguchi design, the robustness of any control elements is measured by the way it affected by the independent factors (noise level). The purpose of Taguchi design is to identify the best control factor which has less variability due to the uncontrolled factors (noise level) such as ambient temperature, engine vibration, etc. The variability in control factors is measured by the Taguchi's signal to noise ratio (S/N). The S/N ratio is the log function of output measured parameter, and these are to be calculated for each output parameter. The higher the S/N ratio means better the control factor and

less variability due to the noise levels (Rao, R. S. *et al.*, 2008; Senthilkumar, N. *et al.*, 2014). The S/N ratio calculated by the three design conditions namely larger the better, smaller the better, and nominal the better. The arrangement of control factors and their levels in a minimum number of experiments called orthogonal array to get the effect of control factors on given responses. However, the Taguchi method is used for single objective optimization. For more than one responses/multi-objective (output parameters) the grey relational analysis (GRA) method proposed by Deng J.L.(1989) is used. In GRA method, all the responses are combined and converted it into single response optimization problem. The Taguchi and GRA methods are combined for optimization of multi-objective responses.

The grey relational analysis (GRA) concept uses two conditions of information. The condition at which not at all any information (black) is available for the system ultimately there is no solution. Another side is with full of information (white) which could have a unique solution for the system of information. However, these kinds of extremities never exist in real world, but somewhere in between. Therefore, GRA uses to solve the problems which have less or partially available information. That converts the multi-objective problem into single objective and Taguchi used for optimization. Many authors have used this combined technique of optimization for solving the problems (Tarng, Y. S. *et al.*, 2002; Kuo, Y. *et al.*, 2008; Tsao, C. C., 2009; Sahu, P. K. and S. Pal, 2015; Pervez, H. *et al.*, 2016; Raju, A. V. S., 2016).

Saaty T. L.(1980;2000) has developed the multiple criterion decision analysis (MCDA) based analytical hierarchy process (AHP) method for solving the complex decision-making problems. The AHP method organizes the decision process in a systematic hierarchical order of objective, conditions, and alternatives. This process helps the people to make the most appropriate arrangement qualitatively and quantitatively for selecting the best option. The use of AHP in many decision-making applications shows its popularity (Agapova, M. *et al.*, 2017; Giacomini, C. *et al.*, 2017; Leong, Y. T. *et al.*, 2017; Sutadian, A. D. *et al.*, 2017).

The TOPSIS method has been used in many applications for optimization purpose. However, the authors (Sanayei et al., 2010) noted its limitations as it does not account for the relative significance of distances it measures from two reference points for the optimal solution. Furthermore, it's been reported that the TOPSIS and grey relational methods have the similarity and the limitation of TOPSIS can be overcome by

integrating with GTM (Tzeng and Tasur, 1994; Chen and Tzeng, 2004). The optimal combination of input parameters has been obtained for performance improvement and reducing the emissions.

2.5 Observations from the literature

In reviewing the literature, the emphasis has been given on the design parameters and modification of the engine along with different optimization techniques for the optimum parameters of the engine. From the literature following observations are noted in brief as follows.

1. The density, viscosity, bulk modulus, and latent heat of vaporization are the main biodiesel properties which limit the use of higher blends satisfactorily.
2. Most of the input variable parameters are CR, load, IT, IP.
3. At higher CR, the engine operates smoothly.
4. On an average, the biodiesel blend B20 has the comparable performance with lesser emission. By increasing the input parameters viz. *CR, IP*, higher blends also possible to utilize in the CI engine but performance goes down.
5. Most of the biodiesel research concentrated on second–generation vegetable oil-based biodiesel.
6. Very little study available for linseed VO based biodiesel and that too using VCR engine.
7. In case of high FFA linseed VO based biodiesel, only blend B10 can be used in the unmodified engine due to its physicochemical properties.
8. The partially modified engine can run on higher blends of biodiesel satisfactorily.
9. Very few studies have been conducted on biodiesel fueled small and high speed (single cylinder) supercharged engine.

2.6 Gaps identified from the literature

1. There is no enough and thorough literature available on linseed biodiesel with variable compression ratio engine.
2. The available literatures are inadequate on the feasibility studies of higher blends of proposed biodiesel on a new or modified engine technology.
3. There is no trace of literature on an experimental study on the combined effect of CR and supercharging on an engine performance fueled with diesel or biodiesel.

4. No much work reported by any researchers on quantification of single cylinder engine's downsizing.

2.7 Objectives of the research work

1) Experimental investigations of higher biodiesel blends by varying *CR* 14, 16, 18 and compared with the PD at the standard operating condition at CR17.5 and full load.
2) To modify the existing engine for supercharging at 0.5 kPa (g), 1 kPa (g), and 1.5 kPa (g) for optimised blends.
3) To investigate the CI engine performance with increasing boost pressure and CR fueled with optimum biodiesel blends and PD.
4) The quantification of downsizing parameters of the engine regarding % increase in specific power, and % decrease in specific weight of the engine.

Chapter 3

Fuel preparation and its experimentation in an unmodified engine

This chapter highlights the preparation of linseed biodiesel, properties and experimental setup considered for further investigations in the subsequent sections. Though there was much information available on the edible and non-edible fuel varieties, fewer contributions have found in the application of linseed in the variable compression ratio engine. It understood that the LB10 fuel shown comparable performance. The objective of this chapter is to understand the causes for the limitation of blends and steps/modifications to be followed when higher blend ratios required.

3.1 Linseed vegetable oil as a source

Fig. 3.1 Linseed crop

Linseed oil is being selected for the present study due to its non-edibility, eco-friendly and vast amount availability. India is the third major producer of linseed oil after Australia and Canada.Linseed is mainly cultivated in India for oil and fibers in October - November as a rabi crop as shown in Fig.3.1. Linseed seed contains around 33 to 47% of the oil. Its seed cake used for feeding cattle and most of the linseed oil (80%) used for industrial purpose. The Fig. 3.2 shows the different steps/procedure followed

for entire research investigations right from the procurement of crude linseed oil to the final objective achievement.

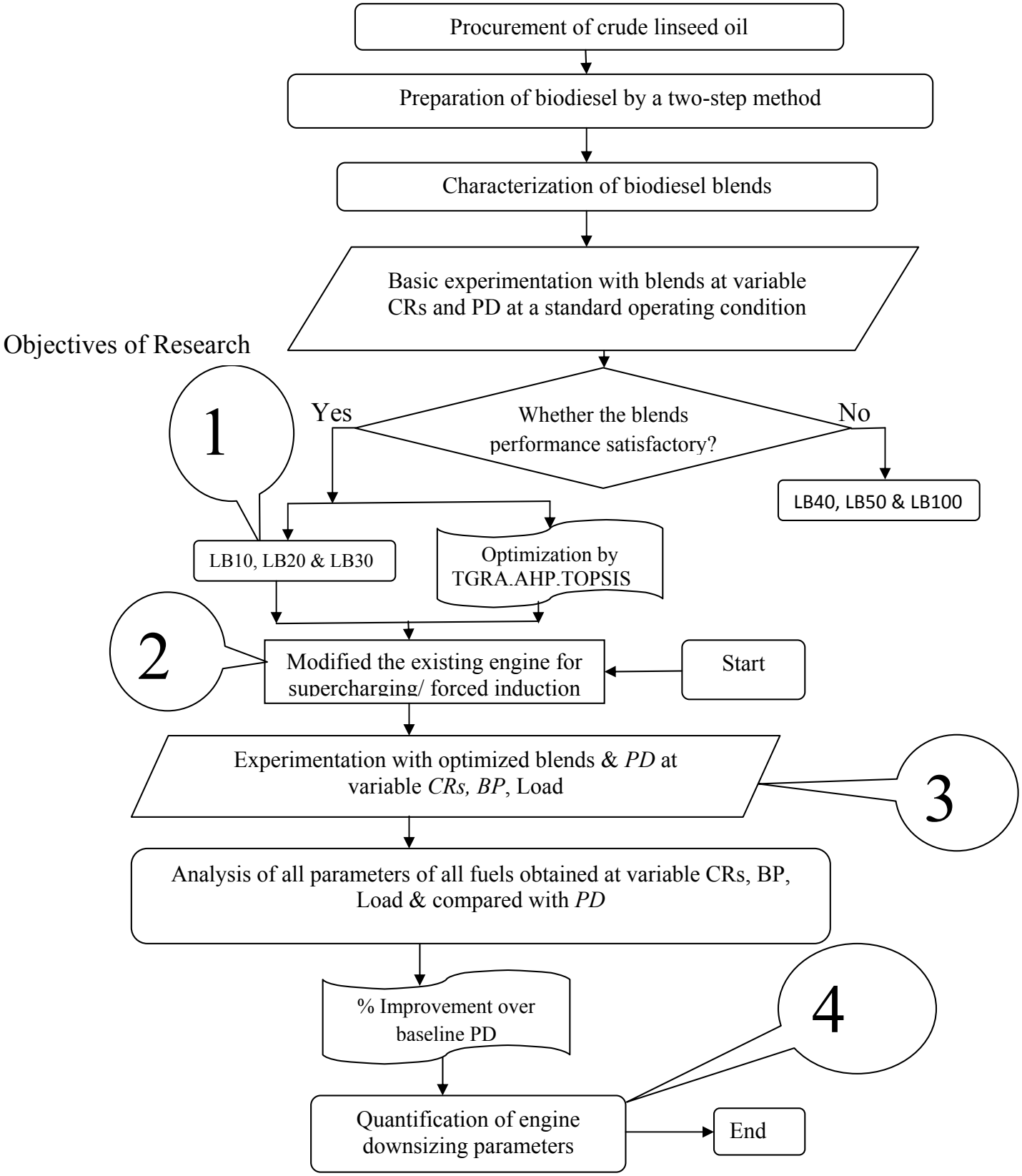

Fig. 3.2 Flow chart of procedure/ steps followed for investigation

3.2 Biodiesel and its blends preparation method

Table 3.1 presents the different amount of free fatty acids present in linseed oil. Most dominant free fatty acids are oleic, linoleic, linolenic and these acids have double bond makes them highly unsaturated. This oil highly unsaturated and has more percentage of linolenic acid (60%), and hence it is highly acidic and viscous (Dlugogorski, B. Z. *et al.*, 2012).

Table 3.1 FFAs in linseed oil (Puhan, S. *et al.*, 2009)

S. No.	% Weight	Compound Name	Formula	Molecular Weight
1	0.045	Myristic	$C_{14}H_{28}O_2$	288
2	0.5	Lignoceric	$C_{24}H_{48}O_2$	368
3	0.357	Arachidic	$C_{20}H_{40}O_2$	312
4	0.222	Behanic	$C_{22}H_{44}O_2$	340
5	6.21	Palmitic	$C_{15}H_{32}O_2$	256
6	5.63	Steanc	$C_{18}H_{36}O_2$	284
7	20.17	Oleic	$C_{18}H_{34}O_2$	282
8	14.93	Linoleic	$C_{18}H_{32}O_2$	280
9	51.12	Linolenic	$C_{18}H_{32}O_2$	278

The FFA value represents the amount of KOH required in mg to neutralize the 1 gm of oil. The FFA value (mg of KOH/gm) of linseed oil is high around 5.4% (Nayak, S. K. and P. C. Mishra, 2016), hence the two-step transesterification method adopted for biodiesel production. The first acid pretreatment, i.e., esterification is followed by second stage transesterification of esterified oil to reduce the FFA level around 1% (Mohite, S. *et al.*, 2016).

The transesterification process uses the catalyst for carrying out the reaction and could be alkali base, acid, enzyme. In this process, initially, esterification of raw oil is performed and followed by the transesterification of esterified oil. In esterification reaction, the reaction takes place between the carboxylic acid group (free fatty acid) present in the fresh linseed oil and with the alcohol in the presence of an acid (H_2SO_4) catalyst. In this reaction, –OH from the carboxylic acid combine with –H from alcohol and produce an ester of linseed oil and H_2O as a byproduct as given in equation 3.1 and Fig. 3.3 (Jindal & Salvi, 2012; Krishnan & Vasudevan, 2015).

$$\underset{FFA}{R-COOH}+\underset{Alcohol}{R_4OH}\xleftrightarrow[Catalyst]{H_2SO_4}\underset{Water}{H_2O}+R-CO-\underset{Ester}{OH_2C-R_4} \quad (3.1)$$

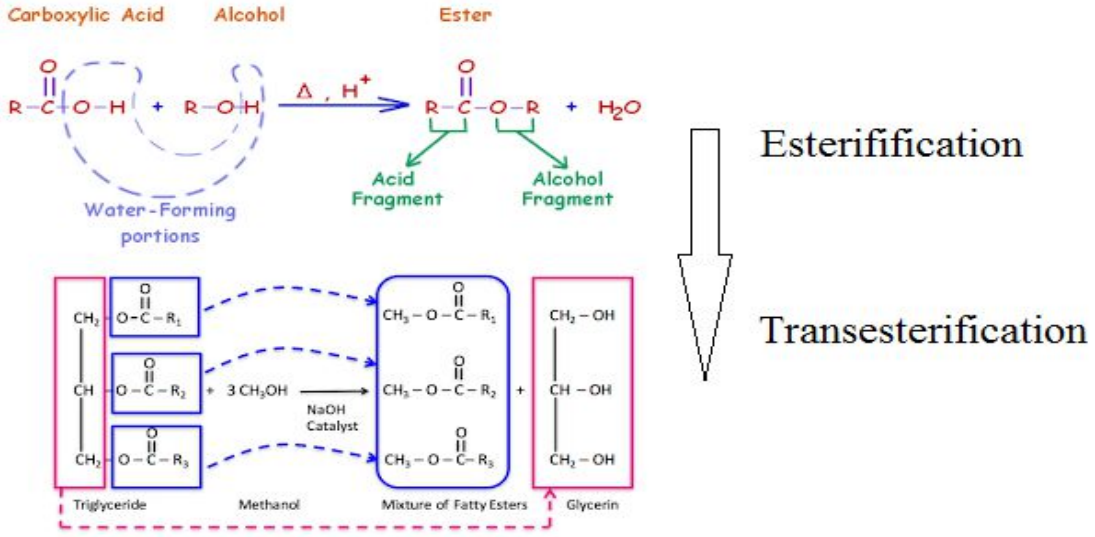

Fig. 3.3 Esterification and transesterification process (Aranda, D. A. G. *et al.*, 2008)

The esterification is neutralization reaction reduces the acid content and adds additional carbon chain. Hence esterified linseed oil has reduced viscosity and increases the cetane number. In esterification reaction, 100 ml of methanol mixed per liter of oil and heated one hour at 60^0 C in the presence of 2.5 ml of sulfuric acid (H_2SO_4) as a catalyst. At this temperature, reaction initiates as shown in equation 1 and form esterified linseed oil. This step followed by transesterification which is a consecutive reversible chemical reaction. In this reversible reaction triglyceride present in the esterified oil/fresh oil converts to diglycerides then monoglycerides known as methyl/ethyl ester or biodiesel (Shahid, E. M. and Y. Jamal, 2011).

The optimization of biodiesel yield from partially processed esterified oil decided by taking the different combination of weight % of NaOH in a fixed amount of esterified oil and methanol heated at 60^0C about one hour for the proper reaction of esterified oil and methanol as represented in the Fig. 3.4. After the reaction, two distinct layers formed the methyl ester of linseed oil at the top and glycerol at the bottom. The different percentage of yield obtained as indicated in Table 3.2. The sample no. 5 has the maximum yield of 85% of biodiesel. This sample's weight proportion of NaOH selected for mass production of biodiesel.

In the process of transesterification, first, the required amount of NaOH flakes and methanol mixed and stirred the solution until the homogeneous solution of methoxide formed. Meanwhile, the esterified oil is stirred and heated around at 60 ^{0}C and then

prepared methoxide poured into heated oil. The solution of methoxide and esterified oil is heated 60 - 65^{0}C and simultaneously stirring at 650 rpm so that reaction should occur. After heating 70-80 minutes, the solution is poured into the separating funnel and kept for 24 hours for settling the glycerol. The settled material at the bottom is the glycerol and above it is the course biodiesel. The coarse biodiesel is water washed two-three times with hot distilled water to remove the any of the soap traces remaining in the biodiesel. Then, after water washing, the biodiesel further boiled at 80 ^{0}C to evaporate the remaining any of the methanol traces in the biodiesel as the methanol has the 60 ^{0}C boiling point. After water washing and boiling, the obtained biodiesel is pure as shown in Fig. 3.4.

Table 3.2 Percentage yield of biodiesel

Sample	Esterified linseed oil (ml)	Methanol (vol. %)	Catalyst (NaOH in %wt.)	Yield (Vol. %)
1	200	20	0.35	80
2	200	20	0.36	80
3	200	20	0.39	75
4	200	20	0.40	66
5	**200**	**20**	**0.50**	**85**

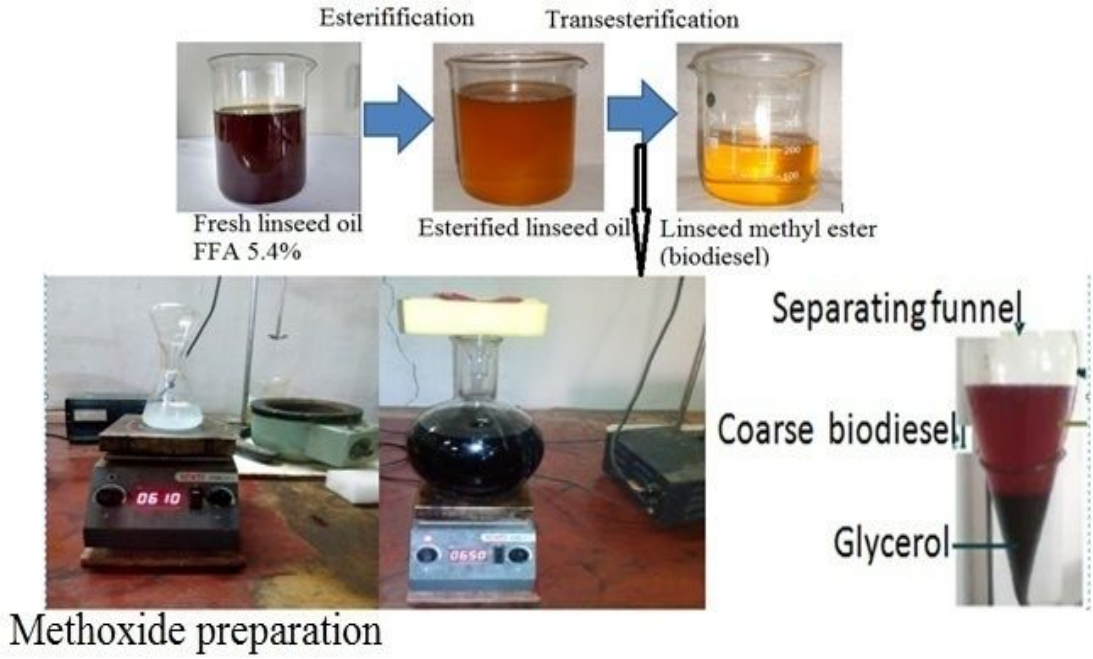

Fig. 3.4 Stages of biodiesel preparation in the laboratory

The neat linseed biodiesel LB100 is mixed with baseline fuel, petro-diesel on the volume basis and prepared the different biodiesel blends for initial primary

investigations. For example, the biodiesel blend LB10 indicates the volume of biodiesel is 10% and remaining 90% is the baseline fuel petro-diesel (PD). Similarly, the different blends of biodiesel prepared as presented in Fig.3.5, and it's physical and chemical properties are determined and tabulated in Table 3.3.

Fig. 3.5 Biodiesel and its different blends

Table 3.3 Properties of petrodiesel, biodiesel and its blends

Properties	Diesel	LB10	LB20	LB30	LB40	LB50	LB100
Density at 40 ^{0}C (kg/m^3)	829	834	842	853	865	877	889
Kinematic viscosity at 40^{0}C (centistokes)	2.68	2.82	3.12	3.3	3.45	3.62	4.22
Flash point (^{0}C)	50	96	102	120	122	132	140
Fire point (^{0}C)	--	102	110	125	130	142	145
Lower calorific value (MJ/kg)	43.5	42.65	42.11	40.83	40.61	38.9	38.3

The purity of the tested biodiesel confirmed with the biodiesel standard for India as per ASTM D6751 as given in Table 3.4. It is found that our neat biodiesel (LB100) is in conformation with ASTM standard.

The ASTM D975-08a, was basically revised to allow the 5% biodiesel in standard petrodiesel. However, the ever-increasing demand for fossil fuel causes a declining its sources, and higher pollution level leads to strict emission regulations for the transport vehicles. This feature has forced the decision makers and researchers to explore a fuel from a sustainable source which produces minimum pollution and should be

renewable like vegetable oil-based biodiesel, alcohols, etc. to replace the conventional fuel shortly.

Table 3.4 Biodiesel standard in India (ASTM D6751) (Giesela Montero, 2011)

Properties	ASTM D6751			Linseed biodiesel (LB100)	
	Test Method	Min.	Max.	Test Method	
Density at 40 ^{0}C (kg/m^3)	ISO 3675 /P 32	860	900	In house	889
Kinematic viscosity at 40^{0}C (centistokes)	ISO 3104 / P25	2.5	6.0		4.22
Flash point (^{0}C) (closed cup)	P21	120	--		140

The vegetable oil-based biodiesel could be the first generation, i.e., edible oil such as coconut, palm, rapeseed, sunflower and second generation (non-edible oil) such as Pongamia pinnata, jatropha curcas, castor, sea mango, neem, mahua, etc. and third generation biodiesel based on microalgae (Katam, G.B. *et al*., 2017).The second or third generation biodiesels does not affect the food security and hence mostly selected for biodiesel production. Therefore, to encourage the agriculture sector, and to ease the fuel shortage, and burden on the economy, India has proposed for blending up to 20% biodiesel and alcohol in transportation fuel by 2017 under the national biofuels policy (Energy, M. of N. & R., 2017).Also, as per the ASTM standard, it is emphasized on energy Independence and security. From detailed literature review, it is already proved that up to 10% linseed biodiesel can be used in unmodified engine satisfactorily. Furthermore, the demand of increase of 20% blend of biodiesel in the petrodiesel, engine or fuel has to modify. We have modified the engine and experimentally showed that in modified engine up to 30% biodiesel can be used with less pollution and improved performance except 10 to 15% penalty on NOx emission.

3.3 Basic experimental setup and methodology

The experimental setup's in photographic view and schematic diagram are as shown in Figs. 3.6 and 3.7 respectively. The experimental investigations conducted with naturally aspirated single cylinder four stroke, variable compression ratio diesel engine. The engine has rated power 3.5 kW at 1500 rpm, bore diameter of 87.5 mm

and stroke length of 110 mm. The capacity of the engine is 0.661liters with connecting rod length of 234 mm.

Fig. 3.6 Photographic view of the experimental setup

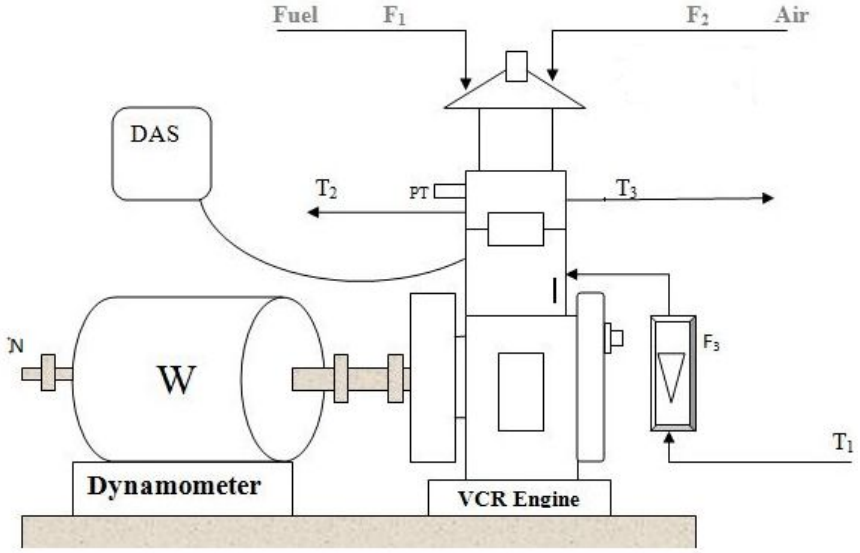

Fig. 3.7 Schematic diagram of the experimental setup

F_1= Fuel flow, F_2 = Air flow, F_3 = Engine cooling water flow, N= Speed of engine in rpm, W = Eddy current dynamometer, PT= Pressure transducer, DAS= Data acquisition system, T_1= Engine inlet cooling water temp.T_2 = Engine outlet cooling water temp. T_3 = Engine exhaust gas temperature

The suitable instruments provided with the experimental setup for measurements of combustion pressure, fuel line pressure, and crank angle. The panel box of the engine

set up consisting of digital temperature indicators, digital voltage indicator, and digital load indicator with load control knob of eddy current dynamometer, air-box with orifice meter for measurement of air flow and graduated glass burette for fuel flow indicator. All these experimentally measured data signals are interfaced with a computer loaded with Labview based data acquisition software "ICEnginesoft" for online performance/combustion evaluation. The strain gauge of 0 – 50 kg loading capacity was coupled to crankshaft for engine loading. The temperature sensors RTD, PT100, and K type thermocouples are used to measure exhaust gas and engine cooling water temperature at various locations with accuracies of ±0.1 ^{0}C. The engine water flow rate adjusted by using suitable rotameter to maintain the engine cooling water temperature around 60^{0}C at the outlet. The combustion pressure and fuel line pressure measured by using the two piezoelectric sensors of range 0 – 5000 PSI and crank angle encoder used for measuring the crank angle with a resolution of 1 degree of crank angle.

The emission parameters measured at variable CRs and load for all tested fuels, using INDUS five gas analyzer (PEA 205N, Make: INDUS).The specification of gas analyzer has tabulated in Table 3.5. The smoke opacity is measured using the NETEL smoke meter model no.NPM-SM-111B in Table 3.6. The five gas analyzer and the smoke meter were also interfaced with the computer for online recording the data.

Table 3.5 INDUS (PEA 205N) Five Gas Analyzer specification

Measurand	Range	Resolution	Accuracy
CO	0 - 15% Vol.	0.01% Vol.	± 0.02% Vol.
CO_2	0 - 20% Vol.	0.01% Vol.	± 0.3% Vol.
HC	0 - 30000 ppm	≤2.000:1ppm vol.	< 2000 ppm vol.: ±4ppm vol.
O_2	0 - 25%	0.01% vol.	± 0.02 % vol.
NO_x	0 - 5000 ppm	1 ppm vol.	± 5 ppm vol.

Table 3.6 Smoke meter specification (NPM-SM-111B)

Parameters	Resolution	Accuracy	Range
HSU	0.1%	-	0-99.9
K	0.01	±0.1 m^{-1}	0- ∞

Initially, all the measurement equipment calibrated for accuracy and reliability of recorded data. In the present work, two lower compression ratios (CR) 14:1, 16:1 and one higher *CR* 18:1 along with the standard *CR* 17.5:1 selected for the experimental investigations. The experimentation performed at *CR* 17.5:1 with petrodiesel as baseline fuel. Further, testing of biodiesel and its blends performed at remaining three *CRs*, i.e., 14:1, 16:1 and 18:1. The injection pressure and timing were kept constant at 210 bar and 23^0 *bTDC* for all observations. Rigorous experimental work was carried out. In each test, before taking the observations, the engine ran for 5 minutes for proper warm-up and stabilizing the set of all working parameters. For reliability and accuracy, a set of observations for output parameters were taken six times for ten cycles each, and the best (less variability) result considered for analysis purpose.

Air consumption is calculated by the using equation 3.2 based on air box with orifice plate and manometer.

$$Air\_flow\_rate(kg/hr) = C_d \times \frac{\pi}{4} \times d^2 \times \rho_a \times 3600 \times \sqrt{2 \times g \times h_w \times \frac{\rho_w}{\rho_a}} \tag{3.2}$$

Where h_w= manometer water column in (m) meter, C_d=coefficient of discharge of orifice, d=dia. of orifice plate in m, ρ_a=density of air at ambient condition in kg/m^3= P/RT, P=Atmospheric pressure in kgf/m^2, R=gas constant =29.27 in kgf.m/kg.^{0}k, T= atmospheric temperature in ^{0}k, ρ_w= density of water in kg/m^3, g=9.81 m/s^2.

The net heat release rate is calculated as per the first law of thermodynamics equations for the fuels from the data collected by the combustion pressure sensor and crank angle encoder (Selvan et al., 2009; Lujaji et al., 2011; Debnath et al., 2012) as given in equation 3.3 and 3.4

$$\frac{dQ_{hr}}{d\theta} = \frac{\gamma}{\gamma - 1} P \frac{dV}{d\theta} + \frac{1}{\gamma - 1} V \frac{dP}{d\theta} + \frac{dQ_{ht}}{d\theta} \tag{3.3}$$

$$\frac{dQ_{hr}}{d\theta} - \frac{dQ_{ht}}{d\theta} = \frac{dQ_n}{d\theta} = \frac{\gamma}{\gamma - 1} P \frac{dV}{d\theta} + \frac{1}{\gamma - 1} V \frac{dP}{d\theta} \tag{3.4}$$

Where $\frac{dQ_{hr}}{d\theta}$ indicates the rate of combustion heat release with crank angle and $\gamma = \frac{c_p}{c_v}$ is the ratio of specific heats, P, V are the instantaneous pressure and volume

of the cylinder measured by the sensors during experimentation, $\frac{dQ_{ht}}{d\theta}$ is the rate heat transfer loss from the cylinder wall by convection, $\frac{dQ_n}{d\theta}$ is the net heat release rate, $\frac{dV}{d\theta}$ is the change of cylinder volume with crank angle and $\frac{dP}{d\theta}$ is the rate of change of cylinder combustion pressure with crank angle.

Similarly, the cumulative heat release rate (Q_{ch}) and in-cylinder mean gas temperature (T_{MGT}) calculated using the following equations 3.5 and 3.6.

$$Q_{ch} = \int_{t_{start}}^{t_{end}} \frac{dQ_{ch}}{dt} dt = m_f Q_{LCV} \tag{3.5}$$

Where t_{start} and t_{end} is the start and end of combustion, m_f is a mass of fuel burned, and Q_{LCV} is the lower calorific value of fuel used (Heywood, 1988).

The in-cylinder mean gas temperature (MGT) has been calculated using the ideal gas law equation, PV= mRT.

$$T_{MGT} = \frac{P.V}{m_{charge}.R} \tag{3.6}$$

Where R is the gas constant and m_{charge} is the mass of charge (fuel plus air) inside the cylinder.

3.4 Results and discussion

Experimental online measured cylinder pressure concerning crank angle for each cycle used for the calculation of all combustion, performance, and emission characteristics. These characteristics have been analyzed for all the biodiesel based fuels at variable *CRs*, % full engine load and compared with baseline *PD* fuel at rated *CR* 17.5.

3.4.1 Combustion characteristics

The combustion characteristics considered for the analysis purpose are cylinder combustion gas pressure, the rate of pressure rise, net heat release rate, cumulative heat release, combustion duration, burning mean gas temperature, ignition delay.

3.4.1.1 Cylinder combustion gas pressure

The nature of variation of in-cylinder combustion pressure (CP) used as a tool to identify the smoothness of operation of compression ignition engine. The fraction of injected fuel burned in the premixed phase of combustion decides the magnitude of peak pressure rise in the compression ignition engine (Heywood, J. B., 1988; Huang, Z. H. *et al.*, 2004).The Fig. 3.8 shows the variation of CP of linseed methyl ester biodiesel (LB) blends at full load at compression ratio (CR) 18:1 and compared with petrodiesel (PD) at rated CR 17.5:1 at the same load. From the figure noticed that the peak pressure for biodiesel is higher, and it is increasing with the fraction of biodiesel in the blends when compared to PD at rated CR. The more elevated CP represents the better ability of the fuel to atomize and mix with air for complete combustion. The CP for LB blends increases with increment of LB in blends with advanced peak combustion pressure due to higher density, viscosity, cetane number, and bulk modulus tends the needle of fuel pump lift early for biodiesel and causes faster pressure wave propagation. The similar kind of results reported by the researchers (Qi, D. H. *et al.*, 2009; Muralidharan, K. and D. Vasudevan, 2011; Amarnath, H. K. *et al.*, 2014).

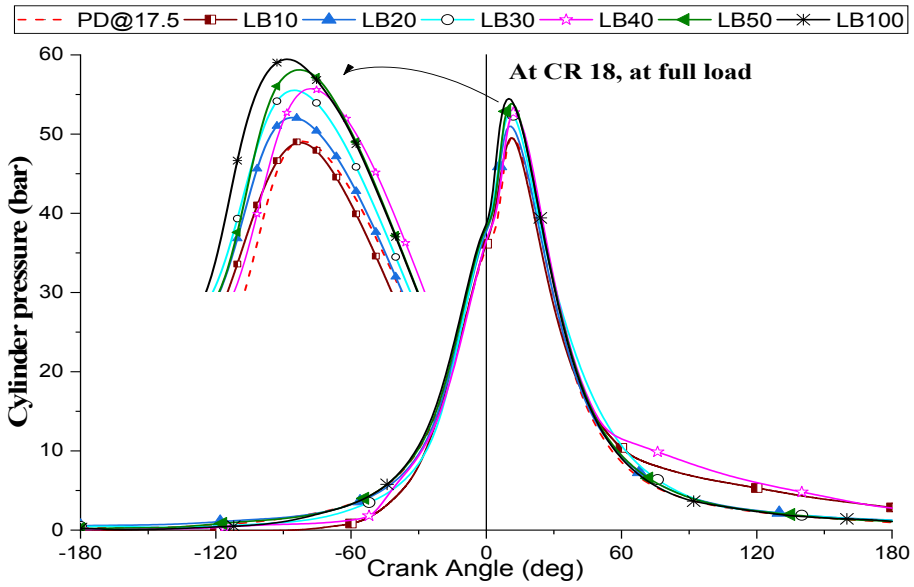

Fig. 3.8 Cylinder gas pressure of biodiesel blends at CR 18 full load

Further the favorable physical and chemical properties and higher operating compression ratio, i.e., 18:1 of biodiesel lead to the higher charge pressure and the temperature inside the cylinder.

The smooth flowability and inbuilt oxygen molecules present in the biodiesel compensates the higher density, viscosity, bulk modulus, low volatility at higher operating CR, and temperature. So initiates the rapid premixed combustion phase by cracking the heavy biodiesel compounds into lighter compounds during the ignition delay period as compared to petrodiesel at rated CR 17.5:1. The noted experimental peak combustion pressure for LB100, LB10, and PD are 50.49 bar at 13^0, 46.99 bar at 14^0, 41.34 bar at 16^0 after top dead center (aTDC) respectively.

The variation of peak combustion pressure of LB blends at different loads and CR varying from 14:1, 16:1, and 18:1 compared with PD at rated CR of 17.5:1 is shown in Fig. 3.9. From the Fig. 3.9, it is inferred that the CP increases with the further addition of load. This increment in CP could be because of the residual gas, wall temperature, amount of injected fuel, and injection duration increases with load. This increased charge temperature and to a lesser extent the charge pressure at injection results in shortening the ignition delay. The Fig. 3.9 (a), depicts the rise in peak CP for biodiesel and blends for operating CR 14:1 and it is increasing with load but less than the PD, which is running at rated CR. Since the biodiesel and blends are operating at relatively lower CR 14:1 attributes the lower charge and wall temperature results in burning inefficiency and relatively lower peak pressure.

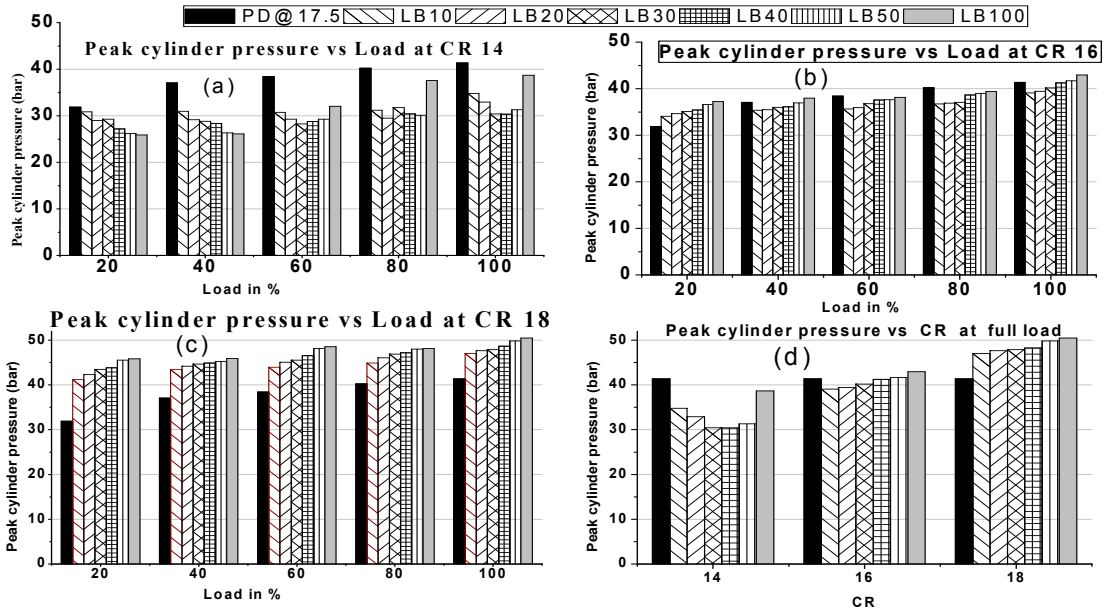

Fig. 3.9 Peak cylinder pressure with load and CR

Moreover, the relatively slower combustion in premixed phase and leads to decrease in CP at lower CR. The peak CP for PD are 31.88 bar, 37.07 bar, 38.42 bar, 40.23 bar,

and 41.34 bar at 20, 40, 60, 80, and 100% loads respectively. Whereas for LB100 these values are 25.89 bar, 26.08 bar, 32.04 bar, 37.56 bar, and 38.68 bar at the corresponding loads. It also observed from Fig.3.9 (a) that at lower loads, i.e., 20% and 40% the peak CP for biodiesel blends is reducing with increment in biodiesel fraction. The charge temperature and pressure are lower at lower loads, leads to improper mixing and atomization with air and hence the reduction in CP for biodiesel and blends. The Fig. 3.9 (b) and (c) show the peak pressure for CR 16:1 and 18:1. In Fig.3.9 (b), the operating pressure is closer to rated pressure of the engine and this increased operating pressure enhances the angle of spray of biodiesel with fine droplets of reduced Sauter mean diameter. This reduced mean diameter and shortened ignition delay improves the mixing of fuel with air and burns smoothly with advanced peak pressure. Similarly, in Fig.3.9 (c), operating pressure further increased to 18:1 for biodiesel, at higher operating pressure viscosity, reduced and ignition delay further get shortened and complete combustion of biodiesel takes place results in higher peak pressure at all loading conditions of the engine. The Fig. 3.9 (d) shows the variations of peak CP of biodiesel and blends at full load with CR. There is a gradual increase in CP at each crank angle (CA) with an increase in CR. This could be because of reduction of cylinder volume and more heat energy gain by the air inside the cylinder during compression stroke with an increase in CR. Consequently, the injected fuel burns rapidly and comprehensively with shortened ignition delay. As a result, at higher CR, smoother combustion is obtained for LB and its blends than PD (Debnath, B. K. *et al.*, 2012). The peak combustion pressure at full load of B10 is 34.8 bar, 39.08 bar, and 46.99 bar at CR 14:1, 16:1, and 18:1 respectively. Similarly for LB100 is 38.68 bar, 42.94 bar, and 50.49 bar at corresponding CR's. Furthermore, it is also seen that increase in CP for each blend at different loads and CR is not uniform, and this could be because of fatty acid methyl ester contents variation in the LB biodiesel blends (Jaichandar, S. *et al.*, 2012; Tesfa, B. *et al.*, 2013).

Therefore, it concluded that as the CR varies from lower to higher value, the CP tends to increase for all fuels under test. This attributed to the fine spray of fuel particles, better mixing of denser fuel charge and complete combustion at higher CR. In the literature similar kind of results reported by the authors (Ozsezen, A. N. *et al.*, 2009; Debnath, B. K. *et al.*, 2012) with canola and palm oil methyl esters in six-cylinder compression ignition engine.

3.4.1.2 Rate of pressure rise

The peak CP and peak rate of pressure rise (RPR) correspond to the amount of fuel burned in the uncontrolled combustion phase (Rajasekar, E. and S. Selvi, 2014). The Fig. 3.10 depicts the RPR at full load of biodiesel blends for a CR 18:1 and with PD for rated CR. The experimental study shows that RPR increases with the amount of biodiesel in the blends with peak value advancing towards the top dead center (TDC) as compared with PD (Hariram, V. and R. Vagesh Shangar, 2015). The higher operating CR of LB and its blends lead to the fine spray particles at a wider angle, higher fuel charge pressure, temperature, and density than PD fuel. In addition to this, a higher value of cetane number of LB blends corresponds to early injection and combustion with relatively shorter ignition delay.

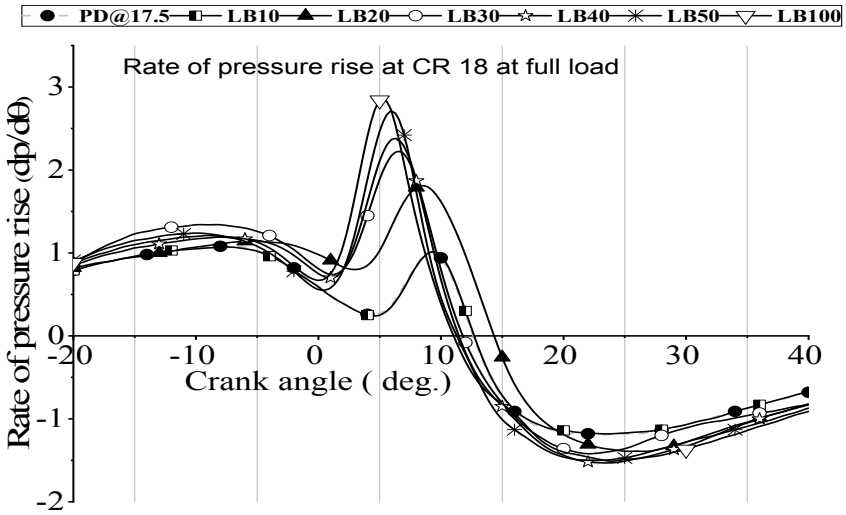

Fig. 3.10 Rate of pressure rise rate at CR 18 full load

The cumulative effects of these physical and chemical properties result in a comparatively larger fraction of mass burned in the premixed combustion phase consequently the RPR increase. The peak value of RPR for PD, LB10, LB20, LB30, LB40, LB50, and LB100 are 1 bar /^{0}CA at 9^0 CA, 1.79 bar/^{0}CA at 9^0 CA, 2.19 bar/^{0}CA at 7^0 CA, 2.37 bar/^{0}CA at 6^0 CA, 2.71/^{0}CA bar at 6^0 CA, and 2.84/^{0}CA bar at 5^0 CA aTDC respectively.

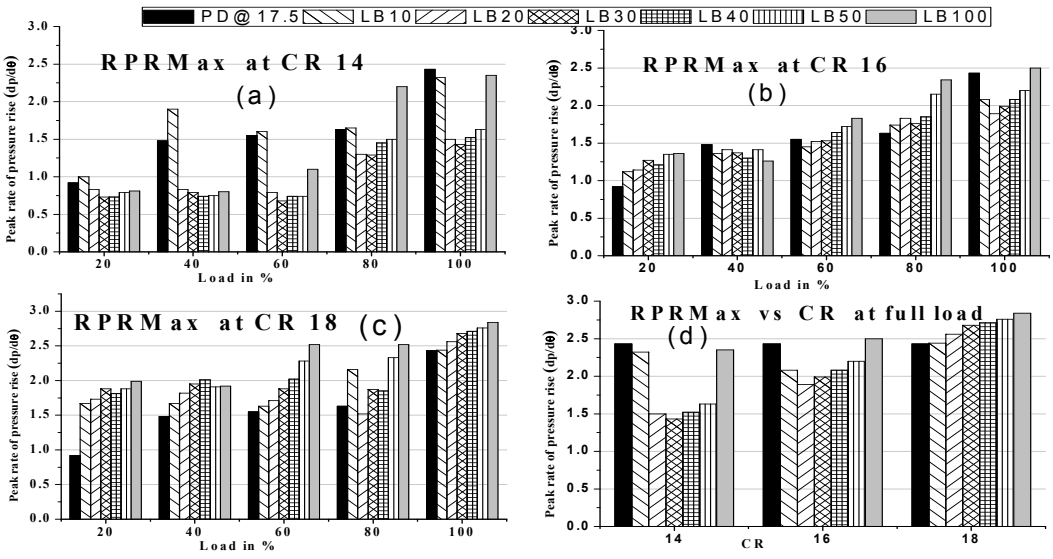

Fig. 3.11 Peak Rate of pressure rise rate with load and CR

The Fig. 3.11 demonstrates the variation of peak RPR with the percentage of load on engine and CR. It observed that the rate of pressure rise increases with increase in engine load, biodiesel fraction, and CR. The synergetic effect of these three parameters improves in-cylinder pressure, temperature and quantity of fuel injected into the cylinder. As a result, the LB blends burns smoothly and efficiently at higher load and CR as shown in Fig, 3.11 (b, c, d) causes the upper value of RPR as compared to PD. However, in Fig. 3.11 (a) which is operating at CR 14:1 result in the lower RPR due to mixing and atomization difficulties for biodiesel. For LB100 the maximum value of RPR is 2.35 bar/^{0}CA, 2.5 bar/^{0}CA, 2.84 bar/^{0}CA at CR 14:1, 16:1, and 18:1 respectively.

3.4.1.3 Net heat release rate

The Fig. 3.12 depicts the net heat release rate (NHR) of LB blends at CR 18:1 compared with PD at CR 17.5 at full load. The baseline PD fuel has higher calorific value (around 13.5% more than biodiesel), greater volatility, lower viscosity, and bulk modulus than LB and its blends. As a result better spray and longer ignition delay of PD during which the relatively more amount of injected fuel mixed with the air. This attributes the significant amount of mixture preparation to ignitable limit and burns the more amount of fuel during uncontrolled combustion phase leads to higher heat release rate (Anand, K. *et al.*, 2008; An, H. *et al.*, 2013).

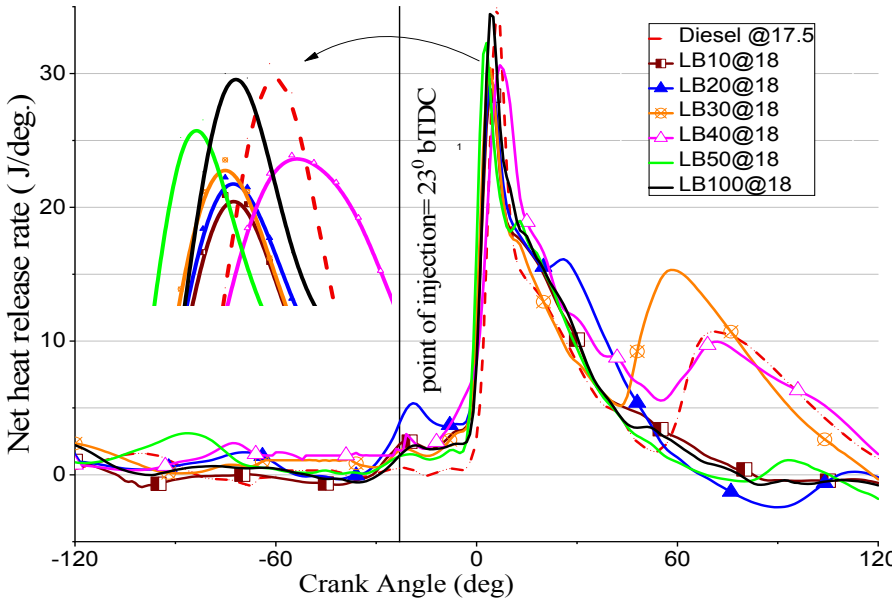

Fig. 3.12 Net heat release rate at CR 18 full load

The NHR of all the LB blends are increasing with the advanced peak with biodiesel fraction but lower than the PD due to lower calorific value. At higher compression ratio, the latent heat of vaporization of biodiesel and its blends increases and therefore, it consumes more heat from surrounding during the ignition delay period for vaporization. The higher cetane number and inbuilt oxygen molecules in biodiesel shorten the ignition delay as compared to PD (Ye, P., 2010).

In spite of lower calorific value, the NHR of biodiesel blends increases from lower to higher blends. This could be because of a higher CR, in-cylinder combustion pressure, temperature, cetane number, and oxygen molecules compensate the higher density, viscosity, and bulk modulus attributes to the complete combustion and higher heat release. The Figs. 3.8 and 3.9 also support this concept of higher NHR for biodiesel blends, which shows the higher CP for blends. The similar kind of results obtained by the researchers for biodiesel blends (Tesfa, B. *et al.*, 2013; Gharehghani, A. *et al.*, 2017). The value of peak NHR for PD, LB50, and LB100 are 41.56 J/^{0}CA at 10 ^{0}CA, 37.56 J//^{0}CA at 6 ^{0}CA, and 39.87 J/^{0}CA at 7 ^{0}CA aTDC respectively.

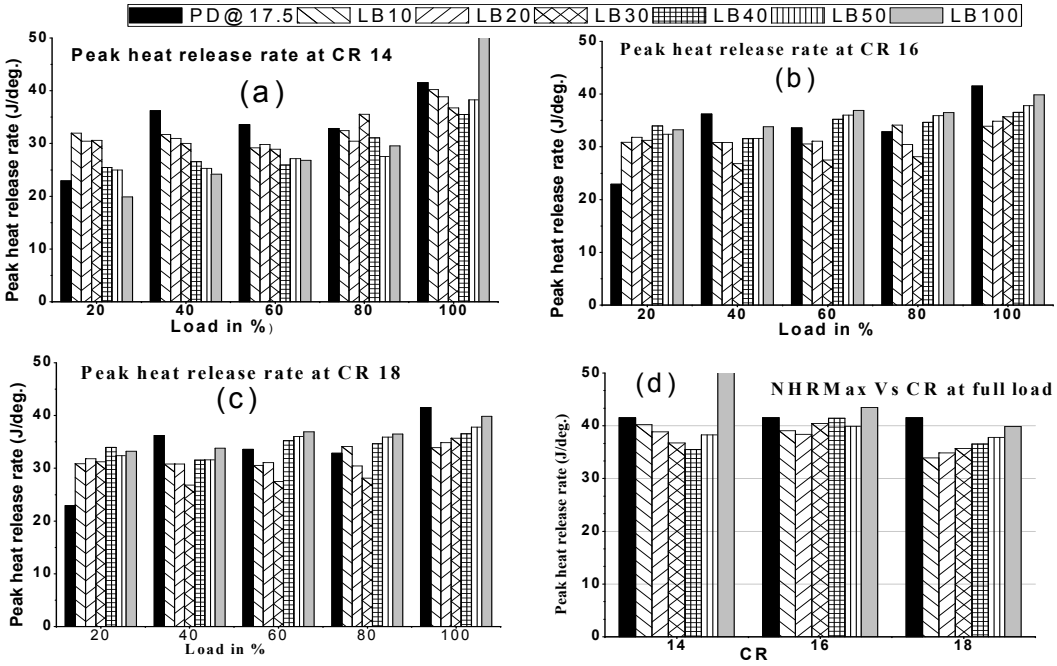

Fig. 3.13 Peak heat release rate with load and CR

The Fig. 3.13 presents the variation of peak instantaneous heat release rate of biodiesel and its blends with an increase in engine load and CR's. The data of heat release rate for PD at rated CR 17.5:1 and compared with the biodiesel blends at different loads and CR's. At lower CR 14:1 the biodiesel and blends have relatively longer ignition delay. Firstly due to higher density, viscosity, and bulk modulus secondly vaporization, atomization and air entrainment difficulties owing to significant accumulated fuel burning (Sharma, A. and S. Murugan, 2015; Singh, B and S. K. Shukla, 2016). With the sudden explosion in the premixed phase of combustion causes a significant amount of pressure rise and net heat release as demonstrated in Fig. 3.13 (a). This substantial amount of LB blends burning compensates and overtakes the higher calorific value of PD fuel. However, this higher pressure rise and net heat release rate occurs away from the TDC (after TDC) during the expansion stroke, and hence the lower heat release sensed by the piezoelectric sensor as shown in Fig.3.13 (a).

For biodiesel and blends, as the CR increases from 14:1 to 18:1, it is noticed that net heat release rate decreases. This could be because of the advanced injection (due to higher density, viscosity, and bulk modulus). The shortened ignition delay for biodiesel blends attributes the lesser quantity of mass burns in the premixed combustion phase, and most of the mass burn in the mixing control combustion (diffusion) phase smoothly and remaining in the late combustion phase. The peak

NHR increases with blends but decreases gradually as CR changes from 16:1 to 18:1 as shown in the Fig. 3.13 (b & c), (Nagaraja, S. *et al.*, 2012). The latent heat of vaporization is a function of operating pressure. At higher CR, the increased latent heat of vaporization of biodiesel and blends absorbs more heat from the surrounding inside the cylinder during premixed, and diffusion combustion phase causes the reduction in the peak NHR as compared to the PD operating at rated CR 17.5:1.

The value of peak NHR for LB100 at CR's 14:1, 16:1, and 18:1 are 61.84 bar at 12^0 CA, 43.49 bar at 11^0 CA, and 39.87 bar at 7^0 CA respectively and for PD at rated CR17.5 is 41.56 bar at 10^0 CA aTDC as shown in Fig.3.13 (d).

3.4.1.4 Cumulative heat release

The total cyclic cumulative heat release has been calculated using the equation 3.5. It is merely the total summation of heat released by the quantity of fuel burned during the start to the end of combustion. The Fig. 3.14 depicts the cumulative heat release (CHR) for LB and its blends at CR 18:1 and PD at rated CR 17.5 at full load. Given figure indicates that peak CHR for baseline data (PD) is less than the LB and its blends. It also observed that a particular load and CR, the peak CHR increases and delayed (i.e., away from the TDC) with the fraction of biodiesel in the blends.

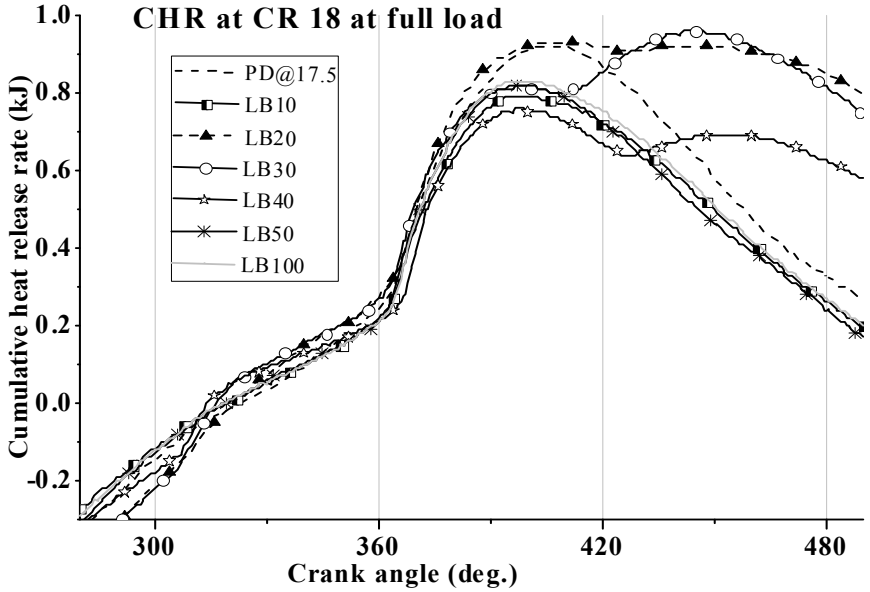

Fig. 3.14 Cumulative heat release at CR 18 full load

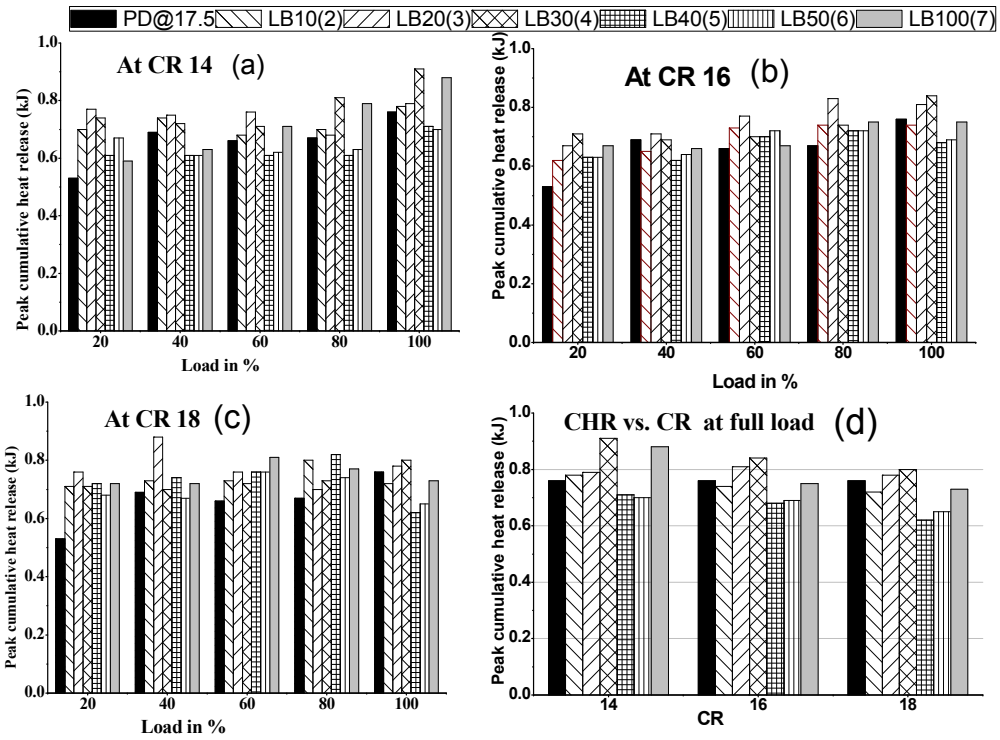

Fig. 3.15 Peak cumulative heat release rate with load and CR

This could be because of shortened ignition delay and presence of inbuilt oxygen in the LB blends burns, the relatively smaller quantity of fuel with lesser duration of premixed combustion phase as compared to PD. This smaller quantity of fuel and lesser duration in premixed combustion phase leads to remaining more quantity of fuel burn in the mixing control combustion phase with longer duration. This effect of combustion phenomena results in the lesser cumulative heat release (%) in premixed phase and more cumulative heat release (%) in the second phase of combustion (Benjumea, P. and J. R. Agudelo, 2010; Ma, F. *et al.*, 2015). However, this higher cyclic heat release for LB blends in the second stage of combustion could not be converted into useful shaft work (brake power) due to its occurrence away from the TDC, i.e., during the expansion stroke. Hence the contribution of later stage combustion for shaft work is very less. The similar kind of investigations reported by the researchers (Puhan, S. *et al.*, 2009b; Tesfa, B. *et al.*, 2013; Pali, H. S. and N. Kumar, 2017).

The Fig. 3.15 (a-c) shows the variation of cumulative heat release with engine load (%) at different CR's (14:1, 16:1, and 18:1) and Fig.3.15 (d) with CR at full load for LB blends and baseline data (PD) at rated CR 17.5:1. The figure shows the rise in CHR with an increase in biodiesel fraction and declines with add to in CR. As the engine

load augmented from 20% to 100%, CHR increases for all fuels at all CR's due to increase in the injection duration and injected mass of the fuel and observed increment is more for LB blends at all CR than PD which is operating at rated CR (Agarwal, A. K. and A. Dhar, 2013; Parida, M. K. and A. K. Rout, 2017). Fukang Ma et al. (2015) reported the total increase in CHR dominated by the heat release during the diffusion of combustion than the premixed phase. The CHR decrease with increase in CR due to the amplified latent heat of vaporization as shown in Fig. 3.15 (d).

3.4.1.5 Ignition delay and combustion duration

The Fig.3.16 depicts the effects of engine load, the fraction of biodiesel in the blends and the CR's on the ignition delay (ID) and combustion duration (CD). The ID defined as the CA interval between the point of fuel injection and a start of combustion point in the cylinder. In this study, the ID is the difference in corresponding CA of peak RPR and peak fuel line pressure, and CD is in between corresponding CA of peak RPR and peak CHR (Gumus, M., 2010). From the Fig. 3.16 (a), it is observed that at fixed CR, the ID decreases with increase in load for all fuels. The ID for PD is more as compared to all biodiesel blends, and it is lessening with the fraction of biodiesel in the blends. The increased temperature and pressure could be the reason for the reduction of ID at higher loads, and cetane number, the oxygen content in the blends causes the further reduction of ID for blends. The decrease of ID for LB blends at fixed CR, varying from 30% to 43% as compared to PD at rated CR.

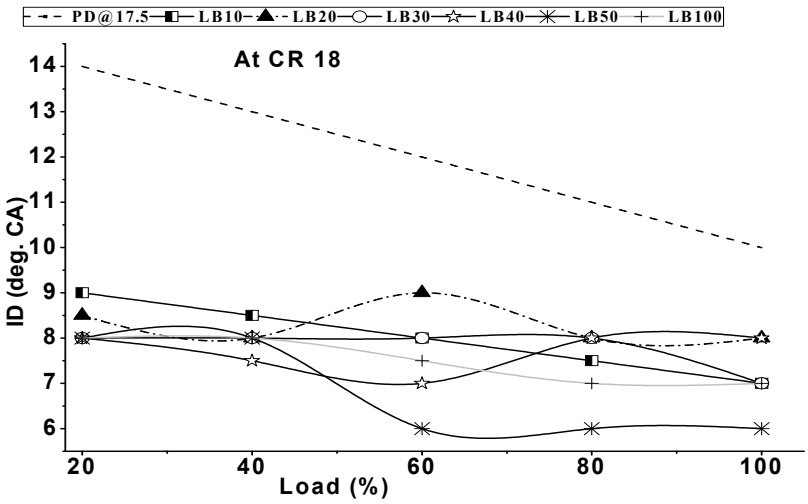

(a) Variation of ignition delay with engine load (%) at CR 18:1

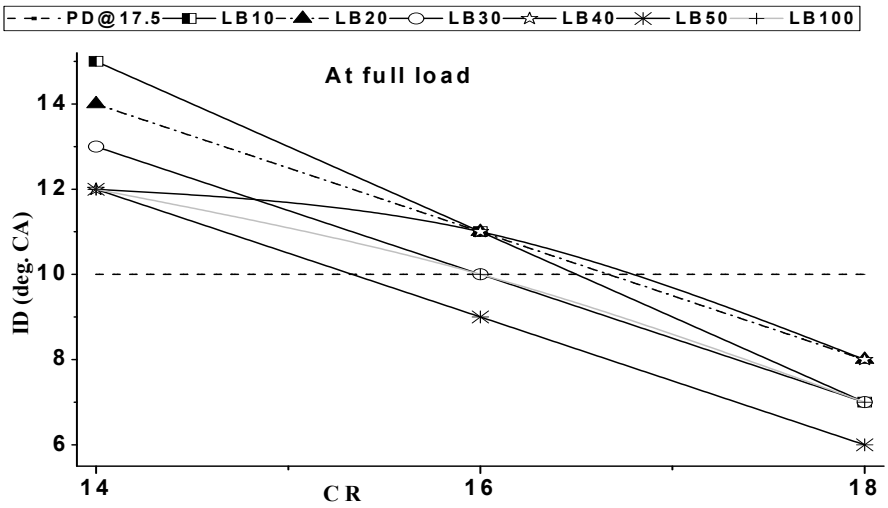

(b) Variation of ignition delay with CR at full load

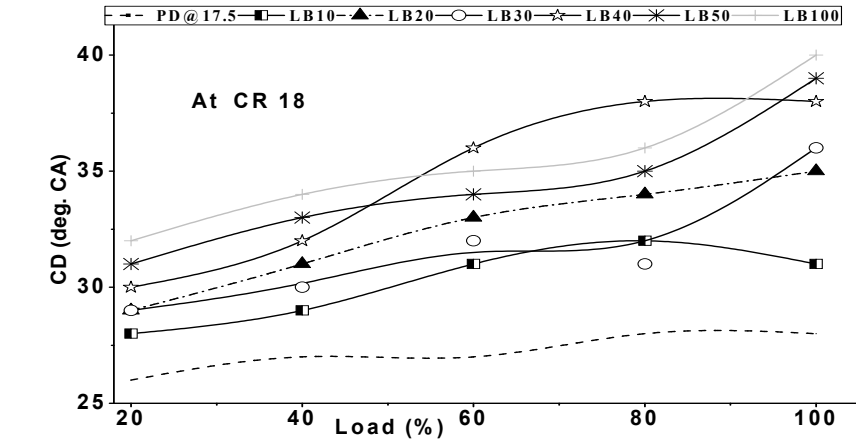

(c) Change of combustion duration with engine load (%) at CR 18:1

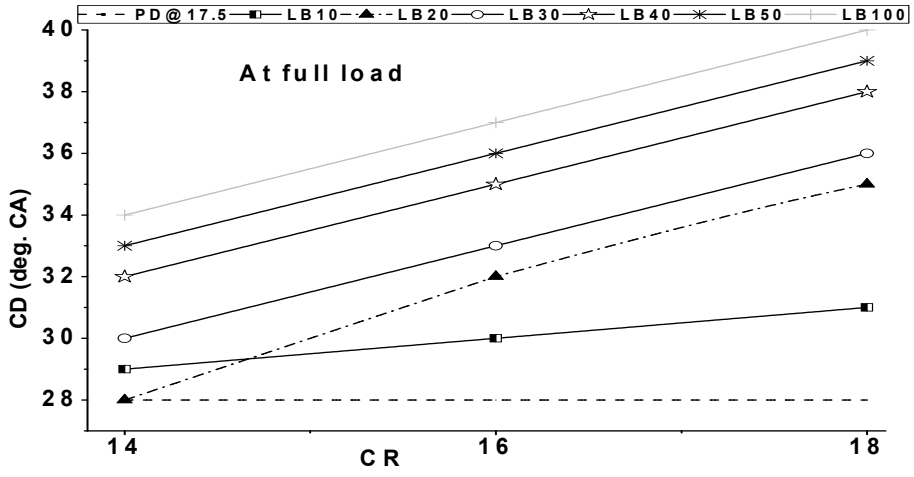

(d) Variation of combustion duration with CR at full load

Fig. 3.16 Variation of ignition delay and combustion duration with load and CR

At fixed load, the ID also decreases with the variation in CR from 14:1 to 18:1. The authors also reported the same results (Banapurmath, N. R. *et al.*, 2008; Sakthivel, G.

et al., 2014; Sakthivel, G. and M. Ilangkumaran, 2017). It is observed from Fig. 3.16 (b), that ID is more at CR 14:1 and further decreases with CR 16:1, 18:1 for LB blends as compared PD. This reduction in ID attributed due to increase in the energy activation at higher CR and at lower CR difficulties in mixing and atomization with air results in more extended ID. The ID for LB and its bends are higher by an average 30% at CR 14:1 and 3.3% at CR 16:1 and decreased by 28.3% at CR 18:1. At fixed CR, the changes of CD concerning amount (Fig.3.16 (c)) and at fixed load; the variations concerning CR (Fig.3.16 (d)) are presented in the figure. The amount of fuel injected into the cylinder increases with load and ID decreases. The amount of fuel burns less in premixed phase (due to reduced ID). Moreover, the remaining amount of fuel takes more time to evaporates and atomize (due to the higher value of density, viscosity, and bulk modulus) in diffusion combustion phase lead to increase in the CD with load and fraction of biodiesel in the blends.

The average increase in CD for LB and its blends was varying from 15% to 30%. At fixed load (full), with CD increases with CR and fraction of biodiesel in the blends and it is higher as compared to PD. The ID and amount of fuel injected decreases with CR. However, the CD increases with the fraction of biodiesel and CR, due to the efficient and smooth burning of fuel at higher CR as also seen from the CHR variation from figures 3.13 and 3.14 and combustion ends away from the TDC. It observed that increase in an average CD from 11% to 30% at fixed load concerning CR as compared to PD at rated CR.

3.4.1.6 Combustion mean gas temperature (MGT)

The combustion mean gas temperature calculated as per ideal gas law using the equation 3.6. The Fig. 3.17 demonstrated the variation of in-cylinder combustion mean gas temperature with the load on the engine at fixed CR. The figure shows the MGT for PD is less than the LB and its blends and it is increasing with engine load and the fraction of biodiesel in the blends. As explained in the former section, with an increase in LB fraction in the blends the ID is lessening, and the fraction of injected fuel burns more in the diffusion combustion phase. This increased amount of fuel burning in the latter stage of combustion leads to higher amount CHR with increased CD results in a rise in the MGT with peak value slightly advanced (Singh, B. and S. K. Shukla, 2016).

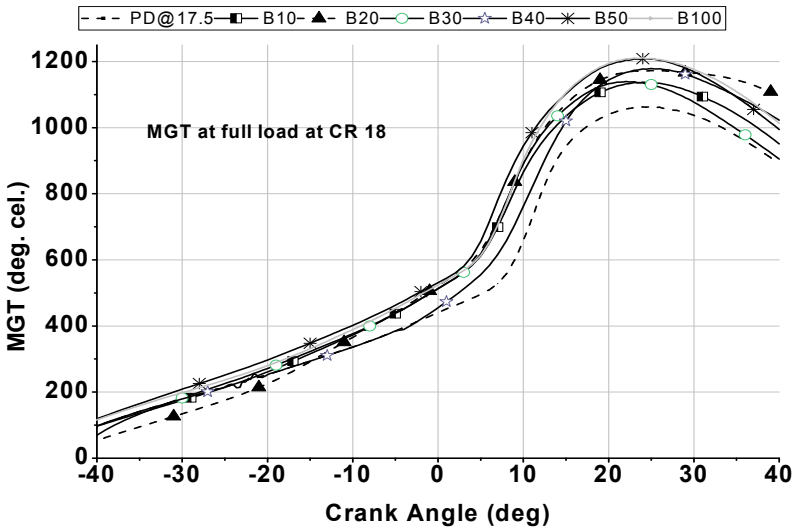

Fig. 3.17 Combustion cylinder means gas temperature at CR 18 full load

The maximum value of MGT for PD, LB10, LB20, LB30, LB40, LB50, and LB100 are 1063.31 0C at 25 0CA, 1137.65 0C at 24 0CA, 1173.2 0C at 25 0CA, 1139.73 0C at 22 0CA, 1179.24 0C at 25 0CA, 1208.98 0C at 24 0CA, and 1211.19 0C at 24 0CA respectively. This higher MGT for LB blends shows the better combustion at higher CR 18:1.

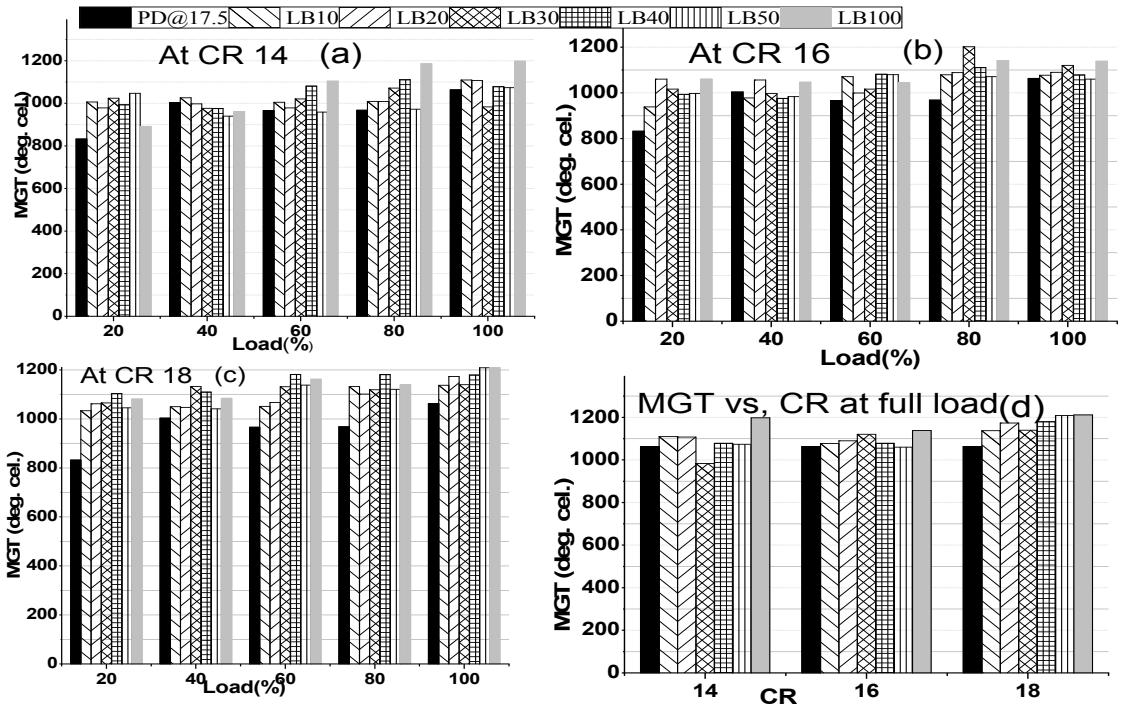

Fig. 3.18 Variation of MGT with load and CR

The maximum MGT is 13% higher for LB100 as compared to PD. The variation of the peak value of MGT with load and CR as illustrated in the Fig. 3.18 (a-d). Given figure

reports that the peak value of MGT gradually increases with engine load, a fraction of biodiesel in the blends, and CR.The Fig.3.18 (a-c) shows the variation of MGT with engine load (%) at different CR's (14:1, 16:1, 18:1) and Fig.3.18 (d) with CR at full load for LB blends and compared with baseline data (PD) at rated CR 17.5:1. The Figs.3.18 (a-c), shows the rise in MGT with an increase in biodiesel fraction and but decreasing trend is observed with rise in CR. As the engine load augmented from 20% to 100%, MGT increases for all fuels at all CR's due to increase in the injection duration and a mass flow rate of the fuel. This results, more amount fuels burns in latter stage of combustion leads to higher MGT. This MGT rise is more for LB blends at all CR due to improvement in diffused combustion. However, reverse trend is observed in Fig.3.18 (d) due to reduced ignition delay and combustion duration and mass of fuel injected as well results in reduced MGT with higher CR.

3.4.2 Performance characteristics

3.4.2.1 Brake thermal efficiency (BTE)

The brake thermal efficiency defined as the brake power as the function of heat energy input of fuel in the internal combustion engine. This term uses to assess, how efficiently the engine converts the heat energy released by fuel in combustion chamber into useful mechanical energy.

The BTE of PD at CR 17.5 is compared with all the biodiesel blends and neat biodiesel at varying loads and CRs as depicted in the Fig. 3.19. In Fig. 3.19(a), the biodiesel and blends are represented at CR 14:1, it is found that the BTE of biodiesel blends increases with load and decreases with the proportion of biodiesel in the mixtures. With increasing the biodiesel fraction in the blends, the density, and viscosity increases and reduces the heating value, results in improper mixing and atomization with air. The overall impact of all these factors leads to lesser energy conversion efficiency of fuel in the cylinder results in the reduction of BTE. With increasing the load, in-cylinder pressure and temperature increases which improves the combustion of biodiesel fuels consequently increases the BTE. The BTE at full load of baseline fuel PD at rated CR is 26.37%, and neat biodiesel is 23.63% and for LB30 is 26.14%. Therefore, the maximum reported reduction was 10.4% for neat biodiesel and minimum0.9% for LB30, as compared to baseline fuel. The further improvement observed in the BTE of biodiesel blends at CR 16:1 as shown in Fig. 3.19(b). This

compression ratio is lower but nearer to the rated CR. Hence the increased in-cylinder pressure, temperature and inbuilt oxygen in the biodiesel, burn the fuel more efficiently and improves the BTE's of neat biodiesel and its blends.

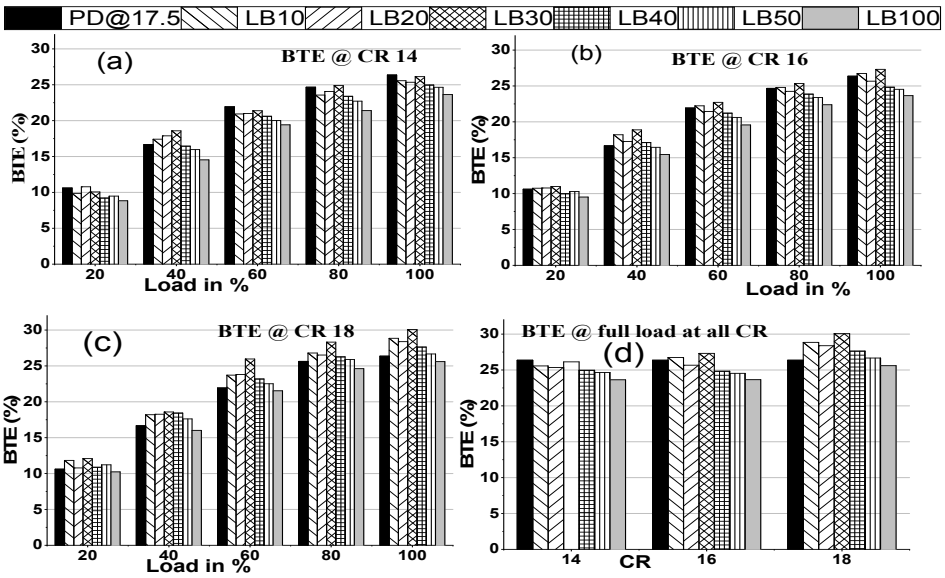

Fig. 3.19 Variation of brake thermal efficiency at three CRs

The BTE's of LB10 and LB30 are 26.73%, and 27.32% respectively. Thus there is an improvement of 1.4% for LB10 and 3.4% for LB30. At CR 18:1, as presented in Fig. 3.18 (c), due to the higher value of CR, an enhancement in BTE's of biodiesel blends has been reported except for neat biodiesel LB100. The maximum improvement of 14% for LB30 and 9.5% observed for LB10 at this CR. The Fig. 3.19 (d) depicts the variation of the BTE's of fuels at full load at varying CR's. At fixed load, the BTE increases with CR and decreases with the biodiesel fraction in the blends (Ananthakumar, S. *et al.*, 2017). The blends LB10, LB20, and LB30 show better performance as compared to PD. Furthermore, LB30 gives the higher BTE due to better combustion.

3.4.2.2 Brake specific fuel consumption (BSFC)

It is the measure of the fuel efficiency of compression ignition engine which gives the quantity of fuel consumed for producing the unit brake power. It used for comparing efficiencies of the engines. Fig. 3.20 shows the variation of BSFC for all tested fuels at different loading conditions and CRs. The BSFC decreases with increase in load and CR for all fuels. At increased load and CR, the heat loss from the engine reduces and

increases in-cylinder pressure and temperature. These three are favorable conditions for better combustion of fuel; as a result, the engine burns a lesser quantity of fuel for producing the unit brake power. Hence the fuel consumption increases with increasing load and decreasing with CR. Again at all loads and CR's, the BSFC increases with fraction biodiesel in the fuel blends. This is because of higher viscosity, density, and bulk modulus of increased proportions of biodiesel in the blends. Since the fuel a pump injects the fuel on a volume basis, hence for the same volume, denser fuel gets injected more quantity in the cylinder. These findings reported at the CR's 14 to 18. At CR 14-18, at full load, the maximum percentage increase in the BSFC for LB100 is 17.6%, 14.7%, and 8.8% respectively as compared to baseline fuel PD. The improvement in BSFC of LB10 has been observed 3 -12 %, whereas it is reported up to 4-6% by authors Jindal S and Salvi BL (Jindal, S. and B. L. Salvi, 2012).

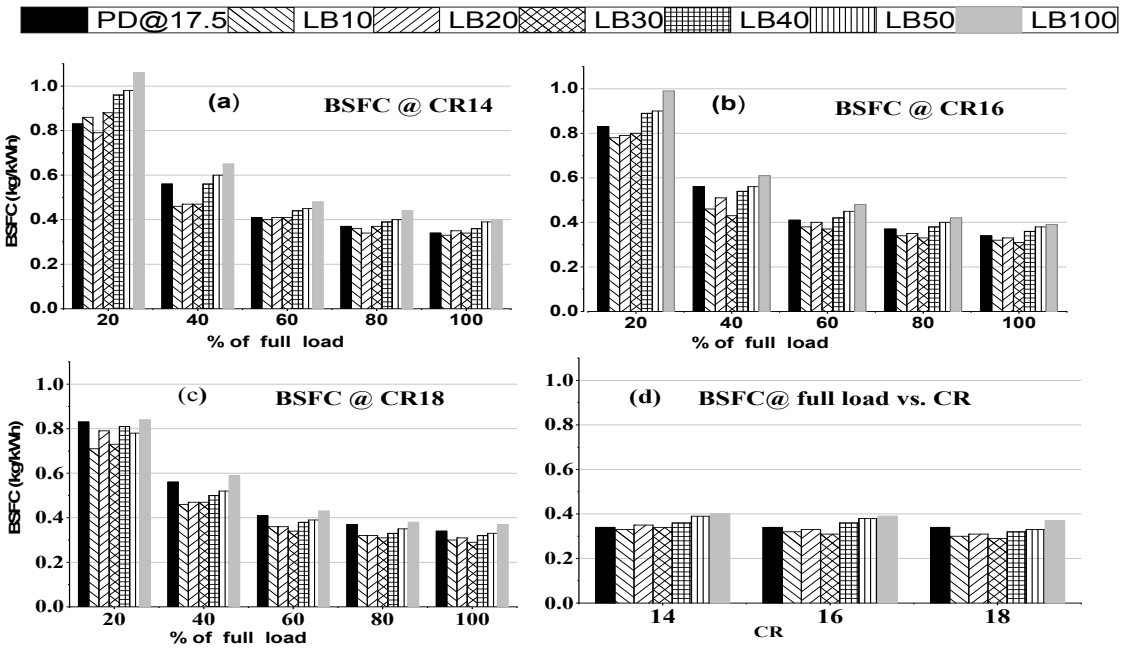

Fig. 3.20 Variation of brake specific fuel consumption at three CRs

3.4.2.3 Exhaust gas temperature (EGT)

The fuel consumption increases, with relatively more prolonged duration of fuel injection to maintain the increased power due to increase in load (Heywood, J. B., 1988). The Fig. 3.21 depicts the variation of EGT for all fuels with load and CR. From the figure noted that EGT increases with a rise in load and amount of biodiesel in the fuel blends (Raheman, H. and S. V. Ghadge, 2008) and decreases with CR. At increasing load, the rise in cylinder pressure, temperature, and minimization of heat

losses to the cylinder wall result in a higher temperature at the exhaust. At CR 18 (Fig. 3.21 (c)), EGT of fuel blends up B40 is lower than the baseline fuel. This attributed due to higher in-cylinder temperature, pressure, and shortened ID. Further supported by oxygen molecules for complete combustion (Debnath, B. K. *et al.*, 2011; Jindal, S., 2011; Raj, M. T. and M. K. K. Kandasamy, 2012; Balakrishnan, N. *et al.*, 2013). At low CRs 14-16 (Fig. 3.21 (a-b)) difficulty in the mixing and atomization of biodiesel fuel blend and causes the incomplete combustion and a higher EGT. At lower CRs, the ignition delay is longer, and amount of fuel mixed with air within combustible limit is more. Hence the more amount of fuel burns in premixed combustion phase leads to higher temperature and causes the higher EGT and vice versa (Sakthivel, G *et al.*, 2014) when compared with baseline fuel PD.

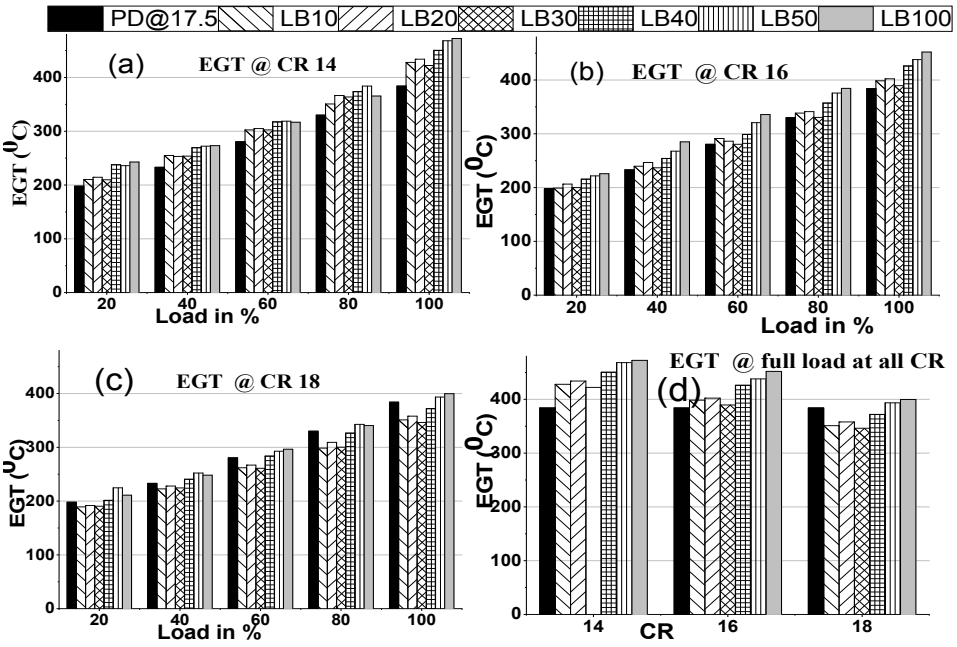

Fig. 3.21 Variation of EGT with load and CR

At higher CR, combustion takes place at low temperature due to shortened ignition delay and presence of oxygen molecules ensuring the complete combustion, results in the lower EGT. At full load, baseline fuel PD has the EGT 383.931^{0}C and at CR 14, LB10, LB20, and LB30 has EGT of 428.071 ^{0}C, 434.025 ^{0}C, 422.33 ^{0}C respectively i.e. 11.5 %, 13% and 10% higher. At CR 16, EGT of LB10, LB40, LB50 has 4%, 14% and 18% higher value whereas it is reduced by 8.6%, 6.8% and 9.8% for LB10, LB20, and LB30 respectively at CR 18 as demonstrated in Fig. 3.21 (d). Moreover, it is also

noticed that minimum EGT are in good agreement with engine operating conditions which has maximum BTE and minimum BSFC (Figs. 3.19 and 3.20).

3.4.3 Emission characteristics

3.4.3.1 Emission of carbon monoxide (CO)

The Fig. 3.22 shows the variation of emission of carbon monoxide concerning the load and CR. At low load condition, the in-cylinder pressure and temperature are not sufficient to breaks fuel droplets; also the air-fuel mixture too lean to make complete combustion leads to the higher emission of CO. At higher loads the blend is rich, and each particle could not get the sufficient oxygen for combustion (Debnath, B. K. *et al.*, 2012, Mahanta, P. *et al.*, 2006). It varies descending to ascending fashion from 20% load to full load and emission of CO lessening with an increase in CR and increases with the increase in biodiesel percentage in the blends. The cylinder combustion temperature rather quite low at lower loads for complete combustion and as the load mounting, the quantity of fuel injected into the cylinder is higher. Consequently, the emission of CO is high at low load and relatively elevated value at higher load (Ananthakumar, S. *et al.*, 2017). At lower CRs 14-16, all the fuel blends have a higher emission of CO due to combustion problems than the baseline fuel as reported in the Fig. 3.22 (a,b).

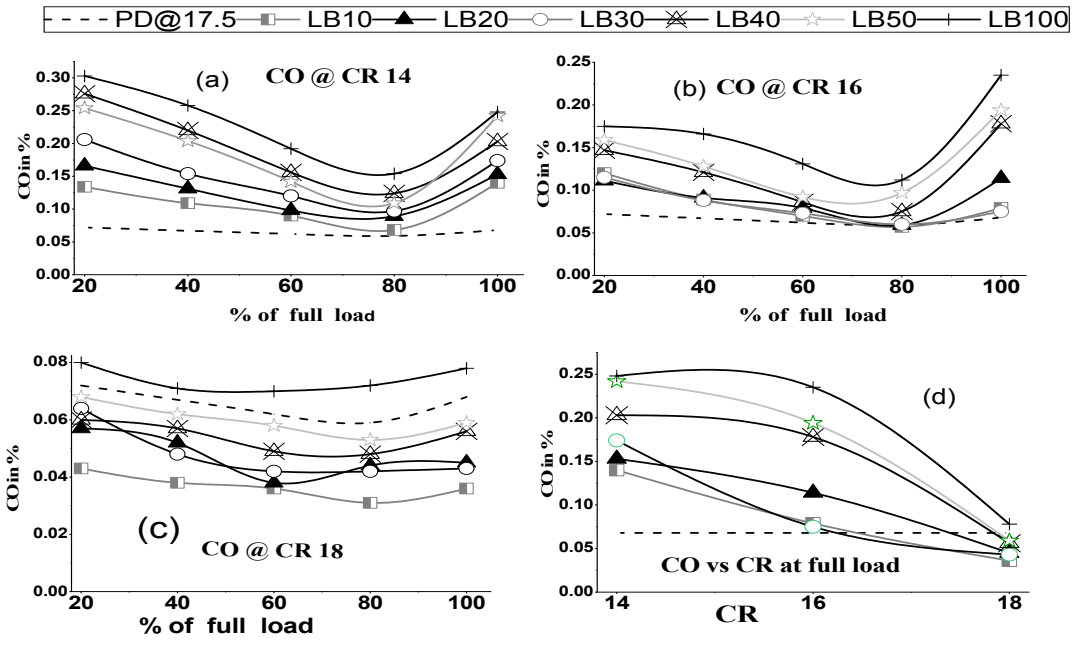

Fig. 3.22 Variation of CO emission with load and CR

The emission of CO has been improved a lot and reduction of emission observed at higher CR 18 (Fig. 3.22(c)). At full load, maximum reductions of emission of CO is 47% for LB10 and 34%, 38%, 18%, and 13% for blends LB20 to LB40 respectively at CR 18.

3.4.3.2 Emission of hydrocarbon (HC)

The trend of variation of emissions of HC is following the emission of CO and for the same reason. From the Fig. 3.23, it is explicitly examined that emission of HC for baseline fuel is slightly varied and increase with load. The HC emission rises with the content of biodiesel in the blends and decreases with increase in CRs. At CR 14, the HC emission is very much high as compared baseline fuel PD. At CR 16, it is higher but quite comparable, and at CR 18 reduced for biodiesel blends except for neat biodiesel. This variation of HC emission reflected by reduced CO and increased NOx. The maximum reduction observed of HC emission at full load at CR 18. The percentage reduction for LB10-LB30 noted as 40.37%, 22.02%, and 26.61% respectively as compared to the PD.

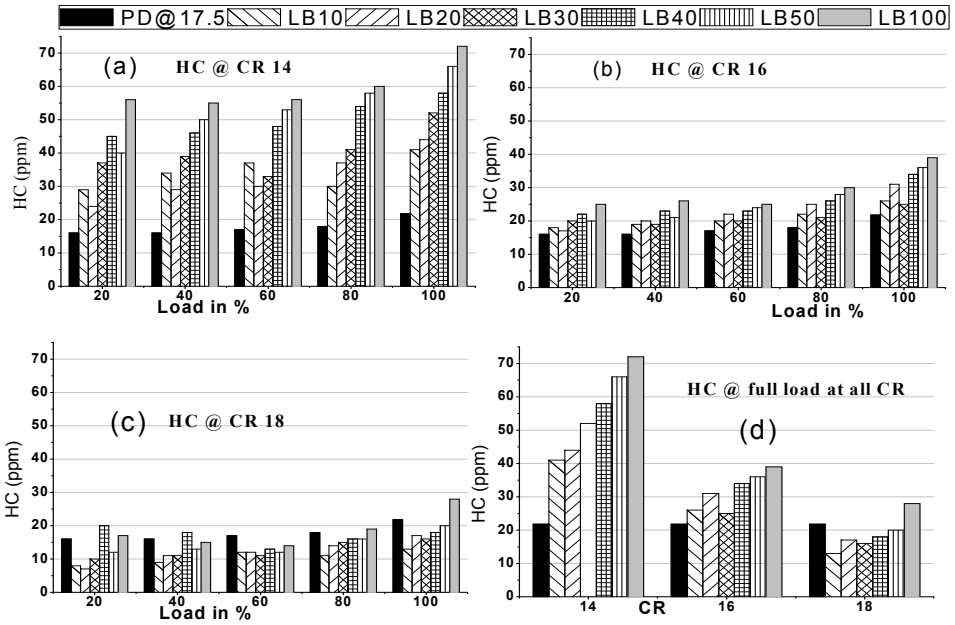

Fig. 3.23 Variation of HC emission with load and CR

3.4.3.3 Emission of oxides of nitrogen (NO_x)

The Fig. 3.24 shows the variations of NOx emissions against load and CR.It increases with a load for baseline fuel due to increased pressure, and temperature burning takes place relatively better. The presence of oxygen content in biodiesels blends leads to the higher amount of NOx emission than PD. The higher content of oxygen during combustion in biodiesel leads to higher combustion temperature and at this high-temperature, nitrogen from air readily combined with oxygen and forms compounds like nitrogen oxide and nitric oxide (Amarnath, H. K. and P. Prabhakaran, 2012). The emission of NOx for biodiesel blends rising to blend LB30, and then it decreases for higher blends of biodiesels at all testing loads and CRs. This variation of NOx emission could be due to the relatively better combustion of blends up to LB30. The higher blends may not have the proper mixing and atomization as compared to the lower blends. At higher CR, the in-cylinder temperature, pressure and reduced loss of heat from cylinder walls easily break the biodiesel blends droplets into fine particles. Each particle exposed to sufficient oxygen of surrounding air along with inbuilt oxygen burns fuel entirely with higher temperatures and forms the more NOx as compared to the blends at lower CR, and baseline fuel at rated CR.

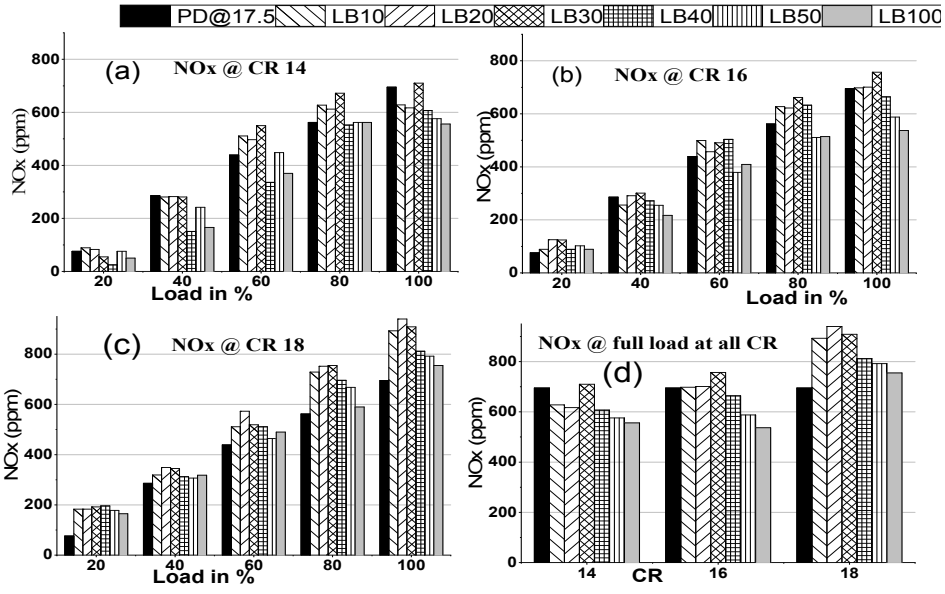

Fig. 3.24 Variation of NOx emission with load and CR

At CR 18, all fuel blends have higher NOx than the baseline fuel PD due to higher temperature, pressure and shortened ignition delay; all fuels burn at high temperature

enhance the NOx formation. At CR 16, blends B10, B20, and B30, B40 showed a more elevated amount of NOx and also at CR 14, blends B10, B20, and B30 have more NOx as compared to diesel fuel. The higher NOx of blends due to the better combustion and confirmed with higher BTE and lower BSFC of these blends. At full load and CR 18, the emissions of NOx was higher for LB10, LB20, and LB30 by 28.5%,35.25%, and 30.8% respectively as compared to PD fuel operated at rated CR.

3.4.3.4 Emission of carbon dioxide (CO_2)

The Fig. 3.25 presents the variation of carbon dioxide emission with different loads and CRs for all fuels. The all tested fuels emission of CO_2 increases with load and volume of biodiesel in the blends and decreases with compression ratios. The emission of CO_2 of biodiesel and its blends is more than baseline fuel at all CRs, and it is higher at lower CRs and vice versa.

The complete combustion of fuel means most of the available carbons converted into carbon dioxide and led to more amount of CO_2 discharge (Muralidharan, K. and D. Vasudevan, 2011). At lower CR 14-16, the neat biodiesel and its blends burn with longer ignition delay and inject the more amount of fuel. Due to more extended ignition delay biodiesel blends burns more amount of fuel and away from the TDC and results with more CO_2 emission.

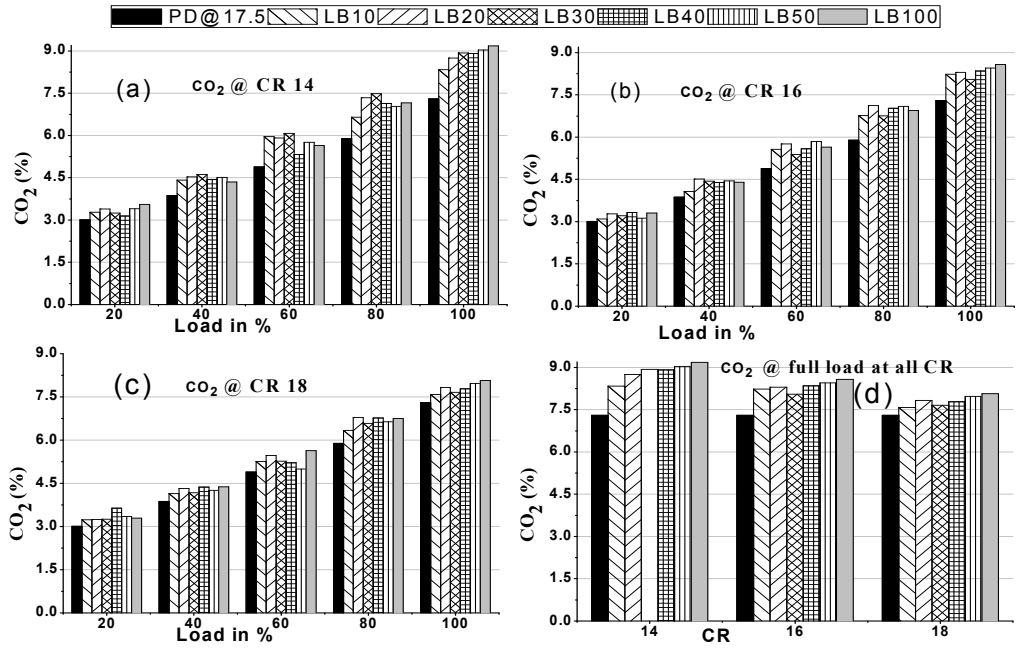

Fig. 3.25 Variation of CO_2 emission with load and CR

This higher emission of CO_2 further supported by the higher EGT, BSFC, and lower BTE. As the fraction of biodiesel increases in the blends means more molecules of oxygen are available for further improving the combustion and results in more amount of CO_2 emissions (Sakthivel, G *et al.*, 2014). From the Fig.3.25 (d), at full load, it is observed that amount of CO_2 decreases with increase in CRs, due to the reduction of biodiesel consumption with the increase in CR, in spite of better combustion and it relates with lower BSFC. As compared to the baseline fuel PD, the higher emission of CO_2 for blend LB10 at CRs 14, 16, and 18 are 14.25%, 12.74%, and 3.84% respectively. Whereas for neat biodiesel LB100 these values are 26%, 17.5%, and 10.6% higher amount of CO_2.

3.4.3.5 Emission of smoke

The smoke is the visible emission at the exhaust of internal combustion engines. This smoke may contain many tiny particles of unburnt carbon particle of the fuel. The emission of smoke occurs mainly due to incomplete combustion of fuels in the engine's combustion chamber.

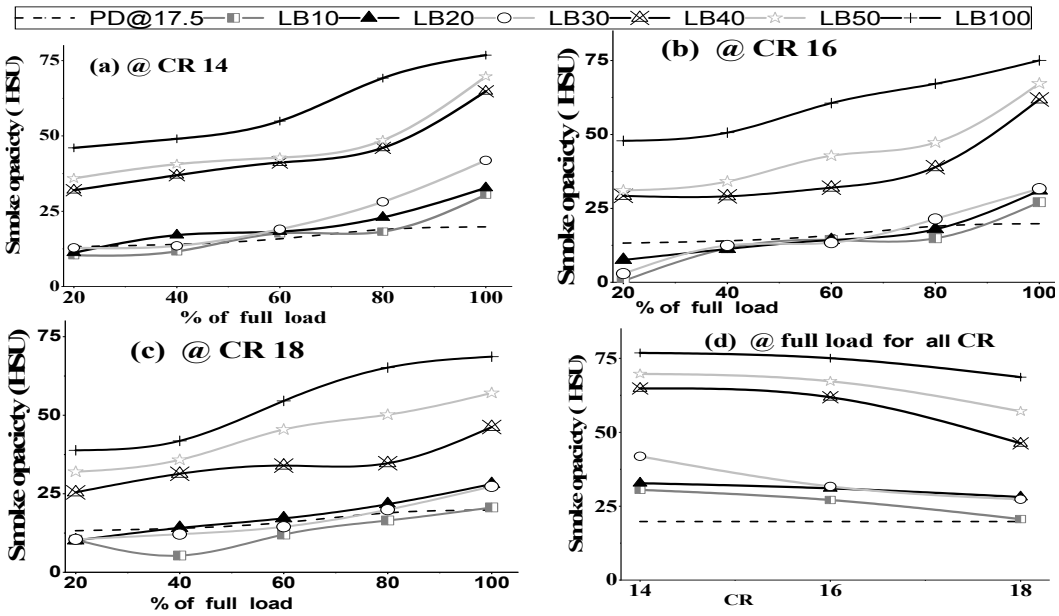

Fig. 3.26 Variation of smoke emissions with load and CR

. The lack of oxygen molecules and improper mixing and atomization of the fuels results in the emission of smoke. The Fig.3.26 shows the variation of smoke opacity with load and CR. The smoke opacity measured regarding Hartridge Smoke Unit

(HSU). With the increase in load increases the injection of fuel and results in rich combustion attributes the higher emission of smoke opacity. The smoke opacity increases, with the addition of biodiesel content in the blends. With the rise in biodiesel content in the blend, the higher viscosity, density, and lower volatility of biodiesel lead to difficulties in atomizing the fuel lead to incomplete combustion of fuel. Lower BTHE observed for biodiesels also support this fact.

3.4.4 Conclusions

Based on the extensive experimental results of linseed methyl ester fueled biodiesel and its blends in the variable CR diesel engine and compared with PD. The following findings were noted.

1. Cylinder gas pressure (CP) for the neat biodiesel and its blends are higher than the standard diesel fuel at all varying loading conditions and CRs. The maximum peak CP was 9 bar higher, and 5^0 advanced for LB100 and for LB10 it is 5 bar, and 2^0as compared to baseline fuel.
2. At CR 14, all the blends have the lower BTE, and as the CR increases from 16 to 18, the BTE improved for all blends except pure biodiesel. At CR16, the maximum BTE the improvement observed was 26.73% for LB30.
3. The marked maximum improvement in BSFC of LB10 for 18 CR is 3 -12% higher than PD.
4. At lower compression ratio the exhaust gas temperature is higher for all blends. As CR and blends ratio increases, EGT lowered as compared to standard diesel fuel. It is reduced by 8.6%, 6.8% and 9.8% for LB10, LB20, and LB30 respectively at CR 18.
5. Emission of CO is higher at lower load. The emission of CO decreases up to the 80% of load and again increase at full load. Maximum reductions of emission of CO are 47% for LB10 and 34%, 38%, 18%, and 13% for blends LB20 to LB40 respectively at CR 18.
6. HC emission increases with load and decreases with CR. The percentage reduction for LB10-LB30 noted as 40.37%, 22.02%, and 26.61% respectively as compared to the PD.
7. NOx emission increases with biodiesel fraction in the blends, load, and CR. At full load and CR 18, the emissions of NOx was higher for LB10, LB20, and LB30 by

28.5%,35.25%, and 30.8% respectively as compared to PD fuel operated at rated CR.

8. Emission of CO_2 is higher for biodiesel and its blends at all CRs and increases with load. It increases with increasing the biodiesel fraction in the blends. As compared to the baseline fuel PD, the higher emission of CO_2 for blend LB10 at CRs 14, 16, and 18 are 14.25%,12.74%, and 3.84% respectively. Whereas for neat biodiesel LB100 these values are 26%, 17.5%, and 10.6% higher amount of CO_2.
9. Emissions of smoke for the fuel blends B10, B20, and B30 is better and lesser as compared to baseline fuel at all compression ratio due to better combustion of these blends. With the increase in CR from 14 to 18, HSU decreases up to 45%. The blends B10, B20, and B30 show the HSU comparable with baseline fuel PD.

From the above discussions and conclusions, it is possible to operate the engine satisfactorily up to LB30 at CR 18 without affecting the engine operating characteristics.

Chapter 4

Optimization techniques for fuel blends, and Input parameters

The objective of the present chapter is to optimize the combination of fuel blend, CR, and a load of linseed methyl ester/ petro-diesel fed single cylinder compression ignition (CI) engine to improve the performance, combustion and to reduce the emission characteristics. The Taguchi optimization technique based grey relational analysis (TGRA) has been used to optimize the responses and to identify the best combination of input parameters. The orthogonal array L_9 used to arrange the input factors and their levels in nine numbers of experiments. An analysis of experimental results was done using the Minitab 17 software. Further, the method of Analytical Hierarchy Process (AHP) and Techniques for Order Preference by Similarity to ideal Solution (TOPSIS) methods confirms the optimized results of TGRA.

4.1 Taguchi and GRA technique for optimization

As mentioned, these two methods combined to solve the multi-objective related problem. The Fig. 4.1 shows the steps in the combined method. The left part of the figure indicates the Taguchi method and right part is GRA.

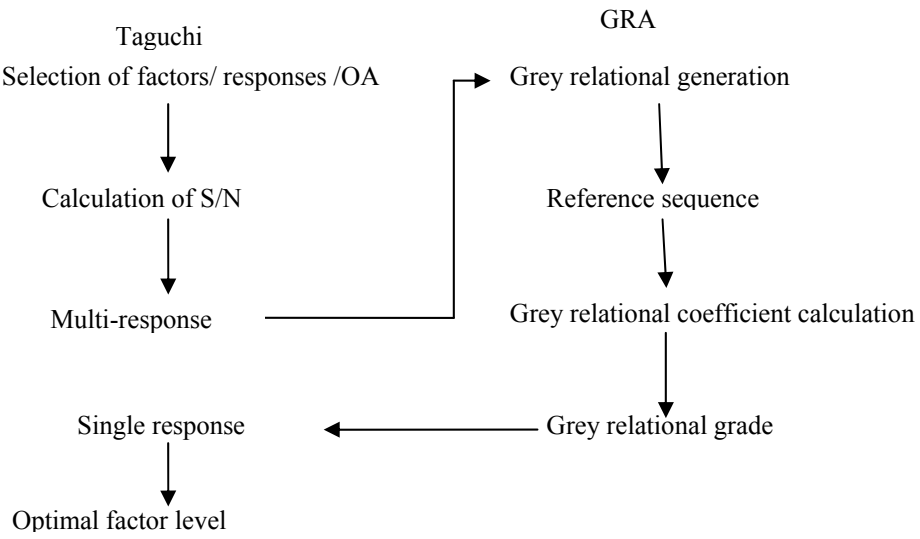

Fig. 4.1 Steps in TGRA method

4.1.1 Selection of factors and their levels

The selection of factors and levels for optimization entirely depends on the designer's level of understanding the experimental setup and its effects on the output responses. In this study, the three input factors viz. fuel blend, CR, and load and their three levels selected as shown in Table 4.1.

Table 4.1 Factors and their levels

Factors	Level 1	Level 2	Level 3
A: Fuel blend	B10	B20	B30
B: CR	14	16	18
C: Load (%)	60	80	100

These selected factors and levels are provided in a Taguchi's orthogonal array (OA), in such a way that optimization should be in a minimum number of experiments/trials (Ross, P. J. P. J., 1996; Mohan, S. V. and P. C. Mouli, 2008; Mukhopadhyay, D. *et al.*, 2013).

Based on the factors and their levels, these are arranged in a minimum number of trials (OA L_9). These combinations along with their experimental results of responses are given the Table 4.2.

Table 4.2 The arrangement of factors and levels in the orthogonal array (L_9) with experimental results

Expt. No.	OA L_9			Output parameters/ Responses									
	Fuel	CR	Load (%)	BTE (%)	BSFC (kg/kWh)	EGT (^{0}C)	CP (bar)	NHR (J/deg)	RPR (bar/deg)	CO %	HC ppm	NOx ppm	Smoke (HSU)
1	B10	14	60	20.93	0.4	302.418	30.74	29.19	0.84	0.09	37	511	17.64
2	B20	14	80	24.06	0.34	366.487	29.5	30.46	0.79	0.089	37	612	22.95
3	B30	14	100	26.14	0.34	422.33	30.41	36.77	1.43	0.174	52	710	41.88
4	B10	16	80	24.8	0.34	338.459	38.73	38.92	2.05	0.057	22	627	14.89
5	B20	16	100	25.67	0.33	402.296	39.43	38.39	1.89	0.114	31	701	31.02
6	B30	16	60	22.71	0.37	280.6	37.76	32.8	1.53	0.073	20	491	13.37
7	B10	18	100	28.85	0.3	350.928	46.99	33.89	2.13	0.036	13	893	20.63
8	B20	18	60	23.8	0.36	266.952	45.38	31.07	1.71	0.038	12	573	17.15
9	B30	18	80	28.31	0.31	300.26	45.9	28.15	1.13	0.042	15	755	19.91

4.1.2 Signal to noise (S/N) ratio calculation

The analyses of results are carried out by calculating the S/N ratio. In this study, for calculation of S/N ratios following two design conditions are used.

For larger the better characteristics

$$\eta_{ij} = -10\times\log\left(\frac{1}{r}\sum_{k=1}^{r}\frac{1}{m_{ijk}^2}\right) \quad (4.1)$$

For smaller the better characteristics

$$\eta_{ij} = -10\times\log\left(\frac{1}{r}\sum_{k=1}^{r}m_{ijk}^2\right) \quad (4.2)$$

Where η_{ij} is the S/N ratio of experiment number i for response j and m_{ijk} is the simulation result for trial i for response j, in k^{th} number of replication and r is the required replication numbers. The BTE, CP, NHR, and RPR taken as 'larger the better' responses and BSFC, EGT, CO, HC, NOx, smoke are 'smaller the better' responses. The S/N ratio calculated by using the equation 4.1 and 4.2 and represented in Table 4.3.

Table 4.3 Signal to noise (S/N) ratio of experimental results

Expt. No.	S/N ratio									
	BTE	BSFC	EGT	CP	NHR	RPR	CO	HC	NOx	Smoke
1	26.42	7.96	-49.61	29.75	29.30	-1.51	20.92	-31.36	-54.17	-24.93
2	27.63	9.37	-51.28	29.40	29.67	-2.05	21.01	-31.36	-55.74	-27.22
3	28.35	9.37	-52.51	29.66	31.31	3.11	15.19	-34.32	-57.03	-32.44
4	27.89	9.37	-50.59	31.76	31.80	6.24	24.88	-26.85	-55.95	-23.46
5	28.19	9.63	-52.09	31.92	31.68	5.53	18.86	-29.83	-56.91	-29.83
6	27.12	8.64	-48.96	31.54	30.32	3.69	22.73	-26.02	-53.82	-22.52
7	29.20	10.46	-50.90	33.44	30.60	6.57	28.87	-22.28	-59.02	-26.29
8	27.53	8.87	-48.53	33.14	29.85	4.66	28.40	-21.58	-55.16	-24.69
9	29.04	10.17	-49.55	33.24	28.99	1.06	27.54	-23.52	-57.56	-25.98

4.1.3 Grey relational generation

The GRA optimization used to solve the multi interdependent responses problem (Moran, J. *et al.*, 2006), the steps are shown in right part of the flowchart of Fig. 4.1.

In this part of optimization, the first step is to linear normalization of calculated S/N ratio between 0 and 1, known as grey relation generation.

The grey relation generation s_{ij} for trial i and response j has been calculated using equation 4.3 and 4.4. The equation 4.3 used for larger the better responses and 4.4 for smaller the better responses for calculating the grey relational generation.

$$s_{ij} = \frac{\eta_{ij} - \min_j \eta_{ij}}{\max_j \eta_{ij} - \min_j \eta_{ij}} \tag{4.3}$$

$$s_{ij} = \frac{\max_j \eta_{ij} - \eta_{ij}}{\max_j \eta_{ij} - \min_j \eta_{ij}} \tag{4.4}$$

The grey relational generations for normalized S/N ratio are tabulated in Table 4.4.

After calculating the grey relational generation, all the performance values are scaled up between 0 and 1. If the performance value s_{ij} for experiment number i of response j is 1 or nearer to 1, then this performance value of i is best for response j. But, these kinds of situation never exist; hence a reference sequence X_0 (best/ideal value) = (X_{01}, X_{02}, ….) = (1, 1, …..) is introduced for comparability.

Table 4.4 Grey relational generations

Exp.No.	BTE	BSFC	EGT	CP	NHR	RPR	CO	HC	NOx	Smoke
X_0	1	1	1	1	1	1	1	1	1	1
1	0.00	1.00	0.73	0.09	0.11	0.08	0.5816	0.2321	0.9333	0.7573
2	0.43	0.44	0.31	0.00	0.24	0.18	0.5745	0.2321	0.6317	0.5268
3	0.69	0.44	0.00	0.07	0.82	0.37	1.0000	0.0000	0.3834	0.0000
4	0.53	0.44	0.48	0.58	1.00	0.94	0.2917	0.5866	0.5912	0.9057
5	0.64	0.33	0.11	0.62	0.96	0.81	0.7316	0.3528	0.4047	0.2629
6	0.25	0.73	0.89	0.53	0.47	0.48	0.4487	0.6516	1.0000	1.0000
7	1.00	0.00	0.40	1.00	0.57	1.00	0.0000	0.9454	0.0000	0.6201
8	0.40	0.63	1.00	0.93	0.30	0.65	0.0343	1.0000	0.7418	0.7819
9	0.94	0.11	0.74	0.95	0.00	0.00	0.0978	0.8478	0.2807	0.6512

4.1.4 Calculation of grey relational coefficient

The grey relational generation compared with reference sequence and determined how close s_{ij} to X_0. This closeness represented by the grey relational coefficient ω_{ij} and calculated as given in Equation 4.5.

$$\omega_{ij} = \frac{\Delta_{\min} + \zeta.\Delta_{\max}}{\Delta_{ij} + \zeta.\Delta_{\max}} \tag{4.5}$$

$$\Delta_{\min} = Min\left(\Delta_{ij}, i = 1,2,....m; j = 1,2,...n\right)$$

$$\Delta_{\max} = Max\left(\Delta_{ij}, i = 1,2,....m; j = 1,2,...n\right)$$

Where $\Delta_{ij} = \left|x_{0j} - s_{ij}\right|$ and ζ is the distinguishing coefficient used for compressing or expanding the range of ω_{ij} responses. The m and n are the numbers of trials/ experiments and responses.

The value of ζ lies between 0 and 1, and most of the researchers have taken the value of it as 0.5. However, any value of it does not affect the ranking of an optimum experimental alternative. The calculated value of, Δ_{ij} $\Delta_{\min}$ and $\Delta_{\max}$ are tabulated in Table 4.5 and grey relational coefficient in Table 4.6.

Table 4.5 Calculation of Δ_{ij}

Exp.No.	BTE	BSFC	EGT	CP	NHR	RPR	CO	HC	NOx	Smoke
1	1.00	0.00	0.27	0.91	0.89	0.92	0.42	0.77	0.07	0.24
2	0.57	0.56	0.69	1.00	0.76	0.82	0.43	0.77	0.37	0.47
3	0.31	0.56	1.00	0.93	0.18	0.63	0.00	1.00	0.62	1.00
4	0.47	0.56	0.52	0.42	0.00	0.06	0.71	0.41	0.41	0.09
5	0.36	0.67	0.89	0.38	0.04	0.19	0.27	0.65	0.60	0.74
6	0.75	0.27	0.11	0.47	0.53	0.52	0.55	0.35	0.00	0.00
7	0.00	1.00	0.60	0.00	0.43	0.00	1.00	0.05	1.00	0.38
8	0.60	0.37	0.00	0.07	0.70	0.35	0.97	0.00	0.26	0.22
9	0.06	0.89	0.26	0.05	1.00	1.00	0.90	0.15	0.72	0.35
Δ_{min}	0	0	0	0	0	0	0	0	0	0
Δ_{max}	1	1	1	1	1	1	1	1	1	1

Table 4.6 Calculation of Grey relational coefficient

Exp.No.	BTE	BSFC	EGT	CP	NHR	RPR	CO	HC	NOx	Smoke
1	0.33	1.00	0.65	0.35	0.36	0.35	0.54	0.39	0.88	0.67
2	0.47	0.47	0.42	0.33	0.40	0.38	0.54	0.39	0.58	0.51
3	0.62	0.47	0.33	0.35	0.74	0.44	1.00	0.33	0.45	0.33
4	0.51	0.47	0.49	0.55	1.00	0.89	0.41	0.55	0.55	0.84
5	0.58	0.43	0.36	0.57	0.92	0.73	0.65	0.44	0.46	0.40
6	0.40	0.65	0.82	0.52	0.49	0.49	0.48	0.59	1.00	1.00
7	1.00	0.33	0.46	1.00	0.54	1.00	0.33	0.90	0.33	0.57
8	0.45	0.58	1.00	0.87	0.42	0.59	0.34	1.00	0.66	0.70
9	0.89	0.36	0.66	0.91	0.33	0.33	0.36	0.77	0.41	0.59

4.1.5 Calculation of grey relational grade

The calculation of grey relational grade needs the suitable weighting factor for each response. The weighting factor is a very crucial factor because it affects the grading of

trials. Hence in this study, weighting factor has been calculated judiciously and logical manner to avoid any error in the performance calculation. The weights (w_j) based on decision makers judgment, but this must be $\sum w_j = 1$. These weights are decided by the AHP's priority matrix as explained in the section 4.5.2.1and values are as follows, BTE=0.25, BSFC=0.16, EGT=0.02, CP=0.11, NHR=0.25, RPR=0.11, CO=0.02, HC=0.02, NOx=0.02, Smoke=0.02. After calculating the weights, the grey relational grades are calculated by using the equation 4.6.

$$\gamma_i = \sum_{j=1}^{n} w_j \omega_{ij} \quad , \qquad \text{i= 1, 2, 3,. . . … m.} \tag{4.6}$$

Where γ_i indicate the grey relational grade for i^{th} experiment and w_j is the weighting factor for j^{th} response.

Grey relational grade (GRG) calculation is converting the multi-objective to a single objective in the form of GRG. Using the above equation grey relational grade has been calculated and shown in Table 4.7. For example, calculation of grey relational grade for experiment number 1 as follows.

0.25*0.33+0.16*1.00+0.02*0.65+0.11*0.35+0.25*0.36+0.11*0.35+0.02*0.54+0.02*0.39+0.02*0.88+0.02*0.67= 0.46

Table 4.7 Grey relational grades (GRG)

Expt.No.	GRG	Rank
1	0.4582	8
2	0.4206	9
3	0.6056	4
4	0.6599	3
5	0.6604	2
6	0.4870	7
7	0.7117	1
8	0.5185	6
9	0.5569	5

The grey relational grade implies the degree of closeness of comparability sequence to the reference sequence. If the comparability sequence (GRG) value is higher, indicates mores closer to the reference sequence (best) (Fung, C. P., 2003). Therefore, the particular experiment number is the best choice whose GRG is higher value. The values of GRG from the Table 4.7, indicates that the test number 7 had the

highest value as compared to others and ranked 1. The operation number 7 is the combination of fuel blend B10, CR 18, and load 100% which gives the best performance characteristics.

4.1.6 Calculation of optimal factor level effect

In Taguchi method, performance characteristics are additive. Then it is possible to predict the factor level effect by knowing the main results. In this study, the effect of fuel at level 1 (A_1) can be calculated by averaging the GRG of all experiments where it has level 1. For example, the factor fuel level 1 is B10, and it has in experiment numbers 1, 4, and 7 as shown in Table 4.2 orthogonal array. Therefore, the effect of factor fuel level 1 has been calculated by taking the average value of GRG at these three experiments.

$$A_1 = \frac{1}{3}(0.46 + 0.66 + 0.71) = 0.61$$

Similarly, all factors level effect calculated and tabulated in Table 4.8 and ranked the influence of factor on performance characteristics based on the higher value. This ranking of factors effect denotes the load has the highest effect on performance characteristics followed by *CR*, and fuel. The analysis of variance (ANOVA) for grey relational grade performed to know the further factor's effect.

Table 4.8 Factor level effects

Factor	L1	L2	L3	Max-Min	Rank
Fuel	**0.61**	0.53	0.55	0.08	3
CR	0.50	**0.603**	0.60	0.10	2
Load	0.49	0.55	**0.66**	0.17	1

4.2 Analytical hierarchy process (AHP) method

It is a multicriteria decision making (MCDM) tool, used for selecting best trial/ experiment from the available set of tests.

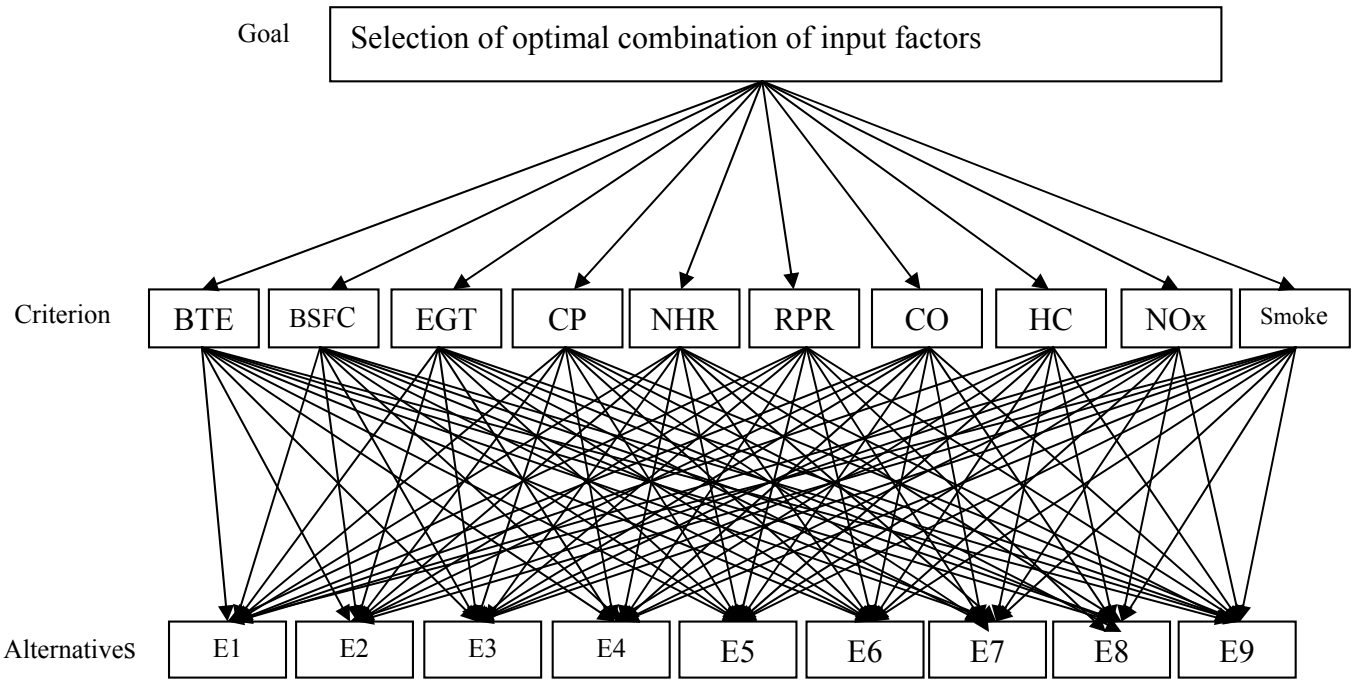

Fig. 4.2 The hierarchy of selection of optimal combination of input factors

It helps to choose the optimal combination of input factors for better performance characteristics in a given trial. The trial/ experiment numbers are designed based on the Taguchi's orthogonal array concept for arranging the input factors and their levels in a minimum number of trials. The beauty of AHP is its flexibility to be combined with Taguchi, GRA, and techniques for order preference by similarity to ideal solution (TOPSIS), linear programming, fuzzy logic, etc. for optimizing the decision making process better way. In this study, AHP is used to rank the experiment numbers as per the performance index values obtained by this method (Rao, R. V., 2007). After arranging the factors and their levels in a nine number of operations, the AHP method used to find the performance index in following steps. The process of decision made in AHP has been presented in the order of hierarchies as shown in Fig. 4.2.

4.2.1 Weights calculation for responses

The weights are calculated by constructing the priority matrix of responses. In this article the number of responses is 10, hence priority matrix is of 10 × 10 has been prepared. In the priority matrix, the values of judgment made by the authors are entered using the basic scale of relative importance from AHP (Wind, Y. and T. L. Saaty,1980). The verbal judgments ‘equally preferred', moderately preferred,' strongly preferred,' ‘very strongly preferred,' and extremely preferred are indicated by the numerical values 1,3,5,7, and 9.If the judgment seems to be in between then the numerical values 2,4,6, and 8 can be used. The preferences of a row over column and vice versa of verbal judgments are tabulated in Table 4.9.

Table 4.9 Numerical values of verbal judgments

Equal 1	⟹ Increasing row importance over the column							
	2	3	4	5	6	7	8	9
	1/2	1/3	1/4	1/5	1/6	1/7	1/8	1/9
	⟹ Increasing column importance over row							

In the priority matrix, the cell entry c_{ij} denotes the numerical value of i^{th} row response compared with j^{th} column response as per the verbal judgments. If i=j, then c_{ij}=1 and c_{ji}= 1/ c_{ij}. Hence in the matrix, all the diagonal entries indicate the response is compared with itself and assigned numerical value 1. The priority matrix has been constructed using the verbal judgments based on their relative importance and tabulated in Table 4.10.Next, multiply the cell values in each row and take the 10^{th} root of multiplication. Then each row’s tenth root product is added and is equal to 16.2370. Row ‘SUM’ denotes the sum of column elements for each response. Weights are calculated for each response by linear normalization of 10^{th} root product. The tenth root of response is divided by the total sum of all responses tenth root product gives the priority vector (weight) for that response. Let us say, weight of response BTE= 3.5887/ 16.2370 = 0.22.

Table 4.10 Priority matrix for the relative importance of responses

Responses	BTE	BSFC	EGT	CP	NHR	RPR	CO	HC	NOx	Smoke	10^{th} root of product	Priority vector (PV)= Weights
BTE	1	2	9	3	1	3	9	9	9	9	4.0054	0.25
BSFC	1/2	1	7	2	1/2	2	7	7	7	7	2.6458	0.16
EGT	1/9	1/7	1	1/6	1/9	1/6	1	1	1	1	0.3707	0.02
CP	1/3	1/2	6	1	1/3	1	6	6	6	6	1.8346	0.11
NHR	1	2	9	3	1	3	9	9	9	9	4.0054	0.25
RPR	1/3	1/2	6	1	1/3	1	6	6	6	6	1.8346	0.11
CO	1/9	1/7	1	1/6	1/9	1/6	1	1	1	1	0.3707	0.02
HC	1/9	1/7	1	1/6	1/9	1/6	1	1	1	1	0.3707	0.02
NOx	1/9	1/7	1	1/6	1/9	1/6	1	1	1	1	0.3707	0.02
Smoke (HSU)	1/9	1/7	1	1/6	1/9	1/6	1	1	1	1	0.3707	0.02
SUM	3.72	6.714	42	10.8	3.722	10.83	42	42	42	42	16.1793	1
SUM* PV	0.9215	1.0980	0.9623	1.2284	0.9215	1.2284	0.9623	0.9623	0.9623	0.9623	10.2092	

4.2.2 Consistency ratio check

The consistency of values entered in the priority matrix has been checked by consistency index (CI) as given by equation 4.7.

$$CI = \frac{\lambda_{max} - n}{n-1} \tag{4.7}$$

Where λ_{max} is the total sum of values in the row 'SUM*PV' and is equal to 10.2092, n is the total number of responses, i.e., 10.

CI= 0.023244

After calculation of CI, next to check, how consistently the author has assigned the values in the relative importance of responses. This has been calculated by the consistency ratio (CR) as follows.

CR= CI / RI = 0.023244/1.49 = 0.0156 < 0.1

Where RI is the random index, and it depends on the number of responses

Table 4.11 Values of RI

Responses	3	4	5	6	7	8	9	10
RI	0.52	0.89	1.11	1.25	1.35	1.4	1.45	1.49

If the value of CR is less than 0.1, then it denotes the decision made by the author is correct, and error is less than 10%, and it is acceptable. The values of RI as given the Table 4.11.

Using the priority matrix, the calculated weights for each of the responses are as follows. BTE=0.25, BSFC=0.16, EGT=0.02, CP=0.11, NHR=0.25, RPR=0.11, CO=0.02, HC=0.02, NOx=0.02, Smoke=0.02.

After calculating the weights of the responses, the experimental values given the Table 4.2 have been normalized. Normalization is done for the sake of uniformity in the all responses, for beneficial (larger the better) responses the maximum value is the denominator and for non-beneficial responses the minimum value is the numerator for calculating the normalized value Table. The experimental values of response given in Table 4.2 used for calculation of normalization. The normalized value calculation of the BTE, CP, NHR, and RPR took as beneficial responses and remaining as non-beneficial.

For beneficial responses $N_{ij} = \frac{E_{ij}}{\max_j E_{ij}}$ i=1 , 2, . . . ; j=1, 2, . . .

.

For non-beneficial responses $N_{ij} = \frac{\min_j E_{ij}}{E_{ij}}$

Where N_{ij} is the normalized value and E_{ij} is the experimental value of responses from Table 4.2 for i^{th} experiment number and j^{th} attribute.

Based on these normalization methods, Table 4.12 depicts the normalized values and corresponding weights for each response and also calculated the performance index of experiment number.

Table 4.12 Normalized value, weights and performance index (P_i)

Expt. No.	Responses											
	BTE	BSFC	EGT	CP	NHR	RPR	CO	HC	NO_x	Smoke	P_i	Rank
w_j	0.25	0.16	0..02	0.11	0.25	0.11	0.02	0.02	0.02	0.02		
1	0.73	0.75	0.88	0.65	0.75	0.39	0.40	0.32	0.96	0.76	0.67	9
2	0.83	0.88	0.73	0.63	0.78	0.37	0.40	0.32	0.80	0.58	0.71	8
3	0.91	0.88	0.63	0.65	0.94	0.67	0.21	0.23	0.69	0.32	0.79	6
4	0.86	0.88	0.79	0.82	1.00	0.96	0.63	0.55	0.78	0.90	0.88	2
5	0.89	0.91	0.66	0.84	0.99	0.89	0.32	0.39	0.70	0.43	0.85	3
6	0.79	0.81	0.95	0.80	0.84	0.72	0.49	0.60	1.00	1.00	0.79	7
7	1.00	1.00	0.76	1.00	0.87	1.00	1.00	0.92	0.55	0.65	0.93	1
8	0.82	0.83	1.00	0.97	0.80	0.80	0.95	1.00	0.86	0.78	0.83	4
9	0.98	0.97	0.89	0.98	0.72	0.53	0.86	0.80	0.65	0.67	0.82	5

4.2.3 Calculation of performance index (p_i)

The performance index (p_i) calculated for each experiment number by multiplying the row cell value with corresponding response's weights. For example, for test number 1 the p_i calculated as follows.

0.25*0.73+0.16*0.75+0.02*0.88+0.11*0.65+0.25*0.75+0.11*0.39+0.02*0.4+0.02*0.32+0.02*0.96+0.02*0.76 = 0.67, similarly the performance index for all experiment has been calculated .

The higher value of p_i indicated better performance for that experiments combination of factors and ranked as 1. The ranking of AHP has compared with TGRA (Table 4.13), and results are almost same for best and second best in both hybrid optimization techniques.

Table 4.13 Ranking comparison of TGRA and AHP

Expt. No.	1	2	3	4	5	6	7	8	9
TGRA	8	9	4	3	2	7	1	6	5
AHP	9	8	6	2	3	7	1	4	5

4.3 The techniques for order preference by similarity to ideal solution (TOPSIS) method

The method of TOPSIS was developed and used by Yoon and Hwang (Opricovic, S. and G. H. Tzeng, 2004) for decision-making problems. The authors have suggested that in decision problems, the preferred alternative should have the shortest distance from the ideal best solution and farthest from the ideal worst solution regarding geometrical sense. The ideal best solution is a hypothetical term indicates the maximum value of the attribute (response) that gives the optimum solution of the problem and ideal worst solution denotes the minimum value of response in the database. The TOPSIS method gives the solution which is closest to the ideal best and farthest from the ideal worst solution. It is a multicriteria decision making (MCDM) tool, used for selecting best trial/ experiment from the available set of tests. It helps to choose the optimal combination of input factors for better performance characteristics in a given trial. The trial/ experiment numbers are designed based on the Taguchi's orthogonal array concept for arranging the input factors and their levels in a minimum number of trials. The TOPSIS method was used for accurate weather forecasting application (Zeyaeyan, S. *et al.*,2017). The optimization of electric discharge machining parameters for the material AISI D2 tool using the TOPSIS method (Raj, S. O. N. and S. Prabhu, 2017). In this study, TOPSIS is used to rank the experiment numbers as per the performance index values obtained by this method. After arranging the factors and their levels in a nine number of operations, the TOPSIS method used to find the performance index in following steps.

4.3.1 Normalization of decision matrix (N_{ij})

In this, the experimental results given in Table 4.2 are normalized by using the equation 4.8 and normalized decision matrix are depicted in Table 4.14. In this method of TOPSIS, alternative means the number of experimental trials and attributes means the output responses.

$$N_{ij} = \frac{m_{ij}}{\left[\sum_{j=1}^{n} m_{ij}^{2}\right]^{\frac{1}{2}}} \tag{4.8}$$

Table 4.14 Normalized decision matrix

Alt.	Attributes									
	BTE	BSFC	EGT	CP	NHR	RPR	CO	HC	Nox	Smoke
1	0.2775	0.3870	0.2960	0.2636	0.2904	0.1782	0.3346	0.4183	0.2567	0.2477
2	0.3190	0.3289	0.3587	0.2530	0.3030	0.1676	0.3309	0.4183	0.3075	0.3223
3	0.3465	0.3289	0.4134	0.2608	0.3658	0.3033	0.6468	0.5878	0.3567	0.5881
4	0.3288	0.3289	0.3313	0.3322	0.3872	0.4348	0.2119	0.2487	0.3150	0.2091
5	0.3403	0.3193	0.3938	0.3382	0.3819	0.4009	0.4238	0.3504	0.3522	0.4356
6	0.3011	0.3580	0.2746	0.3239	0.3263	0.3245	0.2714	0.2261	0.2467	0.1878
7	0.3825	0.2902	0.3435	0.4030	0.3372	0.4518	0.1338	0.1470	0.4487	0.2897
8	0.3155	0.3483	0.2613	0.3892	0.3091	0.3627	0.1413	0.1357	0.2879	0.2408
9	0.3753	0.2999	0.2939	0.3937	0.2801	0.2397	0.1561	0.1696	0.3793	0.2796

4.3.2 Calculation of weighted normalized matrix (V_{ij})

After calculation of normalized decision matrix (Table 4.14) and weights (Table 4.10) for all the attributes, the weighted normalized matrix is calculated using the below equation and tabulated in Table 4.15.

$$V_{ij} = w_j N_{ij}$$

Table 4.15 Weighted normalized matrix

Alt.	Attributes									
	BTE	BSFC	EGT	CP	NHR	RPR	CO	HC	Nox	Smoke
1	0.0610	0.0890	0.0030	0.0422	0.0523	0.0160	0.0067	0.0125	0.0077	0.0074
2	0.0702	0.0757	0.0036	0.0405	0.0545	0.0151	0.0066	0.0125	0.0092	0.0097
3	0.0762	0.0757	0.0041	0.0417	0.0658	0.0273	0.0129	0.0176	0.0107	0.0176
4	0.0723	0.0757	0.0033	0.0531	0.0697	0.0391	0.0042	0.0075	0.0095	0.0063
5	0.0749	0.0734	0.0039	0.0541	0.0688	0.0361	0.0085	0.0105	0.0106	0.0131
6	0.0662	0.0823	0.0027	0.0518	0.0587	0.0292	0.0054	0.0068	0.0074	0.0056
7	0.0841	0.0668	0.0034	0.0645	0.0607	0.0407	0.0027	0.0044	0.0135	0.0087
8	0.0694	0.0801	0.0026	0.0623	0.0556	0.0326	0.0028	0.0041	0.0086	0.0072
9	0.0826	0.0690	0.0029	0.0630	0.0504	0.0216	0.0031	0.0051	0.0114	0.0084

Next step is to calculate the ideal best an ideal worst solution using the following equations.

$$V^{+} = \max_j V_{ij} \left(j \in J \right), \min_j V_{ij} \left(j \in J' \right)$$

$$V^{-} = \min_j V_{ij} \left(j \in J \right), \max_j V_{ij} \left(j \in J' \right)$$

Where i= 1, 2,…..m indicates the alternatives and j= 1, 2, . . . n are the attributes .

The term J used for beneficial term, i.e., larger the better and $J^{'}$ used for non-beneficial terms (smaller the better). Using these equations and conventions the ideal best and ideal worst is calculated for each attribute and tabulated in Table 4.16.

Table 4.16 Calculated ideal best (V^+) and ideal worst (V^-)

	BTE	BSFC	EGT	CP	NHR	RPR	CO	HC	NOx	Smoke
V^+	0.0841	0.0668	0.0026	0.0645	0.0697	0.0407	0.0027	0.0041	0.0074	0.0056
V^-	0.0610	0.0890	0.0041	0.0405	0.0504	0.0151	0.0129	0.0176	0.0135	0.0176

4.3.3 Calculation of separation variables and relative closeness

The separation variable indicates its Euclidean distance from the ideal solutions for each alternative. These variables are calculated using the below-given equations.

$$S_i^+ = \left[\sum_{j=1}^{n}\left(V_{ij} - V_j^+\right)^2\right]^{0.5}$$

$$S_i^- = \left[\sum_{j=1}^{n}\left(V_{ij} - V_j^-\right)^2\right]^{0.5}$$

Where S_i^+ and S_i^- indicates the separation of each alternative from the positive ideal solution and the separation from negative ideal solution respectively.
Table 4.17 shows the calculated separation variables for each alternative.

Table 4.17 Separation variables

Alt.	S^+	S^-
1	0.050258	0.014477
2	0.042929	0.020634
3	0.036049	0.028407
4	0.019162	0.041707
5	0.02004	0.038673
6	0.031437	0.028697
7	0.011324	0.052182
8	0.025779	0.03711
9	0.027789	0.041907

The relative closeness P_i of each alternative has been calculated using the following equation and tabulated in Table 4.18. Based on the value of relative proximity, the alternatives are ranked in descending order for the value of P_i.

$$P_i = \frac{S_i^-}{\left(S_i^- + S_i^+\right)}$$

Table 4.18 Relative closeness of alternatives

Alt.	P_i	Rank
1	0.22364	9
2	0.324625	8
3	0.440723	7
4	0.685191	2
5	0.658678	3
6	0.477218	6
7	0.821683	1
8	0.590088	5
9	0.601279	4

Finally, the ranking of TOPSIS alternatives has been compared with TGRA and depicts in Table 4.19. It is found that the optimal solution is same in both the technique and confirms the results.

Table 4.19 Ranking comparison of TGRA and TOPSIS

Expt. No.	1	2	3	4	5	6	7	8	9
TGRA	8	9	4	3	2	7	1	6	5
TOPSIS	9	8	7	2	3	6	1	5	4

4.4 Results and discussion

4.4.1 Signal to noise ratio analysis for GRG

Table 4.20 Signal to Noise Ratios for GRG

Level	Fuel	CR	Load
1	-4.443	-6.191	-6.207
2	-5.608	-4.471	-5.393
3	-5.175	-4.564	-3.626
Delta	1.165	1.72	2.581
Rank	3	2	1

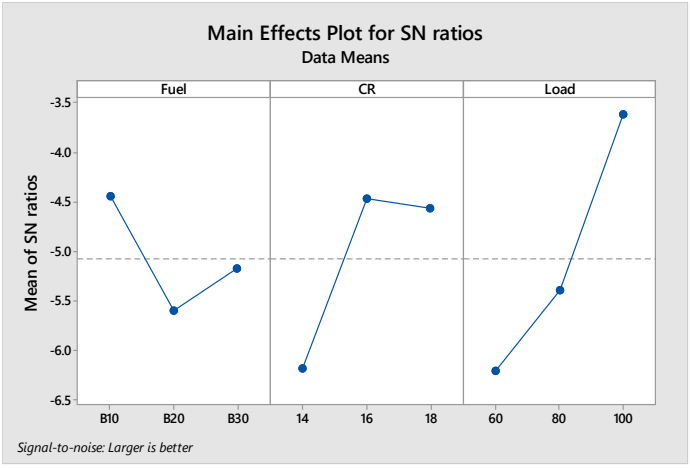

Fig. 4.3 S/N ratio for the grey relational grade (GRG)

The Taguchi method used for analysis of grey relation grade obtained by GRA the optimization technique. The signal to noise ratio of GRG calculated by using the 'larger the better' design condition represented by equation 4.3. The Table 4.20 tabulated the S/N ratio of input factors and their levels. Similarly, Fig.4.3 shows the graphical representation of S/N ratio of GRG for input elements. The inferences have drawn from Table 4.20and Fig. 4.3, about optimal combination of input factors A1B2C3, i.e., fuel blend B10, CR 16, and load 100% for improved performance characteristics.

4.4.2 Analysis of variance

For analyzing the effect of input factors on output responses quantitatively, the statistical tool analysis of variance (ANOVA) used at 95% confidence level. The ANOVA distributes the total variability in responses, among the available factors. This investigation recognizes the factor whose effect is significant on the output responses and quantifying the effect of the factor regarding percentage contribution (Gamst, G. *et al.*, 2008; Montgomery, D. C. and G. C. Runger, 2010). The various terms used for analysis of variance namely sum of squares (SS) mean square (MS) and F-value (Fisher, R. A., 1937) calculated by using below-given equations and the results and tabulated in Table 4.21.

$$SS = \sum_{i=1}^{n} \left(\gamma_i - \gamma_m\right)^2$$

$$MS = \frac{SS}{DF}$$

Where is γ_i the GRG for ith experiment and γ_m is the mean of GRG. The value of F calculated by taking the ratio of factor MS to the error mean square. The percentage contribution is the ratio factor SS to total SS.

The Table 4.21 tabulates the results of analysis of variance of a grey relational grade. The ANOVA result shows the most significant factor is load whose contribution for variation of output responses is 52.82%, followed by the CR (28.38%), and fuel (10.52%). This result implies that by controlling the load and CR, the performance parameters can be varied and improved.

Table 4.21 Analysis of Variance for S/N ratios

Source	DF	Seq SS	Adj MS	F	Contribution (%)
Fuel	2	2.081	1.0405	1.27	10.52
CR	2	5.614	2.8071	3.42	28.38
Load	2	10.449	5.2244	6.37	52.82
Residual Error	2	1.639	0.8197		8.28
Total	8	19.784			100

4.4.3 Experiments for confirmation test

The initial optimal settings of variable compression ratio diesel suggested by the manufacture are fuel petrodiesel, CR 17.5 and load 80. Then at initial settings of the engine, the GRG (0.521) and S/N ratio (- 3.4525) are represented in Table 4.22 and compared with predicted and experimental optimized factor level results.

After getting, the optimal input factor levels from the S/N ratio plots, the grey relational grade ψ predicted at the optimal input factor by the equation 4.9.

$$\psi = \gamma_m + \sum_{i=1}^{n} (\gamma_i - \gamma_m) \tag{4.9}$$

Using this equation 4.9 the predicted grey relational grade at optimal input factor level $A_1B_2C_3$ is 0.8429, and corresponding S/N ratio is -1.4845 tabulated in Table 4.22. Also at the same optimal level, confirmation experiment was conducted and results are reproduced. The results inferred that the improvement in GRG with linseed biodiesel blend is 0.2922, i.e., 56.1% as compared to existing initial setting of a variable compression ratio diesel engine. The optimal combination of input parameters shows the improvement in performance, combustion, and emission parameters justifying the application of Taguchi with GRA.

Table 4.22 Results of an existing and optimal set of input factors

	Initial process parameters	Optimal process parameters	
	Existing VCR engine setting	Predicted	Experimental
Level		$A_1B_2B_3$	$A_1B_2C_3$
GRG	0.521	0.8429	0.8132
S/N ratio	-3.4525	-1.4845	-2.38936

Improvement in GRG = (0.8132-0.521) = 0.2922

4.4.4 Performance of index (p_i) of AHP and TOPSIS

Taguchi's OA, i.e., the arrangement of factors and levels in a minimum number of experiment taken as the alternatives and a corresponding set of output parameters as attributes (responses). This OA has been analyzed using the AHP and TOPSIS for selecting the best option. The performance index p_i for AHP and TOPSIS calculated, and it shows the best alternative is 7. This 7^{th} choice has a combination of B10, CR18, and load 100% and this optimum result exactly matching with TGRA.

4.5 Conclusions

In the variable compression ratio diesel engine the performance, combustion, and emission characteristics affected by the input factor fuel blends, compression ratio, and applied load on the engine. The combined technique TGRA used to identify the best combination of input factor levels for improved performance characteristics in a minimum number of trials. In designing of the experiment, the TGRA method is useful, since it reduces the time to perform the experiments by suggesting the optimal combination of factors in the lesser number of tests. Following conclusion has been drawn.

1. In the study, the optimal combination is fuel blend B10, compression ratio 18 and load on the engine is 100% for better performance and combustion and reduced emission. The optimum factor level effects observed by these techniques are fuel blend B10 and compression ratio 16 and load 100%.
2. The ANOVA analysis for grey relational grade shows the most influencing factor is load with the contribution of 52.28% followed by the factor CR of 28.38% and least effect of fuel blend of contribution only 10.52%.
3. The confirmation test shows the improvement in performance by 56.1% as compared to the existing setting of the engine for fuel as petrodiesel. This confirms the advantage of TGRA techniques for optimization.
4. The TGRA results also confirmed by Taguchi-AHP-TOPSIS for the optimal level of the factor. This means a hybrid method of optimization can be used effectively.

Chapter 5

Engine modification and investigations at variable boost pressures and compression ratios

5.1 Engine modifications

The existing experimental setup of a variable compression ratio single cylinder naturally aspirated (NA) diesel engine is partially modified to supercharged condition to boost the engine. A variable speed centrifugal blower (680 W) type supercharger used for the boosting of the engine. The supercharger connected at the inlet of the airbox, airbox used as surge tanks at the time of boosting the engine. The single phase electrical energy meter used to measure the energy consumption by supercharger during boosting of the engine. At the outlet of the supercharger and the inlet of the airbox, the mercury manometer 2 used to measure the air flow rate with orifice plate at the inlet pipe. Similarly, the glass tube thermometer of range 0-100 ^{0}C and mercury manometer 1 used to measure the air temperature and pressure respectively at the inlet of the engine.

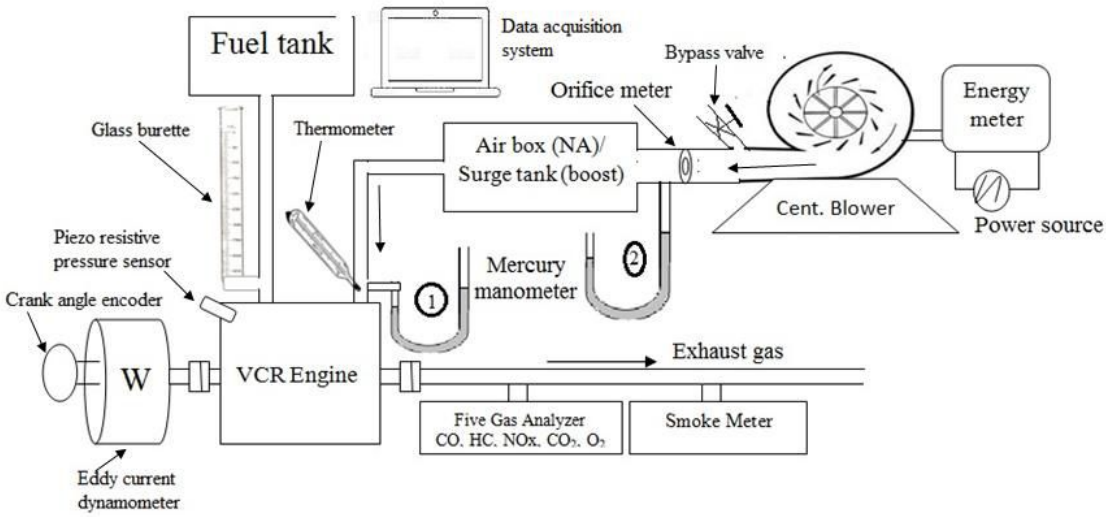

Fig. 5.1 Schematic diagram of the experimentalsetup

The schematic diagram and photographic view of experimental set up as shown in Fig. 5.1 and in Fig. 5.2 respectively.

Fig. 5.2 Photographic view of the experimentalsetup

5.2 Theory and experimental methodology of the modified engine

Many working parameters improve due to the supercharging of the engine. It covers all possible losses and improvement causes due to the supercharging and gives a ratio of concerning an effective brake work to the heat added by fuel equivalent mechanical work. Hence the effective thermal efficiency $\eta_{eff}$of the engine is represented as in equation 5.1.

$$\eta_{eff} = \eta_c \eta_{th} \eta_{cyc} \eta_m \tag{5.1}$$

Where η_c indicates fuel combustion efficiency, i.e., the fraction of added fuel burns to add the heat energy and η_{th} is process efficiency gives the amount of added heat converted into theoretical work. The cycle efficiency η_{cycle} considers the losses due to the gas exchange processes at high BP account the relative closeness of real cycle process efficiency to theoretical efficiency. The η_m is the mechanical efficiency of the engine. The increase in boost pressure has the benefits of the increase in brake thermal efficiency, torque, and improvement in the brake specific fuel consumption. The improvement in these parameters seems to be relevant because of higher energy

released by the same amount of fuel with an increase in boost pressure. Hence the performance characteristics of the engine are the function of brake mean effective pressure (BMEP), effective thermal efficiency η_{eff} ,and air-fuel ratio(AFR). The BMEP can be written as given in the below equation 5.2 (Podevin, P. *et al.*, 1999).

$$BMEP = \frac{\eta_v \rho_a \eta_{eff} . LCV}{AFR} \tag{5.2}$$

Where η_v is the volumetric efficiency, ρ_a air density, and LCV is the lower calorific value of the fuel.

The economy of using supercharger (or downsizing of the engine) is justified by calculating the specific weight, specific volume, and specific power as given in the equations 5.3, 5.4, 5.5.

$$\text{Specific\_weight} = \frac{\text{Engine\_weight}}{\text{Engine\_power}} = \frac{\text{W}}{\text{bp}} \tag{5.3}$$

$$Specific\_volume = \frac{Engine\_volume}{Engine\_power} = \frac{V_d}{bp} \tag{5.4}$$

$$Specific\_power = \frac{Engine\_power}{Piston\_face\_area} = \frac{bp}{A_p} \tag{5.5}$$

Initially, all the measurement equipment calibrated for accuracy and reliability of recorded data. In the present work, two lower compression ratios (CR) 14:1, 16:1 and one higher CR18:1 along with the standard CR17.5:1 selected for the experimental investigations for all fuels, i.e., PD, LB10, LB20, and LB30.

The experimentation performed at CR 17.5:1 with PD treated as a standard operating condition for baseline fuel. The injection pressure and timing were kept constant at 210 bar and 23^0 bTDC for all observations. During the testing, the input parameters such as percentage engine load varied from 20% - 100% in the steps of 20%. Similarly, the engine boost pressure varied from naturally aspirated to 0.5 – 1.5 kPa (g) in steps of 0.5 kPa (g).

Rigorous experimental work was carried out. In each test, before taking the observations, the engine ran for 5 minutes for proper warm-up and stabilizing the set of all working parameters. For reliability and accuracy, a set of observations for

output parameters were taken six times for ten cycles each, and the best (less variability) result considered for analysis purpose.

5.3 Result and discussions

In this section, the experimental observations analyzed and discussed the effect of compression ratios and boost pressures, percentage engine load, and a fraction of biodiesel in the blends on combustion, performance, emission, and downsizing parameters. The combustion parameters include in-cylinder combustion pressure, the rate of pressure rise, and net heat release rate concerning crank angle. The performance parameters considered are brake specific fuel consumption (BSFC), brake thermal efficiency (BTE), and exhaust gas temperature (EGT). Similarly, the emission characteristics HC, CO, NOx, smoke, and downsizing parameters like specific power and specific weight of engine are considered.

5.3.1 Power consumption by the supercharger

The power consumption by the supercharger was measured using the single phase digital energy meter. The energy consumption almost increases linearly with the BPs irrespective of compression ratio used for experimentation in DICI engine as shown in Fig. 5.3.

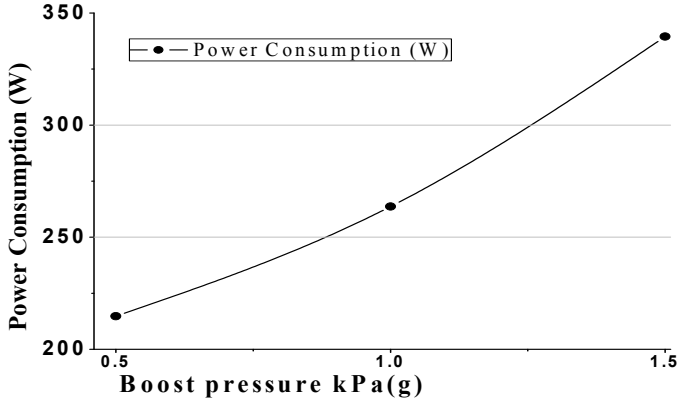

Fig. 5.3 Power consumption by the supercharger

As the CR decreases, the volumetric efficiency of compression ignition engine increases with the boosting pressure. At lower CR clearance volume is more to push the more dense air in the cylinder as compared to higher CR. In spite of this, at high BP, supercharger has to run relatively at higher rpm, and hence it consumes more

power. Therefore, for power consumption, BP is more dominant than CR. It consumes 6, 7.5, and 9.7% of power at the 0.5, 1, and 1.5 kPa (g) respectively.

5.3.2 Effect on combustion characteristics of all tested fuels

In this section the effect of compression ratio, boost pressure, and percentage of engine load discussed for all tested fuel such as PD, LB10, LB20, and LB30. The combustion characteristics considered the variation of in-cylinder combustion pressure, rate of pressure rise, and net heat release rate.

5.3.2.1 Effect on combustion pressure of PD, LB10, LB20, and LB30

The Fig. 5.4 demonstrates the variations of in-cylinder combustion pressure (CP) at different CRs and BPs for PD. It is noted that at higher CR 18, the CP is more and advanced for natural aspiration and further rise and higher value for boost pressures due to improvement in energy conversion of fuel. At high boost pressure, the overall fuel-air mixture is lean and higher density air-fuel charge burns the charge slowly and longer combustion duration results in the higher value of in-cylinder combustion pressure and temperature (Jayashankara, B. and V. Ganesan, 2010).

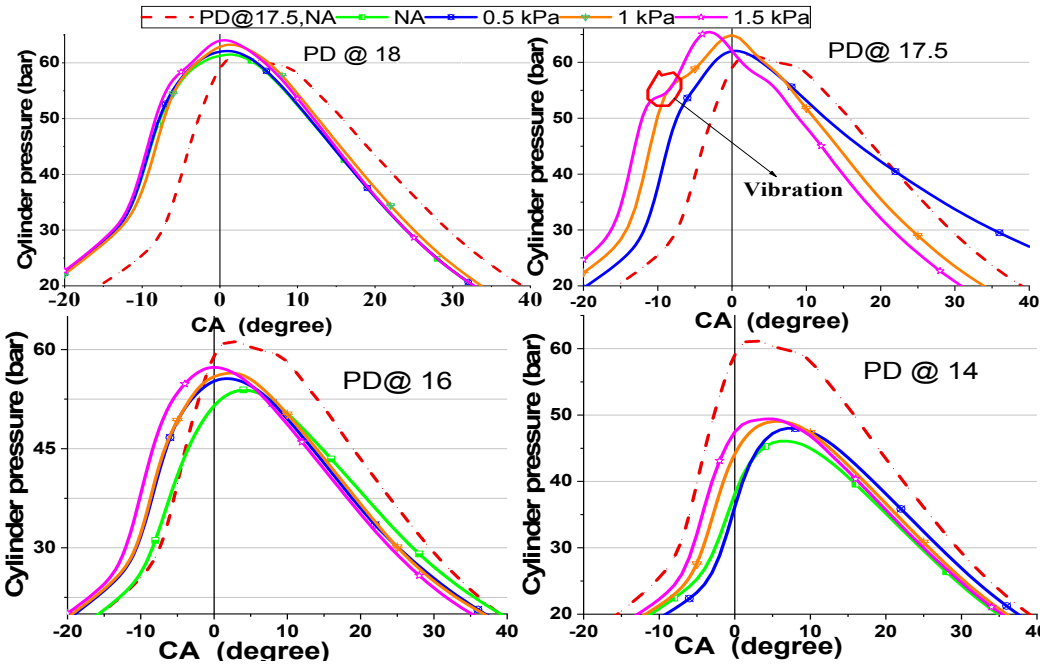

Fig. 5.4 Variation of in-cylinder combustion pressure at different BPs and CRs for PD

As the CR reduces, the CP values also lower due to more prolonged ignition delay as compared to rated natural aspiration (NA) operation. At all BPs, advanced and higher

value of CP observed as compared to NA at respective CR. At rated CR 17.5 at BPs 1 and 1.5 kPa (g), there is a sharp rise in the pressure represents the erratic and vibrating operation of the engine. This could be because of at high boost pressures intensive turbulence and mixing of fuel-air leads to additional fuel mixed to the flammable limit of charge before the end of premixed combustion results in sudden combustion of the fuel charge.

Table 5.1 tabulated the summary of percentage improvements of all CPs at all BP and CR over the naturally aspirated operation condition of the engine.

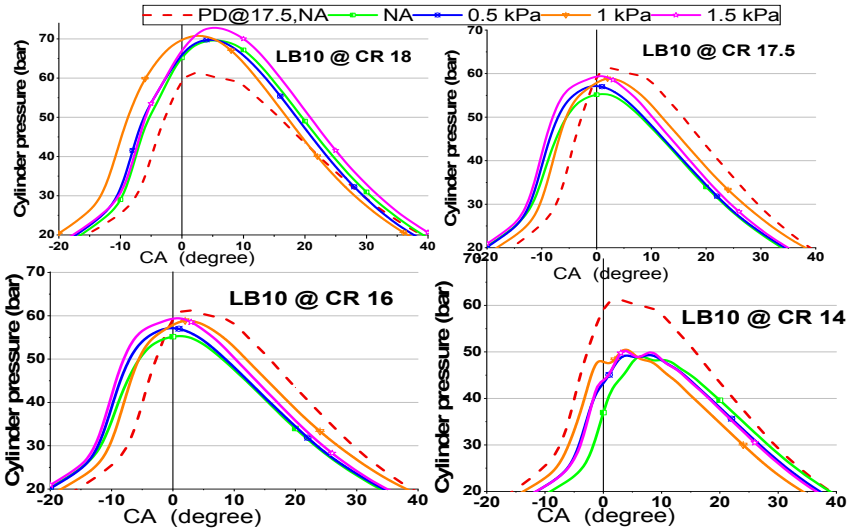

Fig. 5.5 Variation of in-cylinder combustion pressure at different BPs and CRs for LB10

The Fig. 5.5 shows the variation of CP for biodiesel blend LB10 concerning the crank angle at different CR and BP. The change is more in the CPMax. of LB10 as compared to PD. This could be because of inbuilt oxygen, and cetane number of blends enhances the combustion of biodiesel blends. This is further augmented by boost pressure and CR, which compensate the higher density, viscosity, and bulk modulus and improves the combustion efficiency of blends. This results in higher CPMax. However, at CR 14, during more extended ignition delay period more amount of fuel has mixed in boosting condition and has the erratic operation as indicated in the Fig. 4.5.

Similarly, the further improvement observed in the higher blends of biodiesel LB20 and LB30 as shown in Fig. 5.6 and 5.7 respectively. These improvements in higher blends of biodiesel due to enhanced turbulence and mixing at boost pressures, inbuilt

oxygen and comparatively good compression ratio lead to complete combustion of fuel at premixed and relatively better combustion in the latter stage of combustion. From the figures, it noted that all biodiesel blends does not exhibit the smooth burning at CR 14. This could be because of longer ignition delay and boost pressure slightly reduces it but during this duration more amount of fuel mixed with air and burns violently with high heat and temperature release that showed in a later stage in net heat release discussions.

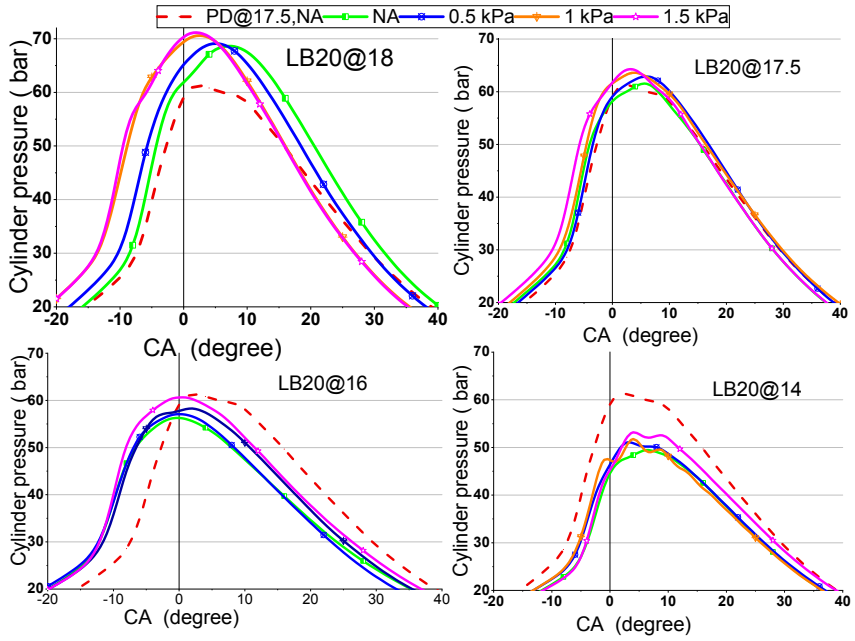

Fig. 5.6 Variation of in-cylinder combustion pressure at different BPs and CRs for LB20

Table 5.1 Percentage improvement of CPMax. over PD @CR17.5, NA at full load

CR	CPMax. % Improvement in PD				CPMax. % Improvement in LB10			
	Boost pressure in kPa (g)				Boost pressure in kPa (g)			
	NA	0.5	1	1.5	NA	0.5	1	1.5
18	0.36	1.42	3.23	7.77	13.6	13.92	15.57	18.89
17.5	--	1.21	5.89	6.79	1.27	3.3	5.03	6.58
16	-12.01	-9.22	-7.88	-6.43	-9.73	-6.68	-3.9	-3.02
14	-24.81	-21.65	-19.9	-19.33	-20.19	-19.33	-17.25	-18.05
	CPMax. % Improvement in LB20				CPMax. % Improvement in LB30			
18	12.01	12.78	15.16	16.13	13.52	14.72	16.31	17.17
17.5	0.39	2.66	3.92	5.06	7.84	8.29	10.14	11.48
16	-8.13	-6.79	-4.85	-1.03	-3.71	-3.09	-2.09	-2.15
14	-19.31	-16.73	-15.51	-13.17	-17.71	-15.88	-14.90	-12.60

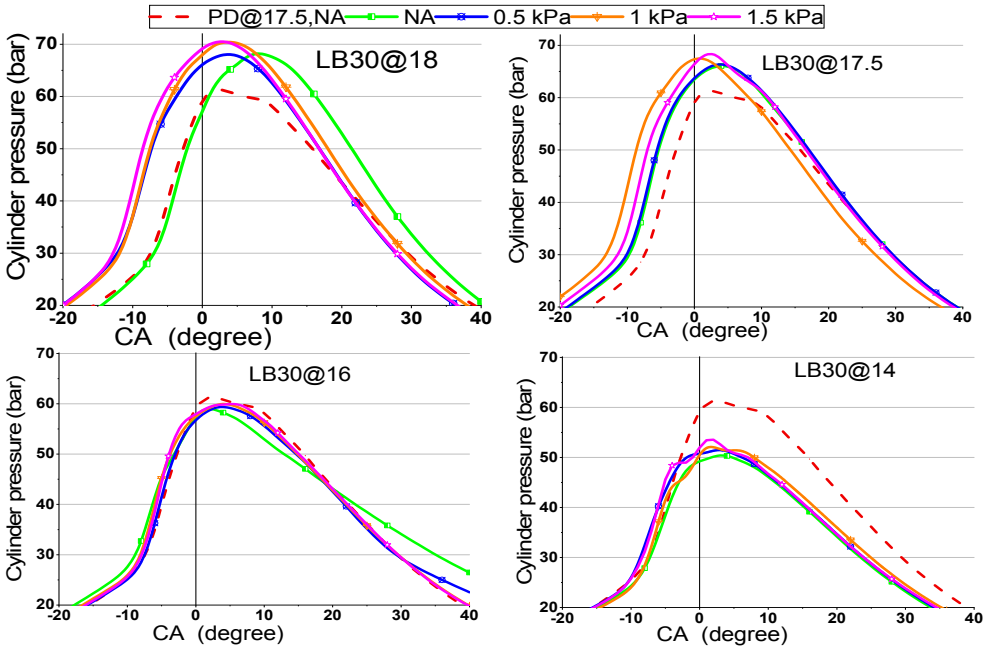

Fig. 5.7 Variation of in-cylinder combustion pressure with BPs and CRs for LB30

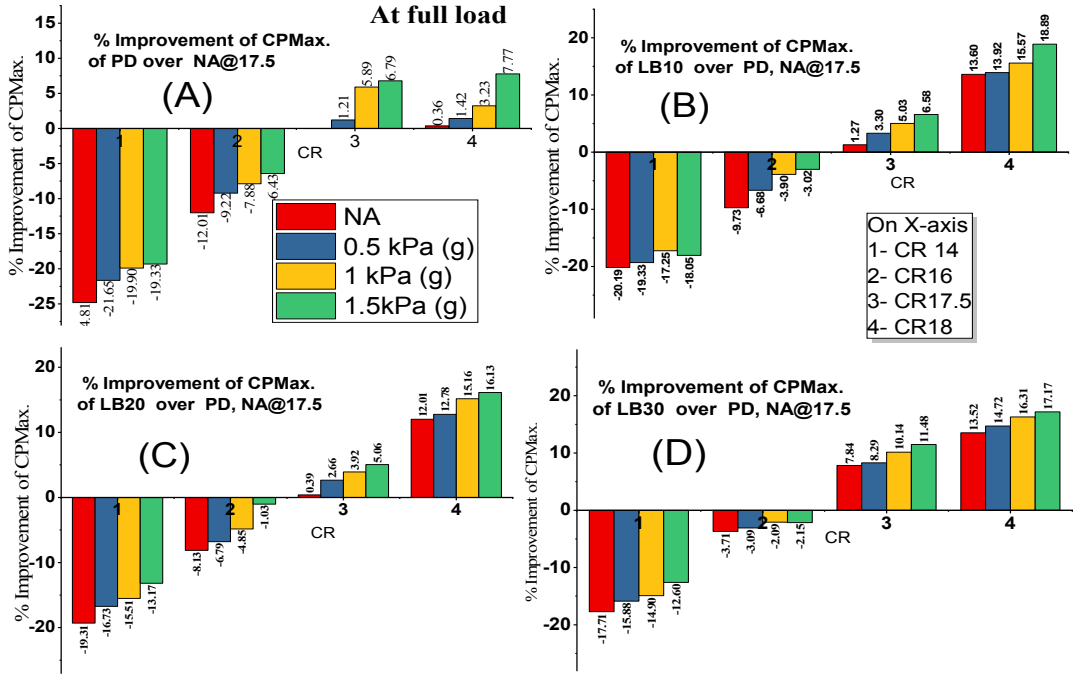

Fig. 5.8 Percentage improvement of CPMax. over @17.5, NA at full load

The percentage improvement of CP over standard operating condition are calculated and tabulated in Table 5.1 for all tested fuels and plotted in the Fig. 5.8. It is noted from the results that percentage improvement increases with increase in compression ratio, boost pressure, and a fraction of biodiesel in the blends. With the increase in these parameters enhanced in-cylinder pressure, temperature, intensive turbulence,

and mixing, inbuilt oxygen, higher cetane number in the blends are responsible for better combustion leads to higher in-cylinder pressure.

5.3.2.2 Effect on rate of pressure rise of PD, LB10, LB20, and LB30

The Fig. 5.9 shows the variation of the rate of pressure at different boost pressures and compression ratios for PD. The variation of the rate of pressure rise indicates the health engine in running condition. The rate of pressure rise increases with increase in CR, and boost pressures. The CR increases in-cylinder pressure, temperature and boost pressure increases the quantity, density, temperature, and turbulence of air leads to better mixing and atomization results in higher rate of pressure rise. As a result, fuel burns smoothly and efficiently at higher CR, boost pressure. However, at rated CR, it shows an erratic rate of pressure rise. This could be because of additional fuel mixed before the end of premixed combustion.

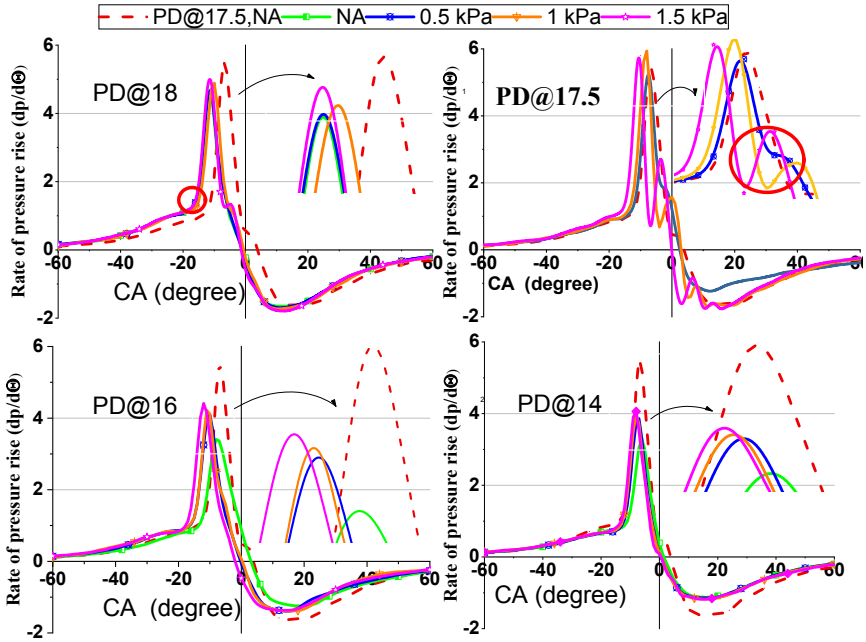

Fig. 5.9 Variation of the rate of pressure rise at different BPs and CRs for PD

The RPR for LB10 blend represented in Fig. 5.10 and it increases with increase in CRs and boost pressures with peak value advancing as compared with PD. The higher operating CR, of LB blends, leads to the fine spray particles at a wider angle, higher fuel charge pressure, temperature, and density than PD fuel. In addition to this, a higher value of cetane number of LB blends corresponds to early injection and combustion with relatively shorter ignition delay. The Boost pressures further

increase the amount of fuel mixed in the air and charge temperature. At CR 18, round highlighted circle shows the early start of diffusion combustion, similarly at CR 17.5 and 14. However, at CR 14, it has many small peaks in diffusion combustion indicates the fuel is mixing fast before the end of first part of mixed fuel combustion.

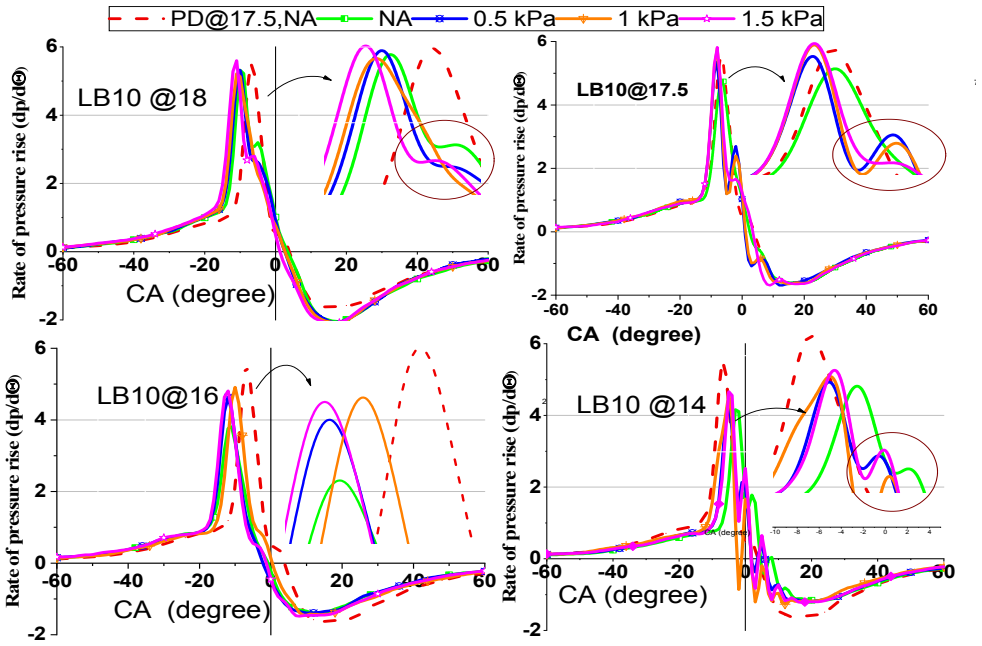

Fig. 5.10 Variation of the rate of pressure rise at different BPs and CRs for LB10

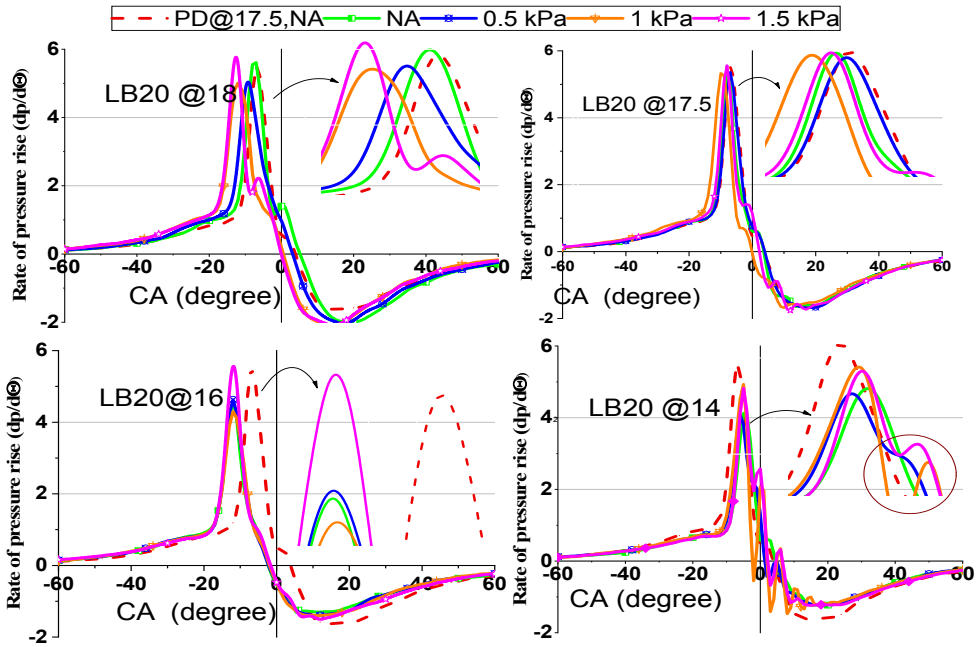

Fig. 5.11 Variation of the rate of pressure rise at different BPs and CRs for LB20

At higher blend LB20, the RPR is smooth and increases with BP and CR as shown in Fig. 5.11. Due to injection of more mass and burning of it, it has the higher rate of

pressure rise. This increased pressure rises from low to high because of the partial effect of CR and mostly dominated by the boost pressure at lower CRs. Furthermore, with higher blend LB30 the effect of boost pressure is dominant at lower compression ratio as shown in Fig.5.12. The improvement in RPR of LB30 is better at lower CRs 16 and 14. This could be because of at lower CR the fuel injection is more and boost pressure, oxygen molecules, and cetane number improves the burning of fuel, results in a rate of pressure rise.

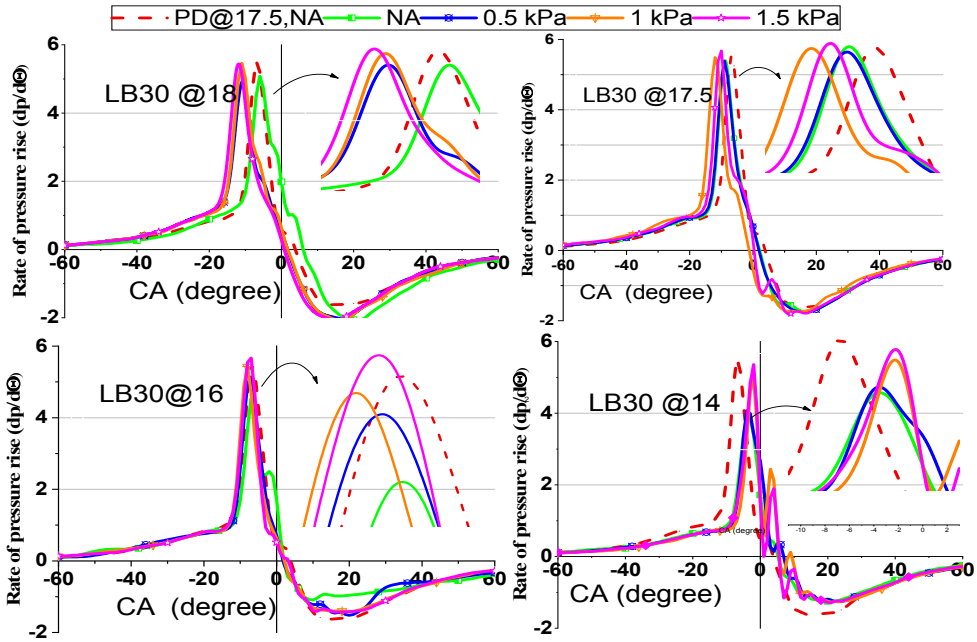

Fig. 5.12 Variation of the rate of pressure rise at different BPs and CRs for LB30

5.3.2.3 Effect on net heat release rate of PD, LB10, LB20, and LB30

At CR 18, NHR for NA reduces due to high CR ID is lower; the lesser mass of fuel burned and increased latent heat of vaporization at higher CR owing to less peak heat release rate. With increasing BPs; high turbulence of air further decreases the ignition delay and improve the combustion efficiency leads to increase in advanced NHR. The value of NHR for PD at CR17.5, NA is 43.31 J/deg. at -7 ^{0}CA and for CR 18 is 37.67 J/deg., 38.04 J/deg., 38.8 J/deg., and 41.99 J/deg. at NA, 0.5 kPa, 1 kPa, and 1.5 kPa boost pressures respectively.

At rated CR17.5, due to increase in BPs, reduction in ID and increase in the NHR observed as 11.91%, 21.6%, and 22.3% respectively for 0.5,1 and 1.5 kPa (g) boost pressures. With the decrease in CR, the mass of fuel injected is more, more

volumetric efficiency and mechanical loss, as well as loss of heat from the cylinder, is less. This leads to increase in NHR due to the vast mass of fuel burned more efficiently in premixed combustion phase at lower CR with boost pressures and almost equals the NHR with the standard operating condition as represented in the Fig. 5.13. From the figure, it also observed that the diffusion combustion heat release is less at all CRs and BPs except the rated CR 17.5. This could be because of at boost pressures fuel-air mixture becomes lean and burns slowly with longer combustion duration.

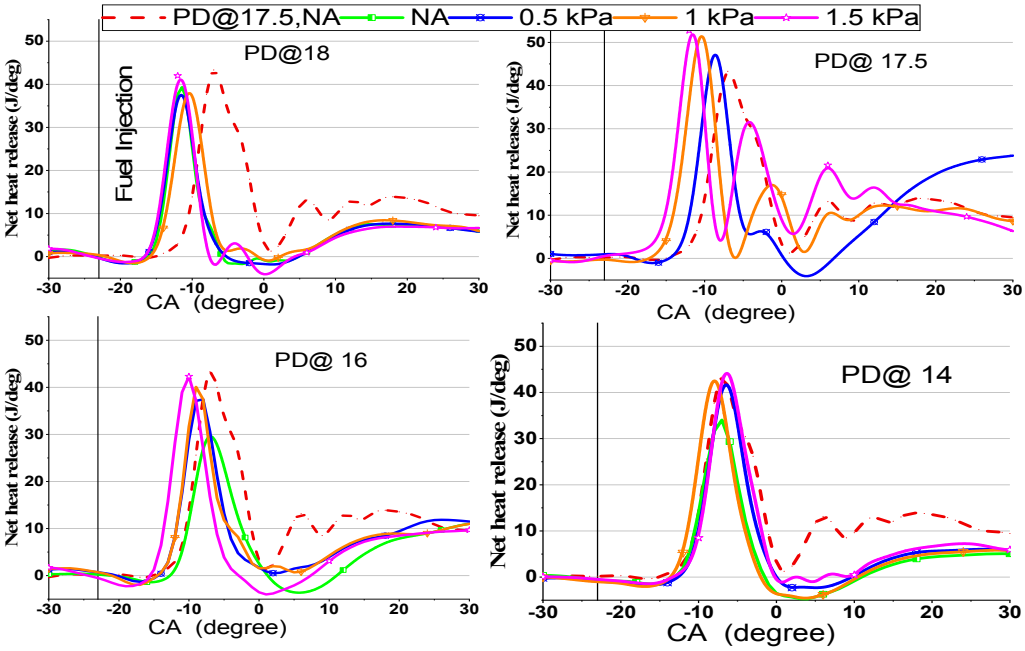

Fig. 5.13 Variation of net heat release rate of PD at different BPs and CRs

The Fig. 5.14 shows the variation of NHR for biodiesel blend LB10. At all CRs the NHR is higher than the baseline fuel, and it is increasing with decrease in CR and rise in boost pressure. At NA operating condition the NHR increases with increase in CR and at lower CR longer ignition delay and hence burns the more fuel and ultimately has the more NHR. The advantage of boost pressures is more at lower CRs. We can observe the more NHR and smooth operation at CR. However,later stage of combustion, i.e., diffusion phase may not correctly burn due to the extra air of boost pressure forms lean air-fuel mixture emits the HC,CO more than PD but less than its natural aspirated condition of its own.

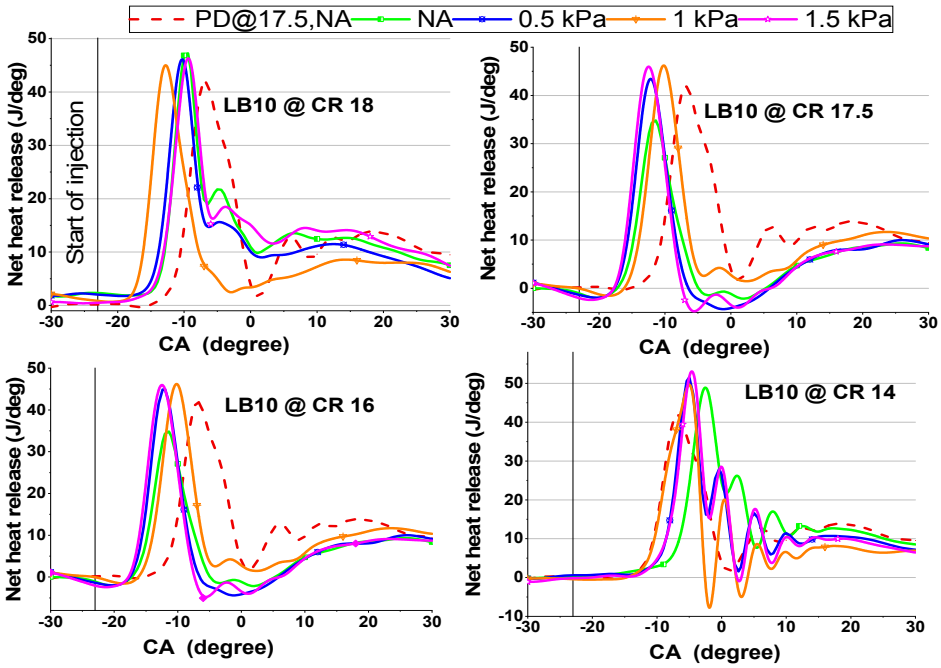

Fig. 5.14 Variation of net heat release rate of LB10at different BPs and CRs

The Fig.5.15 presents the effect of boost pressure in the NHR graphs for LB20. In spite of lower calorific value, the NHR of LB20 increases with increase in boost pressure and decrease with increase in CR. However, in all cases, maybe NA or boost pressure operated engine NHR of LB20 is higher than the baseline fuel. Higher blends of biodiesel inject more fuel due to higher density and inbuilt oxygen molecules, cetane number exhibits the efficient combustion and further improves with BPs leads the more amount of heat release in premixed combustion phase. Hence, it can be concluded that higher blends of biodiesel can be efficiently used in the supercharged engine.

The Fig. 5.16 shows the similar kind of high NHR exhibited by the further higher blend of biodiesel LB30. The net heat release rate of LB30 is increased at NA condition only at CR18, and 17.5 and further at CR 16, 14 decreased due to improper mixing and atomization. However, with an increase in boost pressures, it also increases because of higher volumetric efficiency,density, and turbulence of air.At all boost pressure, it increases with a decrease in CR.

The percentage improvement of all tested fuel's NHR as compared PD at the standard operating condition CR 17.5 are tabulated in Table 5.2. The highest improvement observed for LB30 at a boost pressure of 1.5 kPa (g) is 49.76% at CR 14. The maximum improvement for LB20, at CR16 and 1.5 kPa (g) is 38.33% and LB10 is

25.61% at CR14 and 1.5 kPa (g). For the baseline, PD is 21.68% at rated CR and 1.5 kPa (g).

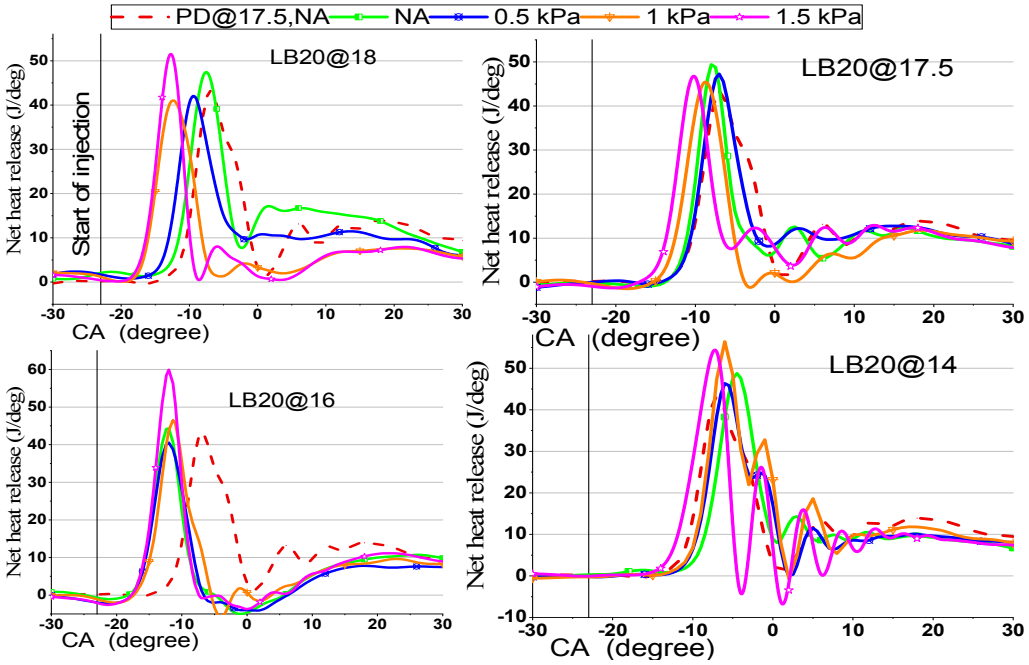

Fig. 5.15 Variation of net heat release rate of LB20 at different BPs and CRs

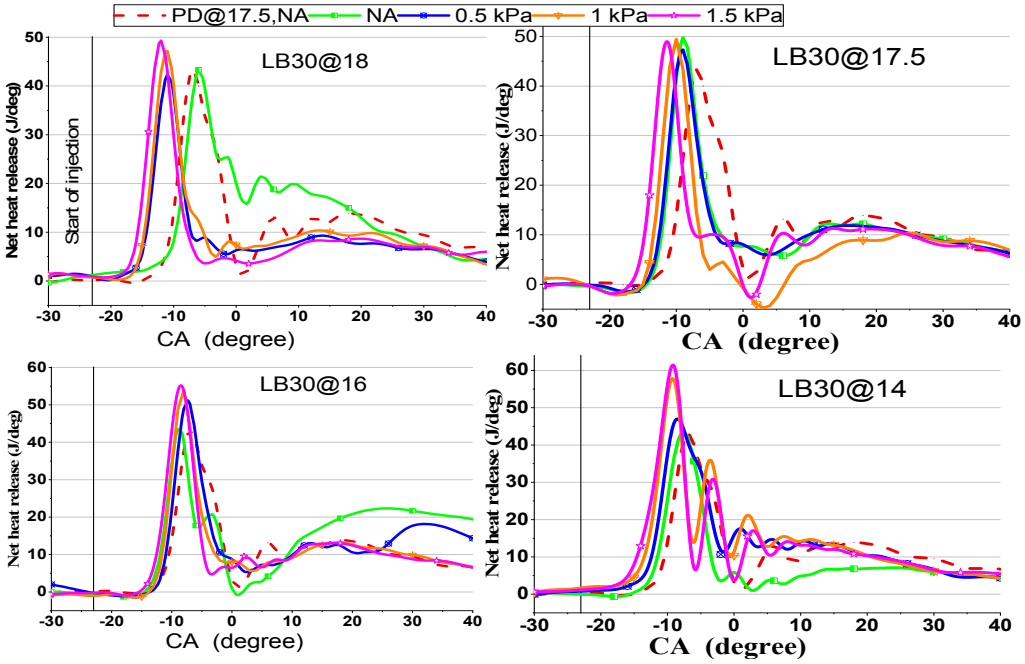

Fig. 5.16 Variation of net heat release rate of LB30 at different BPs and CRs

Table 5.2 Percentage improvement of NHRMax. over PD @CR17.5, NA at full load

CR	NHRMax. % Improvement in PD				NHRMax. % Improvement in LB10			
	Boost pressure in kPa (g)				Boost pressure in kPa (g)			
	NA	0.5	1	1.5	NA	0.5	1	1.5
18	-13.02	-12.17	-10.41	-3.05	8.15	10.69	7.85	10.07
17.5	---	11.91	22.30	21.68	4.09	8.43	18.96	20.23
16	-29.90	-13.48	-7.46	-2.29	-20.80	3.88	10.27	7.16
14	-21.45	-2.49	2.17	4.09	14.18	18.98	20.71	25.61
	NHRMax. % Improvement in LB20				NHRMax. % Improvement in LB30			
18	10.81	-1.27	-4.39	23.53	7.67	3.60	3.97	5.75
17.5	14.13	9.19	7.69	11.89	14.87	9.21	14.11	15.95
16	2.33	-6.40	5.40	38.33	0.55	16.14	24.64	29.05
14	9.95	6.97	31.82	30.27	21.01	8.64	40.08	49.76

In general, at all boost pressures, the improvement increases for all fuels at all CRs. For PD, at CR14, 16, shows the limited improvement because of lower CR and its properties. The % improvement increases with lowering of CRs and with increasing the fraction of biodiesel in the blends. This could be because of boost pressure is dominant with biodiesel blends. It also noted that for all biodiesel blends with increasing CR premixed combustion phase decreases and diffusion phase of combustion phase improves. This could be a reason for high NOx and HC emission at decreasing CR and increasing fraction of biodiesel.

5.3.3 Effect on performance parameters of all tested fuels

Foranalysis, the performance parameters considered are brake specific fuel consumption (BSFC), brake thermal efficiency (BTE), and exhaust gas temperature (EGT).

5.3.3.1 Effect on brake specific fuel consumption (BSFC)

The Fig. 5.17 (a) depicts the brake specific fuel consumption (BSFC) for PD operated at rated compression ratio (CR) 17.5 and at different loading conditions varying from 20% to 100% for all boosting pressures i.e. NA, 0.5 kPa(g), 1 kPa(g), 1.5 kPa (g). It is observed that at NA, BSFC decreases with rising in load due to improvement in-

cylinder pressure and temperature. With the rise in BPs, the BSFC decreases, the improvement is more at low load, and it decreases with load and maximum percentage improvement observed was 44.79% for BP 1.5 kPa (g) at 20% load. Due to the rise in boosting pressure the noted improvement in combustion efficiency of fuel results in an increase in mechanical efficiency, effective torque, and brake power.

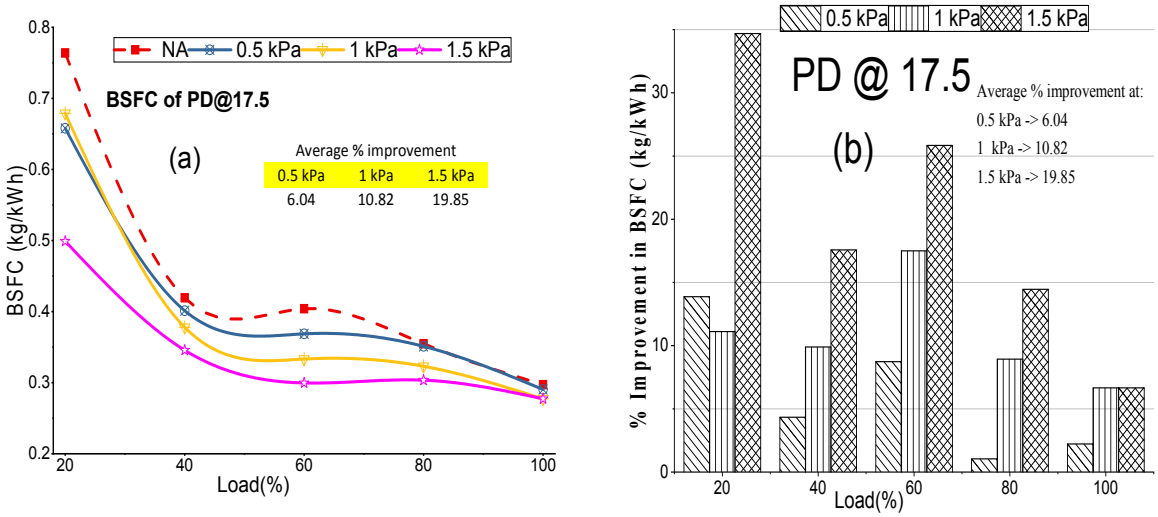

Fig. 5.17 Variation of BSFC with a load for PD at CR 17.5

Also due to the increased volumetric efficiency, density, and turbulence of inlet air improve the lean combustion as shown in the figure. At high load, the effect of supercharging is less as compared to low and medium load.

In the Fig. 5.17(b) presented the percentage improvements (reductions) of BSFC for boosting pressures over NA at CR 17.5. The percentage improvement increases with the boosting pressure, and it is higher at low and partial loads. In the Fig. 5.17(b) demonstrated the percentage improvements (reductions) of BSFC for boosting pressures over NA at CR 17.5. The percentage improvement increases with the boosting pressure, and it is higher at low and partial loads.

At low and partial loads, BP increases the temperature and density of air, high temperature may slightly affect the density, but in overall enhances the combustion of fuel. This increased combustion efficiency of fuel needs the lesser quantity of fuel for developing the required power at the particular load.

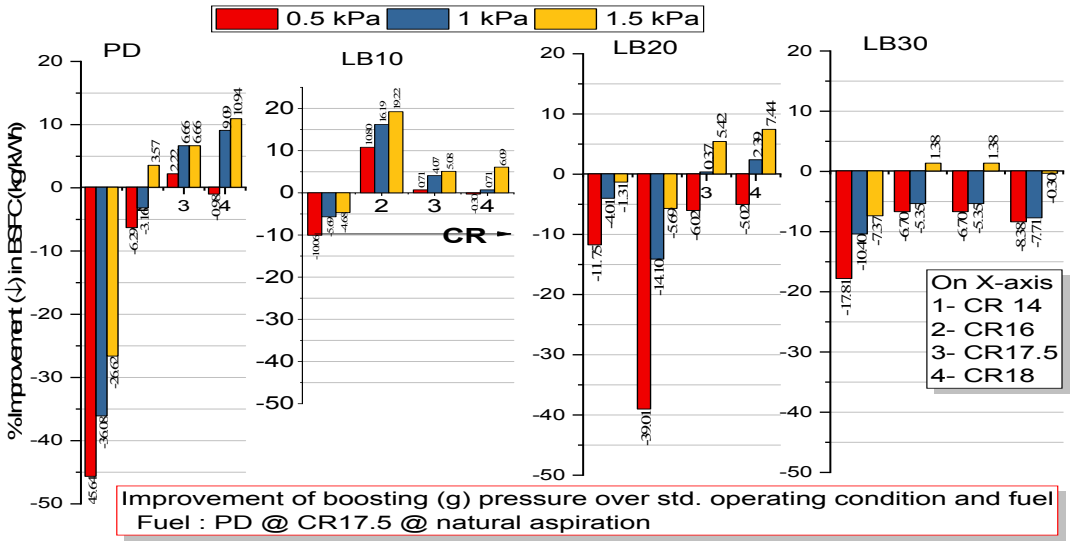

Fig. 5.18 Percentage improvement in BSFC (kg/kW-h) for all fuels at full load

The Fig. 5.18 shows the percentage improvement of BSFC of all tested fuels at full load with varying CRs and BPs over the baseline fuel PD at the standard operating condition. For PD at lower CR 14, the BSFC was 45.64%, 36.08%, and 26.62% higher at three boost pressures 0.5, 1, and 1.5 kPa (g) respectively. At lower CR, the ID is longer, in-cylinder pressure, the temperature is low, and hence the fuel burns inefficiently results in the more amount of fuel for developing the unit power. However, with increasing the BP the high volume and density of air improve the mixing and atomization owing to a reduction in fuel consumption as seen clearly from the figure. At CR16 and onwards the effect of CR increases the in-cylinder pressure, temperature and further conducive environment due to boost pressures reduce the fuel consumption. At CR 18 and 1.5 kPa (g), the maximum observed BSFC reduction of 10.94%.

For biodiesel blend LB10, the physical and chemical properties nearly same as of PD. The presence of oxygen molecules and cetane number further improves the combustion efficiency of biodiesel. Hence the significant reduction is noted at all CRs, and maximum reduction was at rated CR 17.5 as 19.23% at 1.5 kPa (g) boost pressure. In addition to this, further blends LB20 and LB30 showed the improvement at increasing CR and BP, but due to lower calorific value, higher density and viscosity these blends have the higher BSFC except at CR 17.5 and 18 at boost pressure 1.5 kPa (g). The percentage reductions as seen from the figure at CR 17.5and 18 are 5.42%, 7.44% and 1.33%, 1.38% respectively at boost pressure 1.5 kPa (g). This lessening of

BSFC could be because of high effective combustion and thermal efficiency (Ma, Z. *et al.*, 2012).

5.3.3.2 Effect on brake thermal efficiency (BTE)

The BTE increases with load and boosts pressure for PD at CR 17.5 as presented in Fig. 5.19 (a & b). The improvements in BTE are higher at low and medium loads, and it is more at BP 1.5 kPa and supported with an observation of BSFC improvements. The inlet charge pressure, cylinder pressure increases owing to compression of residual gases present in the clearance volume. This positive effect of parameters facilitates the additional filling of air and increase in density and volumetric efficiency and real gas exchange results in further increase in power and BTE.

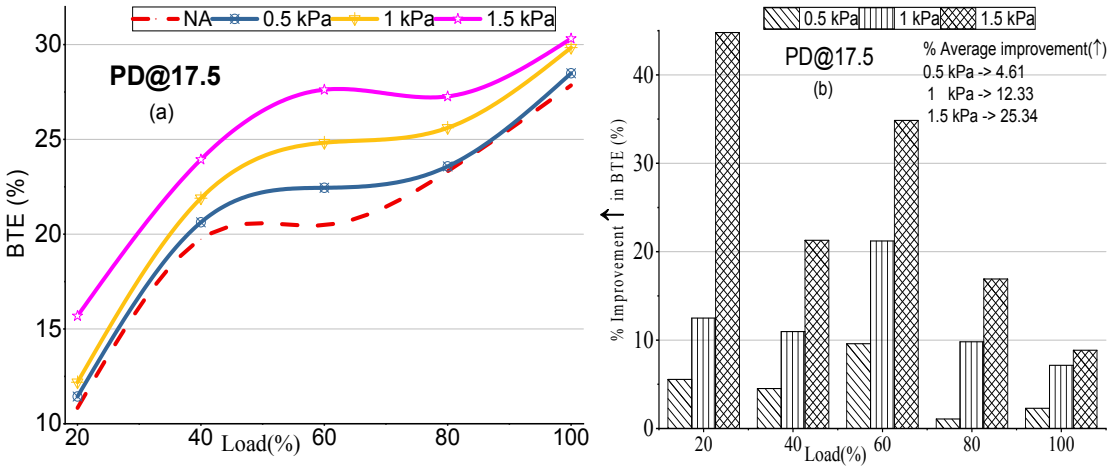

Fig. 5.19 Variation of BTE for PD with load and BP at CR 17.5

In Fig. 5.19 (b) presented the percentage the percentage improvements of BTE at BPs over NA at all loads. The improvement in BTE decreases with increase in load and increases with BPs. With an increase in load, in-cylinder pressure and temperature gradually becomes influential and decreases the effect of boosting pressure. The BP increment causes the reduction in friction loss due to positive gas exchange process and significant reduction of pumping losses. The maximum percentage improvement in BTE was 44.8% at 20% load and average percentage improvement observed for all loads at 0.5,1,1.5 kPa (g) were 4.67 %, 12.33%, and 25.34% respectively.

The Fig. 5.20 depicts an improvement in BTE for all tested fuels at full load concerning BP and CR. This figure shows the combined effect of BP and CR on BTE. The improvement in BTE observed for fuels at all BP and CR irrespective of the type of fuel. For PD fuel, at CR 14, due to lower CR, the in-cylinder pressure and

temperature were not sufficient to burn the fuel entirely at NA has adverse effects, and it is improved with an increase in BPs 0.5, 1, 1.5 kPa (g) but was less than the rated BTE. At CR 16, relatively higher pressure and temperature further supplemented by the BPs and observed improvement in BTE was more, maximum 3.73% at 1.5 kPa (g). This further rise with an increase in CR due to the favorable condition of rated CR and BPs and the improvement was noted 8.66% and 12.3% higher at 1.5 kPa (g) for CR 17.5 and 18 respectively.

For biodiesel blends, the maximum improvement observed in case of LB10 due to its physical and chemical properties nearly same as the PD. The high density and viscosity of biodiesel blends compensated by high CR and the boost pressure. Hence higher CR results in the increase in BTE in spite of lower heating value. The maximum rise in BTE at CR 16 for LB10 was 18.98% at 1.5 BP. Further increase in the fraction of biodiesel in the blends BTE improvement was little bit decreases as compared to LB10 and PD. In spite of the improvement in combustion efficiency at higher blends such as LB20 and LB30, it is not converting into the useful work results lower improvement than the expected (Karabektas, M., 2009).

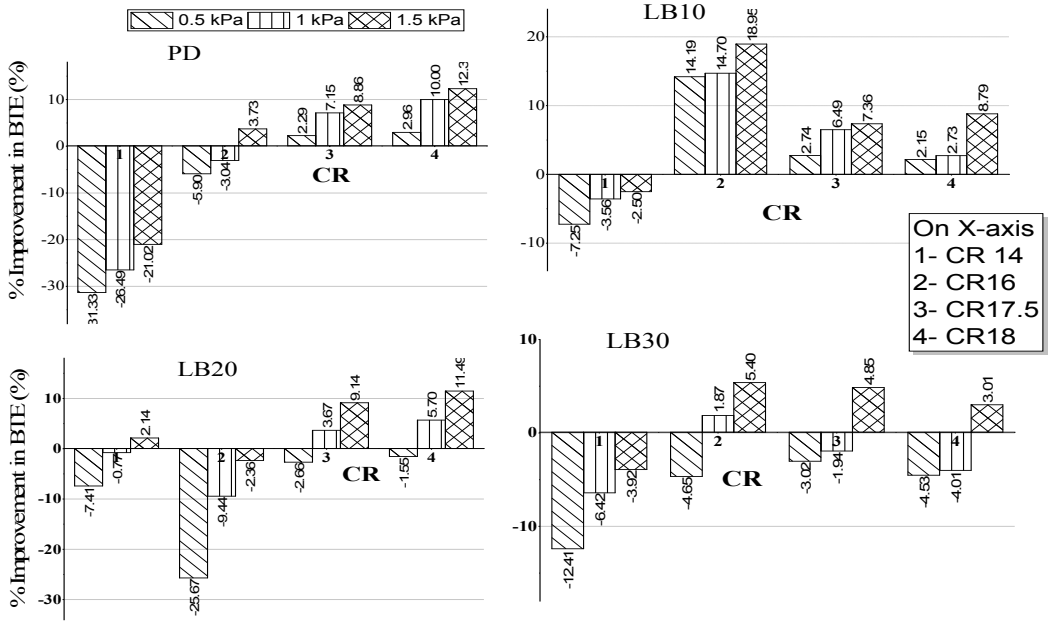

Fig. 5.20 Variation of % change in BTE with BP and CR at full load

5.3.3.3 Effect on exhaust gas temperature (EGT)

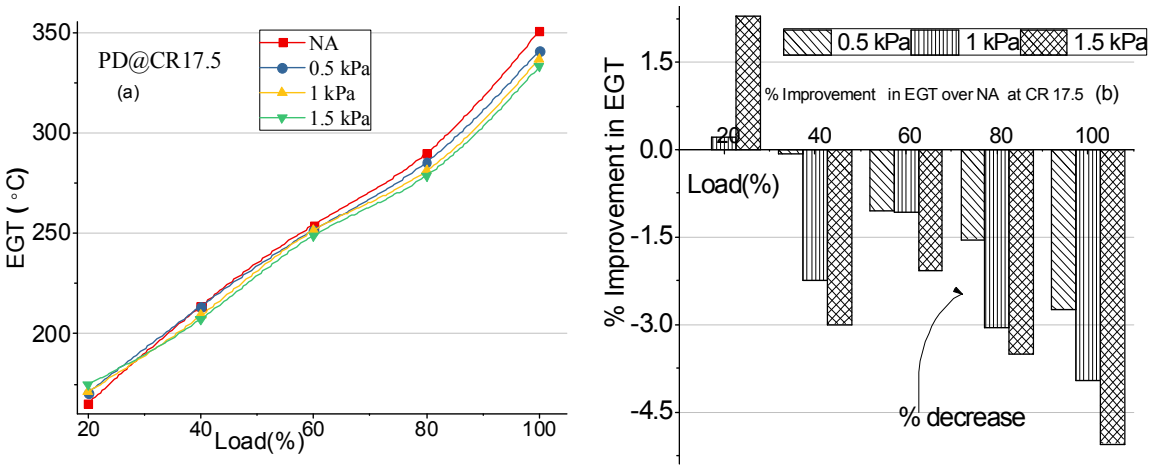

Fig. 4.21 Variation of EGT for PD with load and BP at CR 17.5

The exhaust gas temperature (EGT) indicates how efficiently fuel's energy has been utilized to convert into mechanical energy inside the cylinder. Higher exhaust gas temperature means wastage of energy by late combustion of fuel during the expansion stroke and exhausted without being utilized. The Fig.5.21 (a) depicts the EGT at rated CR 17.5 for PD. It is found that effect of BP increases the EGT at 20% load only and at all subsequent loads it has decreased with increase in BPs. The increase of EGT at 20% load could be because of improvement in first and later stage of combustion (diffusion) and at the middle of the expansion stroke. Hence, even though improvement in combustion efficiency due to boosting pressure it is not utilized efficiently and lost as exhaust gas temperature. However, in the later stage of loading conditions, it is decreased with increase in boosting pressure. This could be because of advancement of combustion towards TDC and efficientlyutilized the energy.

The Fig. 5.21 (b) illustrated the percentage change of EGT due to BPs as compared to NA at each load. At 20% load maximum increase in exhaust gas temperature was 2.3% at 1.5 kPa (g). Further increase in load, the EGT reduces with the BP due to increase in air turbulence and effective thermal efficiency η_{eff}.

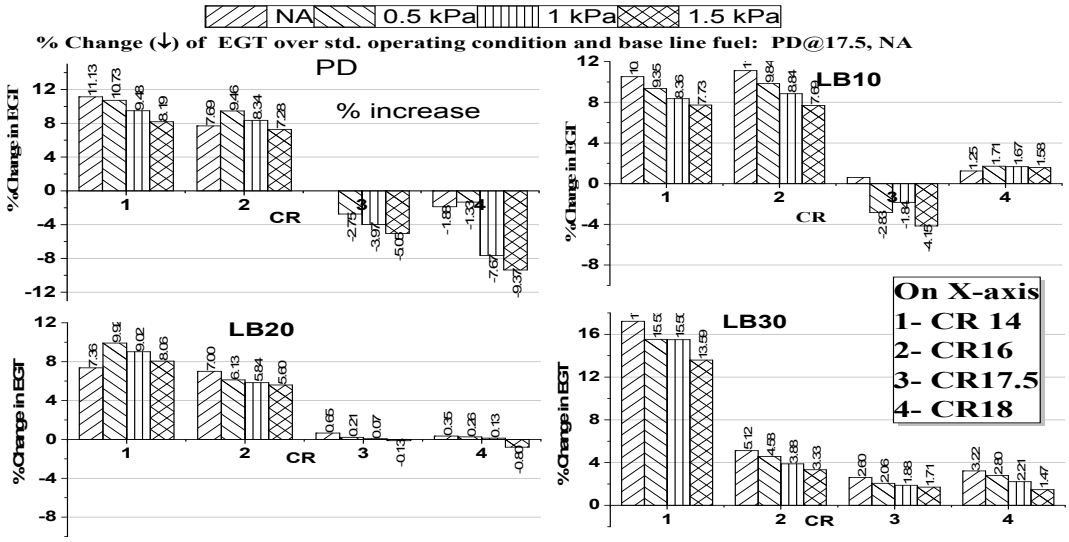

Fig. 5.22 Variation of % change in EGT with BP and CR at full load

The Fig. 5.22 illustrates exhaust temperature variations for all tested fuels concerning CR and boost pressures. The EGT of tested fuels decreases with increase in CR due to shifting of combustion duration left side, i.e., before TDC and with an increase in BPs, the extra air may lean air-fuel mixture and produce the cooling effect on burned gases leads to low EGT. The more efficient combustion of PD due to its low density, viscosity, and high heating value leads to the more % reduction. In biodiesel blends, it increases the amount of biodiesel in the blends. With the increase in the fraction of biodiesel in the blends, the presence of oxygen molecule and cetane number of fuel improves bothphases of combustion, and higher EGT is mainly due to improvement in the diffusion combustion phase. The maximum percentage reduction in EGT for PD, LB10, and LB20 was 9.37%, 4.15%, and 0.8% respectively. However, for LB30 the minimum percentage increases in EGT by 1.47%.

5.3.4 Effect on emission characteristics of all tested fuels

The emission characteristics for analysis considered are carbon monoxide (CO), hydrocarbons (HC), carbon dioxide (CO_2), NO_x, and smoke opacity with the variation of CR and boost pressure. The trade-off analysis of emissions of unburnt hydrocarbons and NO_x has been donefor selection of optimum boost pressure at each CR for each tested fuel.

5.3.4.1 Effect on carbon monoxide (CO) emission

The reduction in CO and HC emissions is the function of better combustion efficiency of fuel with increased boost pressure. For all tested fuels, the emission of CO is demonstrated in Fig. 5.23.

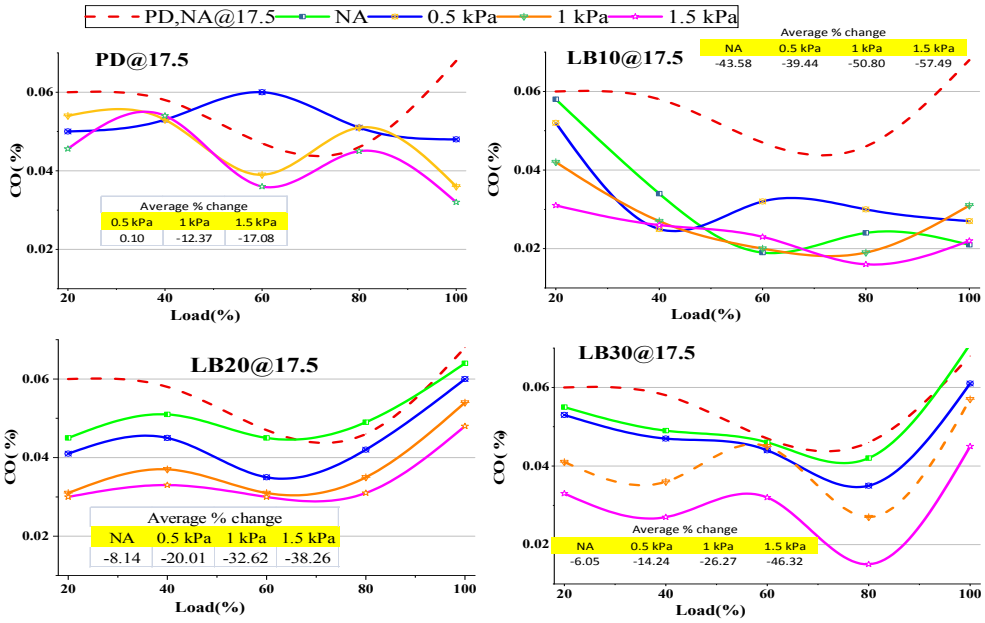

Fig. 5.23 Variation of CO emission for PD with load and BP at CR 17.5

It is found that, at low and higher load, the CO emission is more due to the too lean mixture at low load and comparatively rich mixture at higher load side. As the BP increases, there are more improvements at low load and further increased with the low level of improvements in load and BP. This could be due to the increased turbulence, density, and quantity of air which mixed with fuel and burns the fuel efficiently (Yoshimoto, Y., 2016). The emission of CO depends upon the fuel properties and its combustion characteristics. It reduces with an increase in BPs and fraction of biodiesel. Because of boost pressure, the extra air and inbuilt 11% oxygen molecules may further lead to excellent combustion and oxidation of CO to CO_2 reduce the emission of CO.This can be evidenced by the improvements in the brake thermal efficiency in these loads because of enhanced combustion leading to the low emission of CO.

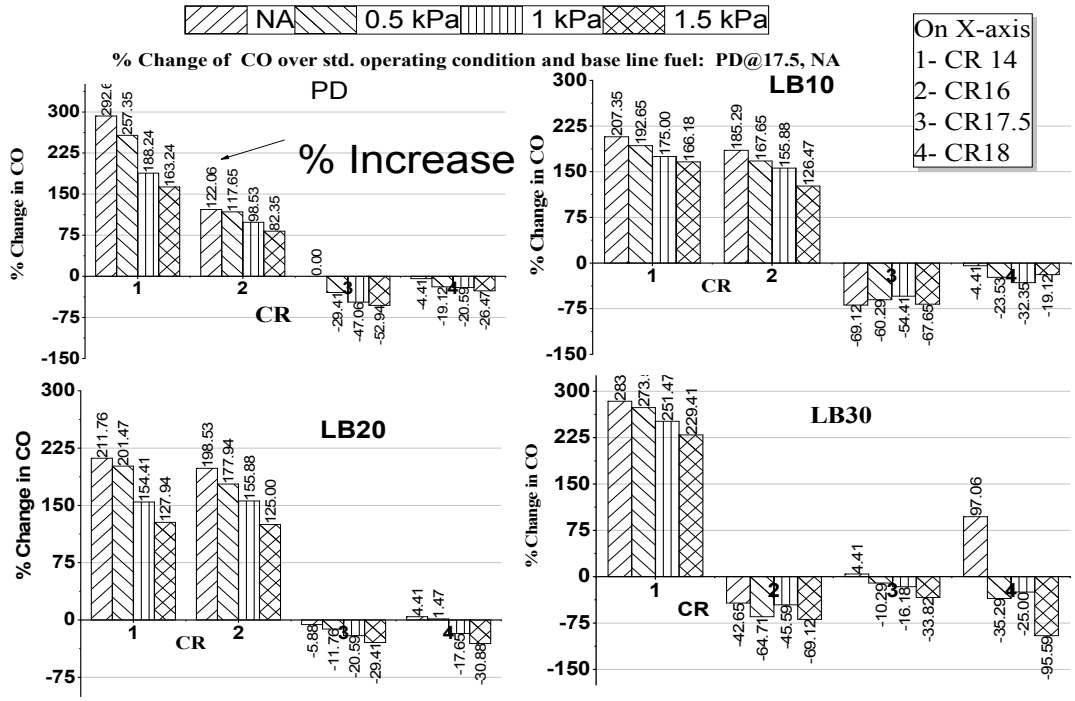

Fig. 5.24 Variation of % change in emission of CO with BP and CR at full load

The emission of CO decreases with increase in CR, BP, and a fraction of biodiesel as illustrated in the Fig.5.24. Ata higher value of CR, a fraction of biodiesel, the increased turbulence, density and temperature of combustion chamber burns the fuel more effectively at both phases of combustion owing to reduction of CO emission. Also at higher CR and BP, the oxidation of CO reduces its amount in the exhaust. However, at low CR, the emission of CO decreases with BPs, but more than the baseline fuel and also it higher for LB3O. At low CR and for higher blends of biodiesel had the atomization and vaporization difficulties owing to comparatively large CO emission. However, these difficulties further improved with BPs. The maximum percentage reduction of emission of CO for PD was 52.94% and for LB10 67.65% at CR 17.5 at 1.5 BP. For LB20 and LB30 was reduced by 30.88% and 95.59% respectively at CR18 and 1.5 BP.

5.3.4.2 Effect on hydrocarbon (HC) emission

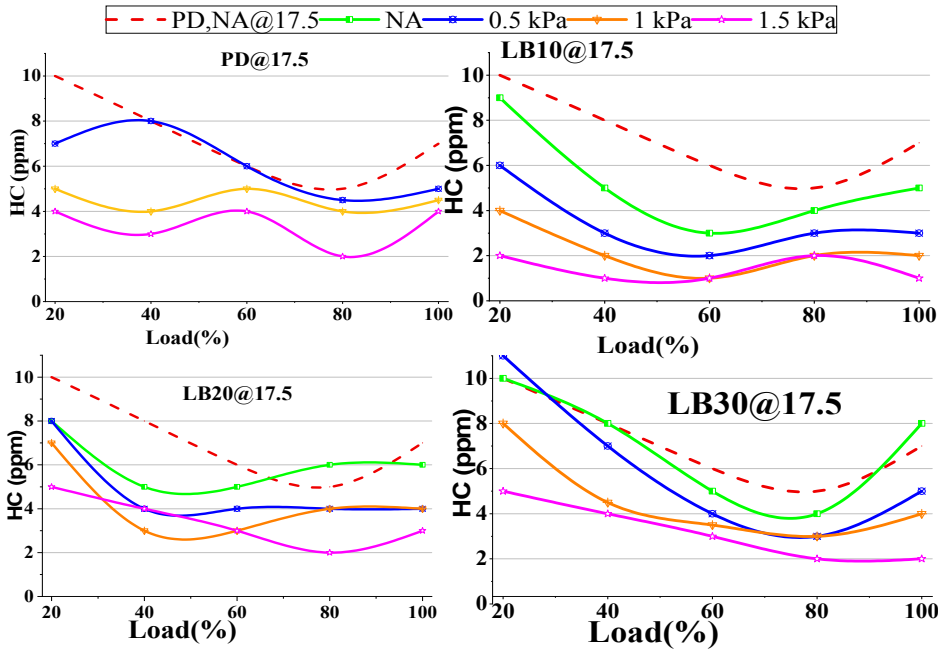

Fig. 5.25 Variation of HC emission for PD with load and BP at CR 17.5

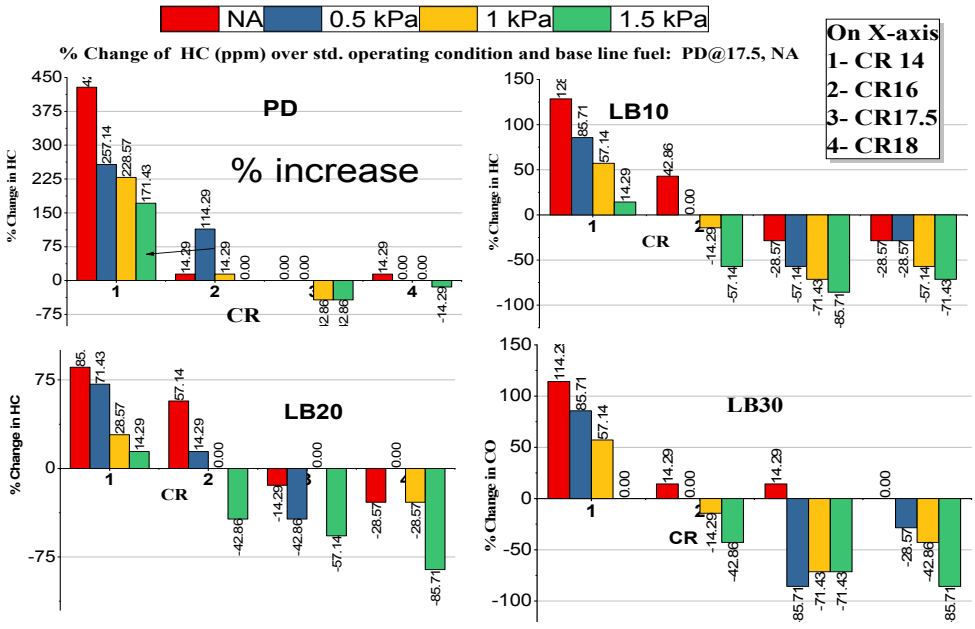

Fig. 5.26 Variation of % change in emission of HC with BP and CR at full load

Fig. 5.25 demonstrates the emission of unburnt hydrocarbons for all tested fuels. It decreases with increase in load and BP. This is obvious due to increase in cylinder temperature and pressure and intensive turbulence of air-fuel charge. The decrement

is further improved for biodiesel blends owing to oxygenated fuels and lower C/H ratio as compared PD.

The Fig. 5.26 demonstrates the % improvement in the emission of HC for all tested fuels concerning BP and CR. The emission of HC decreases with increase CR, BP for tested fuels. The improvement (% decrease) in the HC emission increases with the fraction of biodiesel in the blends. The inbuilt oxygen and cetane number of blends increases with the fraction of biodiesel in the blends has better combustion efficiency. The improvement in the emission of HC is varied from 40% to 86% for the CR varying from 16 to 18 for all boost pressures.

5.3.4.3 Effect on NO_x emission

The Fig. 5.27 shows the variation of NOx emission, plotted against a load at all boost pressures and CR 17.5. The NOx emission is the function of air-fuel ratio, combustion gas temperature, and oxygen content in the fuel. The NOx emission is rising with load and boosts pressure for fuels due to a favorable condition for complete combustion such as high temperature and pressure with the intensive turbulence of air-fuel mixture.

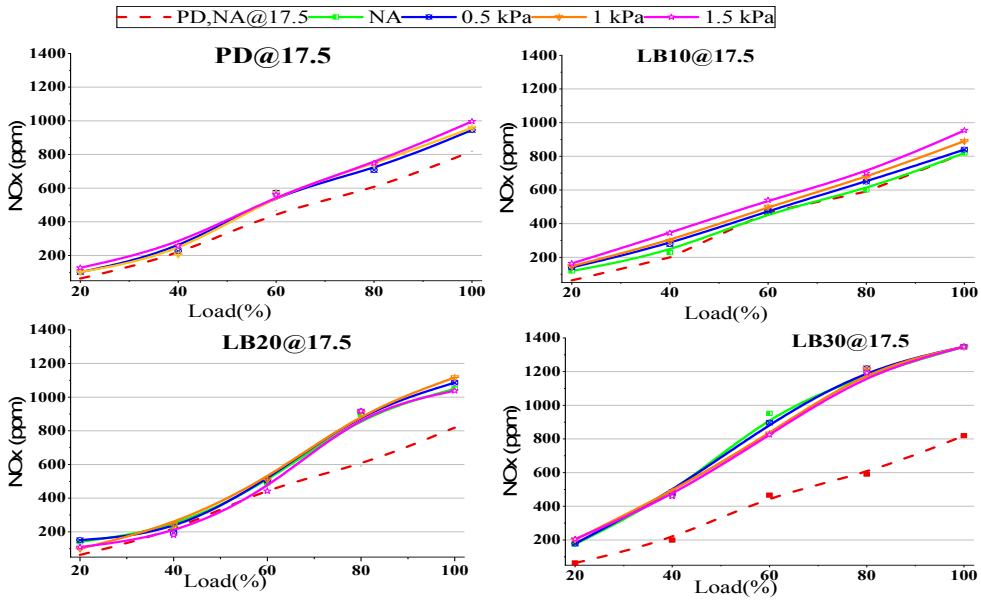

Fig. 5.27 Variation of NO_x emission for all fuels with load and BP at CR 17.5

The NO_x emission for PD and LB10 was practically same due to approximating of their physical and chemical properties. However, it increases with adding the biodiesel content in the blends. In the higher blends of biodiesel, the oxygen content

and cetane number are the primary parameters for causing the higher NOx emission. The oxygen present in the blends reacts with nitrogen in the air and forms NOx, and it is further being raised with BPs as compared to the naturally aspirated condition of the engine.

On an average, the percentage increase in the emission of NOx for biodiesel blends LB10, LB20, and LB30 was 21.19%, 43.45%, and 115.83% respectively at naturally aspirated condition over baseline fuel and rated operating condition. This further increased when the engine operated with boost pressures.

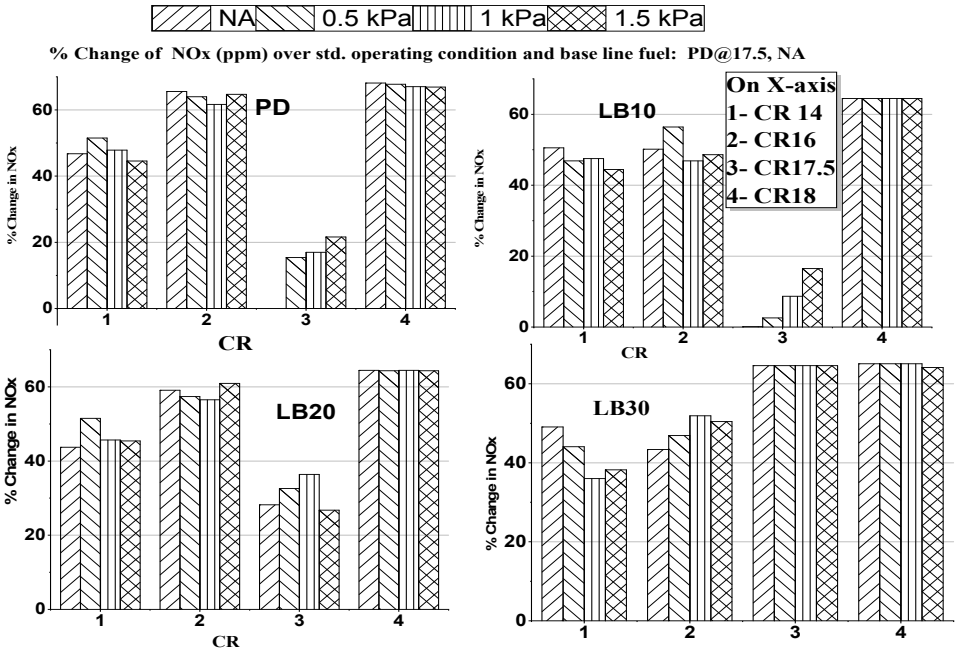

Fig. 5.28 Variation of % change in emission of NO_x with BP and CR at full load

The Fig. 5.28 depicts the % variation of NOx over baseline fuel PD operating at rated condition (CR17.5, NA, at full load). From the figure, it is observed that NOx emission increases with increase in CR except at rated CR17.5. With the increase in CR, the high value of in-cylinder pressure and temperature increases the combustion temperatureleads to the formation of higher NOx. However, it decreases with increase in the boost pressures for fuels PD, LB10, and LB20 up to the CRs 14, 16, and 17.5. The boost pressures force the extra air and effect in two way on the combustion phenomenon of fuels. Firstly, it shortens the ignition delay with intensive turbulence and mixing and secondly due to the extra air has the diluting effect and cooling effect on the remaining combustion gases which inhibits the further formation of NOx. For LB30 the higher density and viscosity injects the more amount and due to boosting air turbulence overtakes itsundesirablephysical and chemical properties and burns the

completely with high combustion efficiency, and it increases the NOx emission with CR and boosts pressure except at CR14. It is also noted that with a decrease in CR, the heat release rate in premixed combustion phase is high as compared to higher CR as shown in the combustion plots. However, the formation of NOx is lesser at low CR and higher at higher compression. For example, for PD, at CR18, in spite of lower peak NHR, the emission of NOx is higher. At this high CR, the impact of boost pressure isn't so convincing because of the low amount of air filling.Moreover, the dominance of CR initiates the early diffusion combustion at a sufficiently high temperature favorable for NOx formation. However, for biodiesel blends, at CR 18 fuel burns the comparatively more amount of fuel and fuels had the oxygen content and hence the in-cylinder combustion temperature, and heat release is high. At this high-temperature oxygen reacts with a vast amount of nitrogen present in the boosted air and forms the NOx. It is also noted at CR 18 NOx emission is high and almost same for all tested fuels due to dominant CR.

5.3.4.4 Effect on smoke (HSU) emission

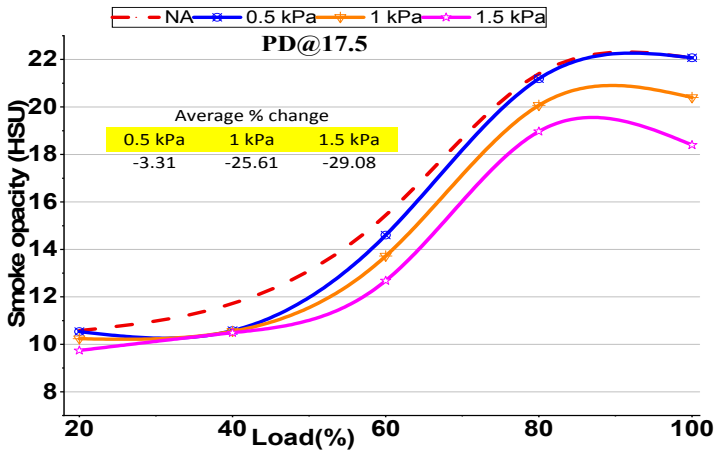

Fig. 5.29 Variation of smoke (HSU) at CR 17.5 for PD

The Fig 5.29 presents the variation of smoke emission for PD at rated CR17.5 for % engine loads and boost pressures. As usual, the smoke emission increases with increase in load and decreases with boost pressures. It is noted from the figure that smoke emission reduction is more and more with an increase in load. This higher amount of smoke emission reduction could be combined effects of high load and boost pressures facilitates the better combustion and responsible for higher NOx emission as well (Amba Prasad Rao, G. and P. R. Mohan, 2003; Ishikawa, N., 2012;

Ma, Z. *et al.*, 2012; Yoshimoto, Y., 2016).On an average, the percentage of smoke emission reduction was observed at boost pressures 0.5, 1, and 1.5 kPa (g) are 3.31%, 25.61%, and 29.08% respectively.

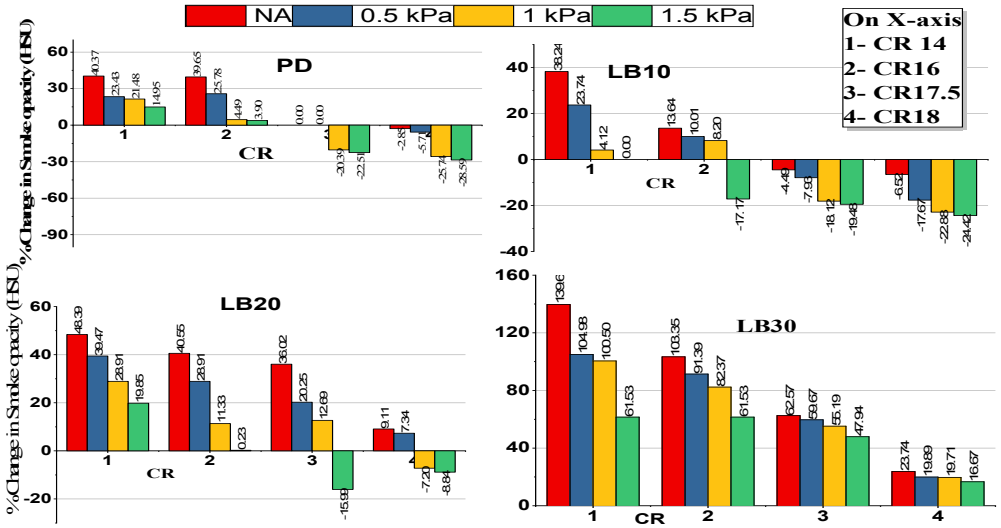

Fig. 5.30 Variation of % smoke (HSU) with BP and CR at full load

The Fig. 5.30 depicts the percentage change of smoke emission over baseline fuel PD operating at rated CR in naturally aspirated diesel engine for all fuel with CRs and boost pressures. The smoke is mainly produced in the diffusive combustion phase (Devan, P. K. and N.V. Mahalakshmi,2009). The figure shows the percentage improvement in emission of smoke is increases with increase in CRs and boost pressure. With the addition in biodiesel content in the blends the smoke emission increases hence in high blend LB30 has improvement in smoke due CR and boost pressure but in overall has the higher value than the baseline fuel. With the rise in biodiesel content, the higher viscosity, density, and lower volatility of biodiesel lead to difficulties in atomizing the fuel. However, boost pressure enhances the combustion of fuel but still has higher smoke emission. Lower BTE observed for higher biodiesels blends support this fact. Smoke is less at higher CR, and boost pressures, because of the heat of the compressed air and turbulence of air-fuel is high enough to cause complete combustion of fuel. At lower CR, temperature and pressure are low and further boost pressure dilutes the mixture in diffusion combustion leads to incomplete combustion of fuel. With the increase in CR from 14 to 18, the blends B10, B20, and B30 show the HSU comparable with baseline fuel PD, because of better combustion of

these fuel blends at all compression ratios (Amarnath, H. K. and P. Prabhakaran, 2012).

5.3.5 Effect on engine downsizing parameters

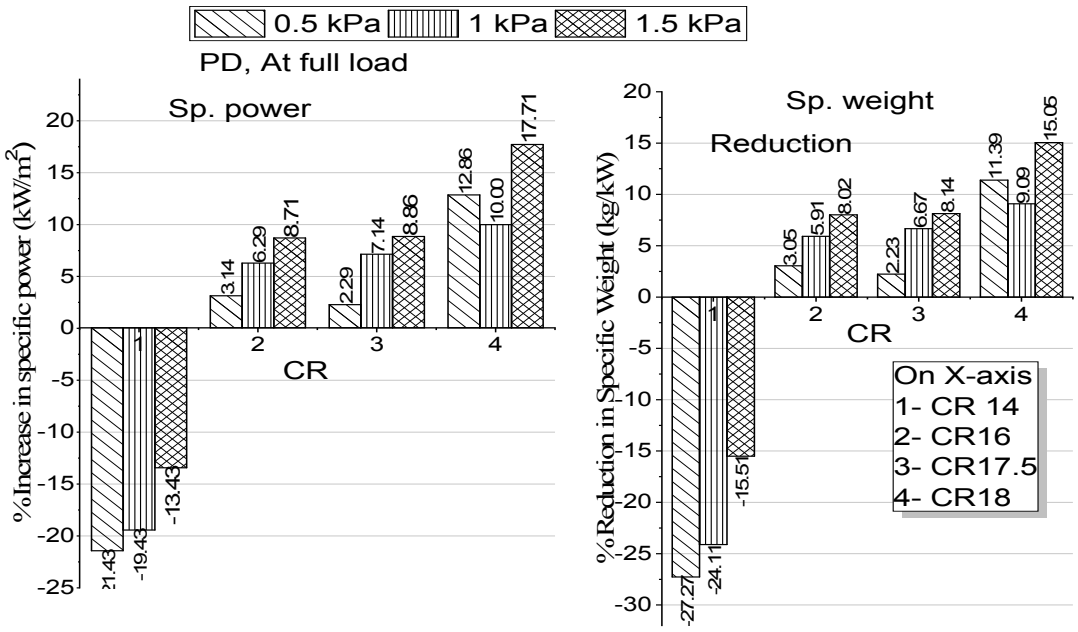

Fig. 5.31 Quantification of parameters for PD fuel

The economy of employing the supercharger for boosting purpose is calculated using the above-said equations 5.2, 5.3, 5.4, and 5.5. As compared to NA at rated CR, the percentage increase in specific power for all BPs and CRs at full loads are presented in the below given figures. The specific power reports how effectively, the piston area is exploited for developing the power irrespective of the size of cylinder. From the figure, it is noted that specific power of engine increases with BPs at all CRs and with the rise in CR; it grows up to 17.5 and slightly decreases. At CR 14, it shows the negative, means power improved but much less than rated CR17.5. At low CR 14, the diesel already has comparatively not as much of performance with less burn and hence the advantage of BP cannot be drawn more as compared to biodiesel blends. Hence the improvement is there but less at CR 14. The BP improves the indicated power at all CR and at the same time it decreases the friction power by reducing the pumping loss owing to improvement in specific power of the engine. The maximum percentage increases in specific power at CRs 16, 17.5, and 18 are 8.71%, 8.86%, and 17.71% respectively at 1.5 BP as indicated in Fig. 5.31.

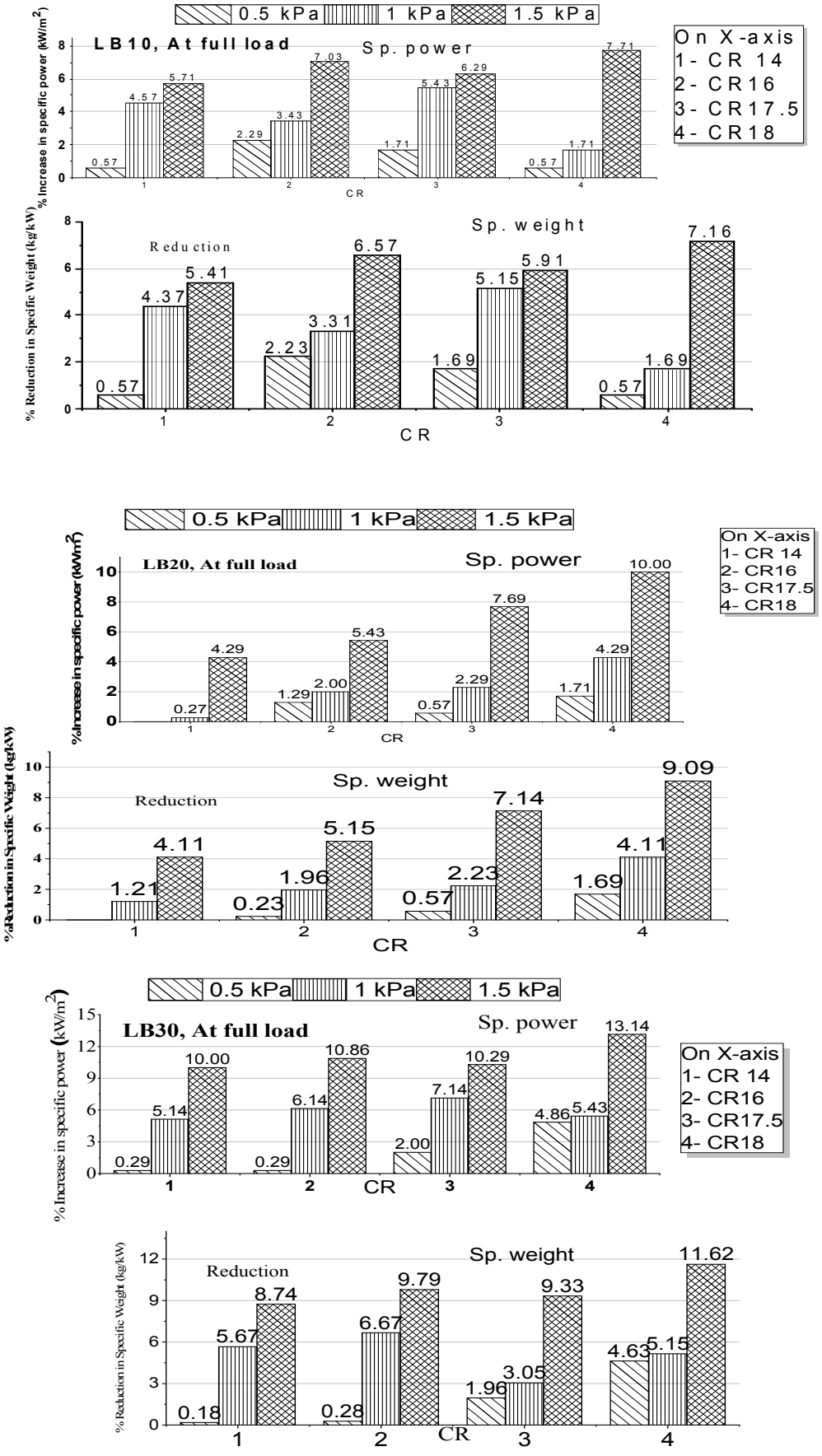

Fig. 5.32 Quantification parameters for LB10, LB20, and LB30 biodiesel blends

Similarly, the economy of engine materials are utilized due to the combined effect of BP and CR is demonstrated in the same figure. The increase in power in the same engine due to CR and boost pressure, hence the weight of engine per unit power has decreased. The maximum percentage decreases in specific weight at CRs 16, 17.5, and 18 are 8.02%, 8.14%, and 15.05% respectively at 1.5 BP.

In all tested biodiesel blends, the improvement in quantification parameters at CR14 improved a lot, as compared to baseline PD. The presence of oxygen molecules in the biodiesel blends compensates the combustion difficulties at low CR14. This improvement further increases with a fraction of biodiesel in the blends solely because of inbuilt oxygen content and cetane number of blends. However, this improvement is less than the improvement for PD because of the lower heating value of biodiesel blends. When comparing the improvements in biodiesel blends, in spite of decreasing the heating value of higher biodiesel content blends, an improvement in downsizing parameters is being increased due to the presence of comparatively more oxygen than the lower blends. The maximum improvements in the specific power of biodiesel blend LB10, LB20, and LB30 are 7.71%, 10%, and 13.14% respectively at CR 18 and 1.5 kPa (g) boost pressure as demonstrated in Fig. 5.32.

5.4 Conclusions

The exhaustive experimental study performed for investigating the combined influence of supercharging and CR on performance, emission, and downsizing characteristics of DICI engine. Obtained results are compared with the standard operating condition at natural aspiration of the engine, and following concluding, comments are made.

- Supercharger consumes 6 - 9.7% of power of the engine and helps to improve the downsizing parameters by 3-18%, 1-8%, 1-10%, and 1-13% for PD, LB10, LB20, and LB30 respectively.
- Boosting improves combustion in both phases, i.e., premixed as well as diffusion phase.
- Maximum BSFC improvement observed at 1.5 BP viz. for LB10 is 22% at CR16, LB20 19.2% at CR17.5, and LB30 is 15.36% at CR16, 17.5.

- All the tested biodiesel blends show the improvement in the range of 30-32% at CR 16 and 17.5 for the boost pressure of 1.5 kPa (g).
- Exhaust gas temperature decreases within boosting pressures and CRs for all tested fuels.
- Better improvement is at higher load in emissions of HC, CO and some penalty for NOx emission.
- On the whole, the engine has been downsized as shown for different tested fuels.
- On an average specific power was higher in the range of 3-17%, 1-8%, 1-10%, and 5-13% for PD, LB10, LB20, and LB30 respectively.
- The maximum improvements in the specific power of biodiesel blends PD, LB10, LB20, and LB30 are 17.71%, 7.71%, 10%, and 13.14% respectively at CR 18 and 1.5 kPa (g) boost pressure.

Chapter 6

The entire investigation has been divided into four parts; the first part describes the biodiesel production from crude linseed oil by two step transesterfication methods and its blends preparation with petro-diesel. The second part is about the comparison of performance of different linseed oil blends and diesel. Third part detailing the optimization techniques that have been carried out and their results are included. This obtained result enables minimum experimental work to draw the conclusion. In the final part, the performance tests were carried out for naturally aspirated and supercharged conditions and the improvement in performance along with expected engine downsizing parameters are discussed.

6.1 Overall conclusions

1. The biodiesel blends LB1 0, LB20, and LB30 shows the more or less similar performance as compared to PD in VCR engine.
2. Using the supercharger with a variable compression ratio in DICI engine is beneficial due to the chemical advantage (improvement in combustion efficiency).
3. The advantage of supercharger boost pressure is higher at lower CR and higher blends of biodiesel.
4. The engine is downsized for tested fuels, and its downsizing parameter further reduces with a fraction of biodiesel in the blends.
5. Lower grade of fuel can be used in VCR supercharged DICI engine.
6. Due to supercharging, satisfactory blends performance shifted from LB10 to LB30.
7. In conventional engine for supercharging, the oil blowing problem needs to be adequately addressed.
8. From experimental findings, it can be recommended that CR16 also has excellent performance with boost pressures.

6.2 Limitations of the study

1. Higher blends of linseed biodiesel are not suitable for engine operation even with modification of engine.

2. In the modified engine supercharging limited up 1.5 kPa (g) due to oil blowing problem of the engine.

Future scope of work

This research work can further be extended by the introducing the few more parameters for overall performance improvement and downsizing of the engine.

- Effect of boost pressure and compression ratio can be researched for other available biodiesels.
- Experimental and simulation study of combined effect of CR, BP, and after cooling air temperature.
- Optimization of after cooling, CR, and BP as per the load requirement.

Publications:

Sr. No.	**Journals**
1.	Warkhade GS, Babu AV. Combustion and emission characteristics of an esterified linseed oil fuelled variable compression ratio diesel engine. World J Eng 2018;15. doi:https://doi.org/10.1108/WJE-04-2017-0083.
2.	Warkhade, G. S., & Babu, A. V. (2018). Impact of supercharging and compression ratio on performance characteristics in a single cylinder DICI engine. *International Journal of Heat and Technology*, *36*(3), 955–961.
3.	Warkhade, G. S., & Babu, A. V. (2018a). Experimental investigations on the feasibility of higher blends of biodiesel in variable compression ratio diesel engine. *International Jounal of Ambient Energy*, *0*(0), 1–14. https://doi.org/10.1080/14484846.2018.1525170.
4.	Warkhade, G. S., & Babu, A. V. (2018). Combustion characteristics of linseed (Linum usitatissimum) methyl ester fuelled biodiesel blends in variable compression ratio diesel engine. *Australian Journal of Mechanical Engineering*, *16*(3), 1–14. https://doi.org/10.1080/14484846.2018.1525170
5.	Ganesh S. Warkhade, A. Veeresh Babu, Katam Ganesh Babu , Optimization of multi-response biodiesel fuelled diesel engine parameters using Taguchi grey relational analysis (TGRA) and analytical hierarchy process (AHP). (**Under review** in *'International Journal of Ambient Energy'*)
6.	Ganesh S. Warkhade, A. Veeresh Babu, 'Optimization of biodiesel fueled variable compression ratio DICI engine parameters using Taguchi based grey relational analysis and TOPSIS'',(**Under review** in *'Australian Journal of Mechanical Engineering'*).
	International Conferences
1.	Ganesh S. Warkhade, A. Veeresh Babu, Katam Ganesh Babu, Gopi Gulivindala M. Vijay Kumar. Effect of compression ratio on combustion characteristics of an esterified linseed oil fuelled diesel engine. Proc. 1st Int. 18thISME Conf. ISME18, held during Feb. 23 – 25,2017 at NIT Warangal, Conference Proceedings pp. 191
2.	Ganesh S. Warkhade, A. Veeresh Babu, Subhash C. Bose P., 'Effect of compression ratio on combustion, performance and emission characteristics of linseed biodiesel fueled compression ignition engine', **International conference** on Energy, Environment and Economics, held on 11-13 December 2017 at Heriot-Watt University, Edinburgh, UK.

References

Abedin, M. J. *et al.* 2016, ‘‘Production of biodiesel from a non-edible source and study of its combustion , and emission characteristics : A comparative study with B5’’, *Renewable Energy*, . Elsevier Ltd. Vol. 88, pp. 20–29.

Agapova, M. *et al.* 2017, ‘‘Using the analytic hierarchy process for prioritizing imaging tests in diagnosis of suspected appendicitis’’, *Academic Radiology*, . ElsevierVol. 24, No.5, , pp. 530–537.

Agarwal, A. K. and Dhar, A. 2013, ‘‘Experimental investigations of performance, emission and combustion characteristics of Karanja oil blends fuelled DICI engine’’, *Renewable Energy*, . Elsevier Ltd. Vol. 52, pp. 283–291.

Alam, M.Song, J.Acharya, R.Boehman, A.and Miller, K. 2004, ‘‘Combustion and Emissions Performance of Low Sulfur, Ultra Low Sulfur and Biodiesel Blends in a DI Diesel Engine’’Vol. , No.724, .

Alam, M.Song, J.Zello, V.and Boehman, A. 2006, ‘‘Spray and combustion visualization of a direct-injection diesel engine operated with oxygenated fuel blends’’, *International Journal of Engine Research*, . SAGE Publications Sage UK: London, England Vol. 7, No.6, , pp. 503–521.

Alonso, J. M. *et al.* 2007, ‘‘Combining Neural Networks and Genetic Algorithms to Predict and Reduce Diesel Engine Emissions’’, *IEEE Transactions on Evolutionary Computation*, Vol. 11, No.1, , pp. 46–55.

Amarnath, H. K. and Prabhakaran, P. 2012, ‘‘A study on the thermal performance and emissions of a variable compression ratio diesel engine fuelled with karanja biodiesel and the optimization of parameters based on experimental data’’, *International Journal of Green Energy*, Vol. 9, No.8, , pp. 841–863.

Amarnath, H. K.Prabhakaran, P.Bhat, S. a.and Paatil, R. 2014, ‘‘A Comparative Analysis of Thermal Performance And Emission Characteristics of Methyl Esters of Karanja And Jatropha Oils Based on A Variable Compression Ratio Diesel Engine’’, *International Journal of Green Energy*, Vol. 11, No.7, , pp. 675–694.

Amba Prasad Rao, G. and Mohan, P. R. 2003, ‘‘Effect of supercharging on the performance of a DI Diesel engine with cotton seed oil’’, *Energy Conversion and Management*, Vol. 44, No.6, , pp. 937–944.

An, H. *et al.* 2013, ‘‘Performance, combustion and emission characteristics of biodiesel derived from waste cooking oils’’, *Applied Energy*, Vol. 112, pp. 493–499.

Anand, K.Sharma, R. P.and Mehta, P. S. 2008, ‘‘Experimental investigations on combustion of jatropha methyl ester in a turbocharged direct-injection diesel engine’’, *Proceedings of the Institution of Mechanical Engineers Part D-Journal of Automobile Engineering*, Vol. 222, No.D10, , pp. 1865–1877.

Ananthakumar, S.Jayabal, S.and Thirumal, P. 2017, ‘‘Investigation on performance, emission and combustion characteristics of variable compression engine fuelled with diesel, waste plastics oil blends’’, *Journal of the Brazilian Society of Mechanical Sciences and Engineering*, . Springer Berlin Heidelberg Vol. 39, No.1, , pp. 19–28.

Aoyagi, Y. *et al.* 2004, ‘‘Diesel Combustion and Emission Study by Using of High Boost and High Injection Pressure in Single Cylinder Engine: The effects of boost pressure and timing retardation on thermal efficiency and exhaust emissions (Diesel Engines, Performance and Emissions’,’ in *The Proceedings of the International symposium on diagnostics and modeling of combustion in internal combustion engines 2004.6*, . The Japan Society of Mechanical Engineers Vol. pp. 119–126.

Aoyagi, Y.Osada, H.Misawa, M.Goto, Y.and Ishii, H. 2006, ‘*Advanced diesel combustion using of wide range, high boosted and cooled EGR system by single cylinder engine*’. SAE Technical Paper.

Aranda, D. A. G.Santos, R. T. P.Tapanes, N. C. O.Ramos, A. L. D.and Antunes, O. A. C. 2008, ‘‘Acid-catalyzed homogeneous esterification reaction for biodiesel production from palm fatty acids’’, *Catalysis letters*, . SpringerVol. 122, No.1–2, , pp. 20–25.

Asif, M. and Muneer, T. 2007, ‘‘Energy supply, its demand and security issues for developed and emerging economies’’, *Renewable and Sustainable Energy Reviews*, . Elsevier Vol. 11, No.7, , pp. 1388–1413.

Babu, A. R.Amba Prasad Rao, G.and Hari Prasad, T. 2016, ‘‘Experimental investigations on a variable compression ratio (VCR) CIDI engine with a blend of methyl esters palm stearin-diesel for performance and emissions’’, *International Journal of Ambient Energy*, Vol. 0750, No.July 2016, , pp. 1–8.

Balakrishnan, N.Mayilsamy, K.and Nedunchezhian, N. 2013, ‘‘Effects of Compression Ratio on Performance and Emission of Internal Combustion Engine with Used Vegetable Oil Methyl Easter’’, *Energy Efficient Technologies for Sustainability*, Vol. 768, pp. 250–254.

Banapurmath, N. R.Tewari, P. G.and Hosmath, R. S. 2008, ‘‘Performance and emission characteristics of a DI compression ignition engine operated on Honge, Jatropha and sesame oil methyl esters’’, *Renewable Energy*, Vol. 33, No.9, , pp. 1982–1988.

Bauer, H. 2004, ‘*Diesel-engine management*’. John Wiley & Sons.

Bazari, Z. and French, B. A. 1993, ‘*Performance and Emissions Trade-Offs for a HSDI Diesel Engine-An Optimization Study*’. SAE Technical Paper.

Benajes, J.Molina, S.García, J. M.and Novella, R. 2004, ‘Influence of boost pressure and injection pressure on combustion process and exhaust emissions in a HD diesel engine’. *SAE Technical Paper*.

Benjumea, P. and Agudelo, J. R. 2010, ‘‘Effect of the Degree of Unsaturation of Biodiesel Fuels on Engine Performance , Combustion Characteristics , and Emissions’’, *Energy & Fuels*, Vol. 25, No.1, , pp. 77–85.

Bentley, R. W. 2002, ‘‘Global oil & gas depletion: an overview’’, *Energy policy*, . ElsevierVol. 30, No.3, , pp. 189–205.

Briggs, I.Mccullough, G.Spence, S. W. T.Mccullough, G.and Seaman, R. 2013, ‘‘A parametric Study of an Exhaust Recovery Turbogenerator on a Diesel-Electric Hybrid Bus’’Vol. , No.JUNE, .

Can, Ö. 2014, ‘‘Combustion characteristics, performance and exhaust emissions of a diesel engine fueled with a waste cooking oil biodiesel mixture’’, *Energy Conversion and Management*, Vol. 87, pp. 676–686.

Canakci, M. 2007, ‘‘Combustion characteristics of a turbocharged DI compression ignition engine fueled with petroleum diesel fuels and biodiesel’’Vol. 98, No.2, , pp. 1167–1175.

Carsguide, 2018, ‘Reviews,news and advice’. Available at: https://www.carsguide-.com.au/oversteer/tech-through-time-supercharging-58592# (Accessed: 13 April 2018).

Chang, D. Y. Z.Gerl, I. H. VanJohnson, L. aHammond, E. G.and Marley, S. J. 1996, ‘‘Fuel Properties and Emissions of Soybean Oil Esters as Diesel Fuel’’, *Journal of the American Oil Chemists' Society*, Vol. 73, No.2, , pp. 1549–1555.

Channapattana, S. VKantharaj, C.Shinde, V. S.Pawar, A. A.and Kamble, P. G. 2015, ‘‘Emissions and Performance Evaluation of DI CI - VCR Engine Fuelled with Honne oil Methyl Ester / Diesel Blends’’, *Energy Procedia*, . Elsevier B.V. Vol. 74, pp. 281–288.

Chen, M.-F. and Tzeng, G.-H. 2004, ‘‘Combining grey relation and TOPSIS concepts for selecting an expatriate host country’’, *Mathematical and Computer Modelling*, . ElsevierVol. 40, No.13, , pp. 1473–1490.

Colban, W. F.Miles, P. C.and Oh, S. 2007, ‘‘Effect of Intake Pressure on Performance and Emissions in an Automotive Diesel Engine Operating in Low Temperature Combustion Regimes’’.

Datta, A. and Mandal, B. K. 2017, ‘‘An experimental investigation on the performance, combustion and emission characteristics of a variable compression ratio diesel engine using diesel and palm stearin methyl ester’’, *Clean Technologies and Environmental Policy*, . Springer Berlin Heidelberg Vol. 19, No.5, , pp. 1297–1312.

Datta Bharadwaz, Y.Govinda Rao, B.Dharma Rao, V.and Anusha, C. 2016, ‘‘Improvement of biodiesel methanol blends performance in a variable compression ratio engine using response surface methodology’’, *Alexandria Engineering Journal*, . Faculty of Engineering, Alexandria UniversityVol. 55, No.2, , pp. 1201–1209.

Debnath, B. K.Saha, U. K.and Sahoo, N. 2011, ‘‘Effect of Compression Ratio on the Performance Characteristics of a Palm Oil Methyl Ester Run Diesel Engine’’, in

Proceedings of the ASME 2011 International Mechanical Engineering Congress & Exposition IMECE2011 November 11-17, 2011, Denver, Colorado, USA, Vol. pp. 1–8.

Debnath, B. K.Saha, U. K.Sahoo, N.and Asme 2012, ‘‘Effect of compression ratio on the performance characteristics of a palm oil methyl ester run diesel engine’’, *Proceedings of the Asme International Mechanical Engineering Congress and Exposition, 2011, Vol 4, Pts a and B*, Vol. pp. 1315–1322.

Debnath, B. K.Sahoo, N.and Saha, U. K. 2013, ‘‘Thermodynamic analysis of a variable compression ratio diesel engine running with palm oil methyl ester’’, *Energy Conversion and Management*, . Elsevier Ltd. Vol. 65, No.1, , pp. 147–154.

Deng, J. L. 1989, ‘‘Introduction to Grey system theory’’, *The Journal of Grey System*, Vol. 1, No.1, , pp. 1–24.

Devan, P. K. and Mahalakshmi, N. V. 2009, ‘‘A study of the performance, emission and combustion characteristics of a compression ignition engine using methyl ester of paradise oil-eucalyptus oil blends’’, *Applied Energy*, . Elsevier Ltd. Vol. 86, No.5, , pp. 675–680.

Dhar, A.Kevin, R.and Kumar, A. 2012, ‘‘Production of biodiesel from high-FFA neem oil and its performance , emission and combustion characterization in a single cylinder DICI engine’’, *Fuel Processing Technology*, . Elsevier B.V.Vol. 97, pp. 118–129.

Dlugogorski, B. Z.Kennedy, E. M.and Mackie, J. C. 2012, ‘‘Low temperature oxidation of linseed oil: a review’’, *Fire science reviews*, . SpringerVol. 1, No.1, , p. 3.

Dorian, J. P.Franssen, H. T.and Simbeck, D. R. 2006, ‘‘Global challenges in energy’’, *Energy Policy*, . Elsevier Vol. 34, No.15, , pp. 1984–1991.

El-Kassaby, M. and Nemit-Allah, M. A. 2013, ‘‘Studying the effect of compression ratio on an engine fueled with waste oil produced biodiesel/diesel fuel’’, *Alexandria Engineering Journal*, Vol. 52, No.1, , pp. 1–11.

Energy, M. of N. & R. 2017, ‘*National Policy on Biofuels*’. Available at:

http://mnre.gov.in/file-manager/UserFiles/biofuel_policy.pdf (Accessed: 25 April 2017).

European Commision 2010, '*Standards - Air Quality - Environment - European Commission*'. Available at: http://ec.europa.eu/environment/air/quality/standards.htm (Accessed: 13 April 2018).

Fisher, R. A. 1937, '*The design of experiments*'. Oliver And Boyd; Edinburgh; London.

Fu, J. *et al.* 2014, ''A comparative study on various turbocharging approaches based on IC engine exhaust gas energy recovery'', *Applied Energy*, . Elsevier Ltd. Vol. 113, pp. 248–257.

Fung, C. P. 2003, ''Manufacturing process optimization for wear property of fiber-reinforced polybutylene terephthalate composites with grey relational analysis'', *Wear*, . Elsevier Vol. 254, No.3, , pp. 298–306.

Gamst, G.Meyers, L. S.and Guarino, A. J. 2008, '*Analysis of variance designs: A conceptual and computational approach with SPSS and SAS*'. Cambridge University Press.

Ganapathy, T.Murugesan, K.and Gakkhar, R. P. 2009, ''Performance optimization of Jatropha biodiesel engine model using Taguchi approach'', *Applied Energy*, . Elsevier Ltd. Vol. 86, No.11, , pp. 2476–2486.

Gandure, J. and Ketlogetswe, C. 2011, ''Marula oil and petrodiesel: a comparative performance analysis on a variable compression ignition engine''. Scientific Research Publishing, http://www. scirp. org/.

Gharehghani, A.Mirsalim, M.and Hosseini, R. 2017, ''Effects of waste fish oil biodiesel on diesel engine combustion characteristics and emission'', *Renewable Energy*, . Elsevier Ltd. Vol. 101, pp. 930–936.

Giacomini, C.Longo, G.Padoano, E.and Zornada, M. 2017, ''An AHP-based method to assess the introduction of electric cars in a public administration'', in *Environment and Electrical Engineering and 2017 IEEE Industrial and Commercial Power*

Systems Europe (EEEIC/I&CPS Europe), 2017 IEEE International Conference on, . IEEEVol. pp. 1–6.

Gisela Montero, 2011, " Biodiesel- Quality, Emissions and By-Products", Rijeka, Croatia : In Tech Europe.

Gonca, G. *et al.* 2015, ‘‘Application of the Miller cycle and turbo charging into a diesel engine to improve performance and decrease NO emissions’’, *Energy*, Vol. 93, No.February, , pp. 795–800.

Gul, M.Shah, A. N.Jamal, Y.and Masood, I. 2016, ‘‘Multi-variable optimization of diesel engine fuelled with biodiesel using grey-Taguchi method’’, *Journal of the Brazilian Society of Mechanical Sciences and Engineering*, Vol. pp. 621–632.

Gumus, M. 2010, ‘‘A comprehensive experimental investigation of combustion and heat release characteristics of a biodiesel (hazelnut kernel oil methyl ester) fueled direct injection compression ignition engine’’, *Fuel*, . Elsevier Ltd. Vol. 89, No.10, , pp. 2802–2814.

Hariram, V. and Vagesh Shangar, R. 2015, ‘‘Influence of compression ratio on combustion and performance characteristics of direct injection compression ignition engine’’, *Alexandria Engineering Journal*, . Faculty of Engineering, Alexandria University Vol. 54, No.4, , pp. 807–814.

Heywood, J. B. 1988, ‘*INTERNAL COMBUSTION ENGINE FUNDAMENTALS*’. New York: Mcgraw-hill New York.

Hirkude, J. and Padalkar, A. S. 2014, ‘‘Experimental investigation of the effect of compression ratio on performance and emissions of CI engine operated with waste fried oil methyl ester blend’’, *Fuel Processing Technology*, . Elsevier B.V.Vol. 128, pp. 367–375.

Holman, J.B. 1988, ' Experimental Techniques for Engineers', New York: Mcgraw-hill New York.

Huang, Z. H. *et al.* 2004, ‘‘Combustion characteristics and heat release analysis of a compression ignition engine operating on a diesel/methanol blend’’, *Proceedings of*

the institution of mechanical engineers, part D: Journal of Automobile Engineering, . Sage Publications Sage UK: London, EnglandVol. 218, No.9, , pp. 1011–1024.

Hugh Maclnnes 1976, '*Turbochargers*'. Tuscon, AZ 85703: H.P.Book, P.O. Box 5367.

Ishikawa, N. 2012, ''A study on emissions improvement of a diesel engine equipped with a mechanical supercharger'', *International Journal of Engine Research*, Vol. 13, No.2, , pp. 99–107.

Jadhav, S. D. and Tandale, M. S. 2016, ''Part load and full load multi-objective performance optimization of a single-cylinder diesel engine operating on Mangifera indica biodiesel as biofuel''. Taylor & Francis Vol. 7269, No.November, .

Jagadish, D.Ravi Kumar, P.and Murthy, K. M. 2011, ''The effect of supercharging on performance and emission characteristics of compresion ignition engine with diesel-ethanol-ester blends'', *Thermal Science*, Vol. 15, No.4, , pp. 1165–1174.

Jaichandar, S.Senthil Kumar, P.and Annamalai, K. 2012, ''Combined effect of injection timing and combustion chamber geometry on the performance of a biodiesel fueled diesel engine'', *Energy*, . Elsevier Ltd. Vol. 47, No.1, , pp. 388–394.

Jayashankara, B. and Ganesan, V. 2010, ''Effect of fuel injection timing and intake pressure on the performance of a di diesel engine - A parametric study using CFD'', *Energy Conversion and Management*, . Elsevier Ltd. Vol. 51, No.10, , pp. 1835–1848.

Jindal, S. 2011, ''Experimental investigation of the effect of compression ratio and injection pressure in a direct injection diesel engine running on Karanj methyl ester'', *International Journal of Sustainable Energy*, Vol. 30, No.5, , pp. 442–448.

Jindal, S.Nandwana, B. P.Rathore, N. S.and Vashistha, V. 2010, ''Experimental investigation of the effect of compression ratio and injection pressure in a direct injection diesel engine running on Jatropha methyl ester'', *Applied Thermal Engineering*, . Elsevier Ltd. Vol. 30, No.5, , pp. 442–448.

Jindal, S. and Salvi, B. L. 2012, ''Sustainability aspects and optimization of linseed biodiesel blends for compression ignition engine'', *Journal of Renewable and Sustainable Energy*, Vol. 043111, No.4, , pp. 1–10.

Joshi, D.Viswanath, P. Vand Sandeep, B. 2014, ‘‘The Effects of Supercharging on the Performance of C . I Engine Using Blends of Pre-Heated Cotton Seed Oil and Diesel as Alternate Fuel’’, in *Advance Research and Innovations in Mechanical, Material Science, Industrial Engineering and Management - ICARMMIEM-2014*, Vol. pp. 110–113.

Karabektas, M. 2009, ‘‘The effects of turbocharger on the performance and exhaust emissions of a diesel engine fuelled with biodiesel’’, *Renewable Energy*, . Elsevier Ltd. Vol. 34, No.4, , pp. 989–993.

Katam, G.B. et al.," Review on Algae for Biodiesel fuel production, its Characteristics comparison with other and their Impact on Performance, combustion and emissions of Diesel engine", *World Journal of Engineering,Emrald. Vol. 14, No. 2, pp. 127-138.*

Kegl, T. 2012, ‘‘Transformation of Heat Energy inot Mechanical Work at Low Environmental Pollution’’, *Journal of Young Investigators*, Vol. 24, No.6, .

Kjärstad, J. and Johnsson, F. 2009, ‘‘Resources and future supply of oil’’, *Energy Policy*, . Elsevier Vol. 37, No.2, , pp. 441–464.

Kolakoti, A. and Rao, B. V. A. 2017, ‘‘Effect of fatty acid composition on the performance and emission characteristics of an IDI supercharged engine using neat palm biodiesel and coconut biodiesel as an additive’’, *Biofuels*, Vol. 7269, No.June, , pp. 1–15.

Kommana, S.Banoth, B. N.and Kadavakollu, K. R. 2016, ‘‘Performance and Emission of VCR-CI Engine with palm kernel and eucalyptus blends’’, *Perspectives in Science*, . Elsevier GmbH Vol. pp. 4–6.

Krishnan, P. N. and Vasudevan, D. 2015, ‘‘Performance , Combustion and Emission Characteristics of Variable Compression Ratio Engine Fuelled with Biodiesel’’, *International Journal of ChemTech Research*, Vol. 7, No.01, , pp. 234–245.

Krishnan, S. R.Srinivasan, K. K.and Raihan, M. S. 2016, ‘‘The effect of injection parameters and boost pressure on diesel-propane dual fuel low temperature combustion in a single-cylinder research engine’’, *Fuel*, . Elsevier Ltd. Vol. 184, pp. 490–502.

Kruiswyk, R. W. 2008, ‘‘An engine system approach to exhaust waste heat recovery’’, in *Proceedings of DEER Conference,* . Dearborn, MI,USA Vol. p. Vol. 1316.

Kruiswyk, R. W. 2012, ‘‘The role of turbocompound in the era of emissions reduction’’, *10th International Conference on Turbochargers and Turbocharging*, Vol. m, pp. 269–280.

Kuo, Y.Yang, T.and Huang, G.-W. 2008, ‘‘The use of a grey-based Taguchi method for optimizing multi-response simulation problems’’, *Engineering Optimization*, Vol. 40, No.6, , pp. 517–528.

Laguitton, O.Crua, C.Cowell, T.Heikal, M. R.and Gold, M. R. 2007, ‘‘The effect of compression ratio on exhaust emissions from a PCCI diesel engine’’, *Energy Conversion and Management*, . Elsevier Vol. 48, No.11, , pp. 2918–2924.

Lee, S. and Reitz, R. D. 2007, ‘*Effects of engine operating parameters on near stoichiometric diesel combustion characteristics*’. SAE Technical Paper.

Leong, Y. T.Lee, J.-Y.Tan, R. R.Foo, J. J.and Chew, I. M. L. 2017, ‘‘Multi-objective optimization for resource network synthesis in eco-industrial parks using an integrated analytic hierarchy process’’, *Journal of Cleaner Production*, . Elsevier Vol. 143, pp. 1268–1283.

Lijiang W., Rupeng C. Hongjun, M. Peng, G. Yanjie Z., K. Y. 2018, "Combustion process and NOx emissions of a marine auxiliary diesel engine fuelled with waste cooking oil biodiesel blends", *Energy*, Vol.144, No. February, pp. 73–80.

Lujaji, F.Kristóf, L.Bereczky, A.and Mbarawa, M. 2011, ‘‘Experimental investigation of fuel properties, engine performance, combustion and emissions of blends containing croton oil, butanol, and diesel on a CI engine’’, *Fuel*, . Elsevier Ltd. Vol. 90, No.2, , pp. 505–510.

Ma, F. *et al.* 2015, ‘‘An Experimental Investigation on the Combustion and Heat Release Characteristics of an Opposed-Piston Folded-Cranktrain Diesel Engine’’, *Energies*, Vol. 8, No.7, , pp. 6365–6381.

Ma, Z.Zhang, C.Li, Y.and Song, J. 2012, ‘‘Performances and emissions of a DI supercharged diesel engine fuelled with soybean biodiesel and its blends’’, *Renewable and Sustainable Energy Ii, Pts 1-4*, Vol. 512–515, pp. 545–551.

MacMillan, D.La Rocca, A.Shayler, P. J.Murphy, M.and Pegg, I. G. 2009, ‘‘The effect of reducing compression ratio on the work output and heat release characteristics of a DI diesel under cold start conditions’’, *SAE International Journal of Engines*, . JSTOR Vol. 1, No.1, , pp. 794–803.

Mahanta, P.Mishra, S. C.and Kushwah, Y. S. 2006, ‘‘An experimental study of Pongamia pinnata L . oil as a diesel substitute’’Vol. 220, pp. 803–808.

Maheshwari, N.Balaji, C.and Ramesh, A. 2011, ‘‘A nonlinear regression based multi-objective optimization of parameters based on experimental data from an IC engine fueled with biodiesel blends’’, *Biomass and Bioenergy*, Vol. 35, No.5, , pp. 2171–2183.

Mahmood Mousavi, S.Abolfazli Esfahani, J.and Yazdi Mamaghani, M. 2013, ‘‘Alternative Equations to Compute the Network and the Thermal Efficiency of the Irreversible Diesel Cycle Using Genetic Algorithm’’, *American Journal of Mechanical Engineering*, Vol. 1, No.5, , pp. 119–125.

Maina, P. 2014, ‘‘Investigation of fuel properties and engine analysis of Jatropha biodiesel of Kenyan origin’’, *Journal of Energy in Southern Africa*, Vol. 25, No.2, , pp. 107–116.

Mendez, S. and Thirouard, B. 2009, ‘‘Using multiple injection strategies in diesel combustion: potential to improve emissions, noise and fuel economy trade-off in low CR engines’’, *SAE International Journal of Fuels and Lubricants*, . JSTOR Vol. 1, No.1, , pp. 662–674.

Merker, G. P.Schwarz, C.and Teichmann, R. 2011, ‘*Combustion engines development: mixture formation, combustion, emissions and simulation*’. Springer Science & Business Media.

Mohan, S. V. and Mouli, P. C. 2008, ‘‘Assessment of aerosol (PM 10) and trace elemental interactions by Taguchi experimental design approach’’, *Ecotoxicology and*

environmental safety, . Elsevier Vol. 69, No.3, , pp. 562–567.

Mohanraj, T. and Kumar, K. M. M. 2013, ‘‘Operating characteristics of a variable compression ratio engine using esterified tamanu oil’’, *International Journal of Green Energy*, Vol. 10, No.3, , pp. 285–301.

Noor, A. M. *et al.* 2016, ‘‘Exhaust Energy Recovery with Turbo Compounding in a Heavily Downsized Engine’’, *Applied Mechanics and Materials*, . Trans Tech Publications Ltd.Vol. 819, p. 432.

Mohite, S.Kumar, S.Maji, S.and Pal, A. 2016, ‘‘Iranica Journal of Energy & Environment Production of Biodiesel from a mixture of Karanja and Linseed oils : Optimization of process parameters’’Vol. 7, No.1, , pp. 12–17.

Montgomery, D. C. and Runger, G. C. 2010, ‘*Applied statistics and probability for engineers*’. John Wiley & Sons.

Moran, J.Granada, E.Míguez, J. L.and Porteiro, J. 2006, ‘‘Use of grey relational analysis to assess and optimize small biomass boilers’’, *Fuel Processing Technology*, . ElsevierVol. 87, No.2, , pp. 123–127.

Moscherosch, B. W.Polonowski, C. J.Miers, S. A.and Naber, J. D. 2010, ‘‘Combustion and emissions characterization of soy methyl ester biodiesel blends in an automotive turbocharged diesel engine’’, *Journal of Engineering for gas turbines and power*, . American Society of Mechanical Engineers Vol. 132, No.9, , p. 92806.

Mukhopadhyay, D.Sarkar, J. P.and Dutta, S. 2013, ‘‘Optimization of process factors for the efficient generation of biogas from raw vegetable wastes under the direct influence of plastic materials using Taguchi methodology’’, *Desalination and Water Treatment*, . Taylor & Francis Vol. 51, No.13–15, , pp. 2781–2790.

Muralidharan, K. and Vasudevan, D. 2011, ‘‘Performance, emission and combustion characteristics of a variable compression ratio engine using methyl esters of waste cooking oil and diesel blends’’, *Applied energy*, . Elsevier Vol. 88, No.11, , pp. 3959–3968.

Muralidharan, K. and Vasudevan, D. 2011, ‘‘Performance, emission and combustion

characteristics of a variable compression ratio engine using methyl esters of waste cooking oil and diesel blends'', *Applied Energy*, . Elsevier Ltd. Vol. 88, No.11, , pp. 3959–3968.

N. Logothetis, A. H. 1988, ''Characterizing and optimizing multi-response processes by the taguchi method'', *QUALITY AND RELIABILITY ENGINEERING INTERNATIONAL*, Vol. 4, No.October 1987, , pp. 159–169.

Nagai, T. and Kawakami, M. 1989, ''Reduction of NOx emission in medium-speed diesel engines'', *SAE*, . SAE Technical Paper.

Nagaraja, S.Sakthivel, M.and Sudhakaran, R. 2012, ''Comparative study of the combustion, performance, and emission characteristics of a variable compression ratio engine fuelled with diesel, corn oil methyl ester, and palm oil methyl ester'', *Journal of Renewable and Sustainable Energy*, Vol. 4, No.6, .

Nagaraja, S.Sakthivel, M.and Sudhakaran, R. 2013, ''Combustion and performance analysis of variable compression ratio engine fueled with preheated palm oil-diesel blends''. NISCAIR-CSIR, India.

Nayak, S. K. and Mishra, P. C. 2016, ''Emission characteristics of diesel fuel composed of linseed oil (Linum Usitatissium) blends utilizing rice husk producer gas'', *Energy Sources, Part A: Recovery, Utilization, and Environmental Effects*, Vol. 38, No.14, , pp. 2001–2008.

Opricovic, S. and Tzeng, G. H. 2004, ''Compromise solution by MCDM methods: A comparative analysis of VIKOR and TOPSIS'', *European Journal of Operational Research*, Vol. 156, No.2, , pp. 445–455.

Ozsezen, A. N.Canakci, M.Turkcan, A.and Sayin, C. 2009, ''Performance and combustion characteristics of a DI diesel engine fueled with waste palm oil and canola oil methyl esters'', *Fuel*, . Elsevier Ltd. Vol. 88, No.4, , pp. 629–636.

Pali, H. S. and Kumar, N. 2017, ''Combustion , performance and emissions of Shorea robusta methyl ester blends in a diesel engine'', *Biofuels*, . Taylor & Francis Vol. 7, No.5, , pp. 447–456.

Pakaj, D., R. G. 2018,"Influences of dual bio-fuel (Jatropha biodiesel and turpentine oil) on single cylinder variable compression ratio diesel engine", *Renewable Energy*, Vol. 115, No. January, pp. 1294–1302.

Parida, M. K. and Rout, A. K. 2017, ‘‘Environmental Effects Combustion analysis of Argemone mexicana biodiesel blends’’, *Energy Sources, Part A: Recovery, Utilization, and Environmental Effects*, . Taylor & Francis Vol. 39, No.7, , pp. 698–705.

Pehan, B. K. • M. K. • S. 2013, ‘*Green Diesel Engines*’. New York: Springer London Heidelberg New York Dordrecht.

Pervez, H.Mozumder, M. S.and Mourad, A. H. I. 2016, ‘‘Optimization of injection molding parameters for HDPE/TiO2 nanocomposites fabrication with multiple performance characteristics using the Taguchi method and grey relational analysis’’, *Materials*, Vol. 9, No.8, .

Pešić, Radivoje, Davinić, Aleksandar, Veinović, S. 2005, ‘‘One engine for all fuels-one fuel for all engines’’, in *10th EAEC European Automotive Congress, Belgrade*, Vol. pp. 1–10.

Peterson, C. L. *et al.* 1996, ‘‘Ethyl ester of rapeseed used as a biodiesel fuel—a case study’’, *Biomass and Bioenergy*, . Elsevier Vol. 10, No.5–6, , pp. 331–336.

Peterson, C. L.Reece, D. L.Hammond, B.Thompson, J. C.and Beck, S. 1995, ‘‘Commercialization of Idaho biodiesel (HySEE) from ethanol and waste vegetable oil’’, in *Annual ASAE Meeting. Paper*, Vol. pp. 49085–49659.

Podevin, P.Descombes, G.and Charpentier, C. 1999, ‘‘Effect of supercharging pressure on internal combustion engine performances and pollutants emissions’’, *From Thermo-eEonomics to Sustainability (GG Hirs editor), Part*, Vol. 2, pp. 703–713.

Puhan, S.Jegan, R.Balasubbramanian, K.and Nagarajan, G. 2009a, ‘‘Effect of injection pressure on performance, emission and combustion characteristics of high linolenic linseed oil methyl ester in a DI diesel engine’’, *Renewable Energy*, . Elsevier Ltd. Vol. 34, No.5, , pp. 1227–1233.

2009b, ‘‘Effect of injection pressure on performance, emission and combustion characteristics of high linolenic linseed oil methyl ester in a DI diesel engine’’, *Renewable Energy*, . Elsevier Ltd. Vol. 34, No.5, , pp. 1227–1233.

Pundir, B. P. 2010, ‘*IC engines: combustion and emissions*’. Alpha Science International.

Qi, D. H. *et al.* 2009, ‘‘Combustion and performance evaluation of a diesel engine fueled with biodiesel produced from soybean crude oil’’, *Renewable Energy*, . Elsevier Ltd. Vol. 34, No.12, , pp. 2706–2713.

Raheman, H. and Ghadge, S. V. 2008, ‘‘Performance of diesel engine with biodiesel at varying compression ratio and ignition timing’’, *Fuel*, Vol. 87, No.12, , pp. 2659–2666.

Raheman, H. and Ghadge, S. V 2008, ‘‘Performance of diesel engine with biodiesel at varying compression ratio and ignition timing’’, *Fuel*, . Elsevier Vol. 87, No.12, , pp. 2659–2666.

Raj, M. T. and Kandasamy, M. K. K. 2012, ‘‘Tamanu oil - an alternative fuel for variable compression ratio engine’’, *International Journal of Energy and Environmental Engineering*, Vol. 3, No.1, , p. 18.

Raj, S. O. N. and Prabhu, S. 2017, ‘‘Analysis of multi objective optimisation using TOPSIS method in EDM process with CNT infused copper electrode’’, *International Journal of Machining and Machinability of Materials*, . Inderscience Publishers (IEL) Vol. 19, No.1, , pp. 76–94.

Rajasekar, E. and Selvi, S. 2014, ‘‘Review of combustion characteristics of CI engines fueled with biodiesel’’, *Renewable and Sustainable Energy Reviews*, . Elsevier Vol. 35, No.x, , pp. 390–399.

Raju, A. V. S. 2016, ‘‘Optimization of Diesel Engine Parameters for Performance, Combustion and Emission Parameters using Taguchi and Grey Relational Analysis’’, *Global Journal of Researches in Engineering: A Mechanical and Mechanics Engineering*, Vol. 16, No.3, .

Rakopoulos, C. D.Dimaratos, A. M.Giakoumis, E. G.and Rakopoulos, D. C. 2010,

‘‘Investigating the emissions during acceleration of a turbocharged diesel engine operating with bio-diesel or n-butanol diesel fuel blends’’, *Energy*, . Elsevier Ltd. Vol. 35, No.12, , pp. 5173–5184.

Rao, R. S.Kumar, C. G.Prakasham, R. S.and Hobbs, P. J. 2008, ‘‘The Taguchi methodology as a statistical tool for biotechnological applications: a critical appraisal’’, *Biotechnology journal*, . Wiley Online Library Vol. 3, No.4, , pp. 510–523.

Rao, R. V. 2007, ‘*Decision Making in the Manufacturing Environment*’. Londan: Springer.

Ravikumar, K. S. P. 2013, ‘‘Optimization of operational parameters on performance and emissions of a diesel engine using biodiesel’’, *International Journal of environmental science and technology*, Vol. 11, No.4, , pp. 949–958.

Roberts, M. 2002, ‘‘Benefits and challenges of variable compression ratio (VCR)’’, *SAE Technical Paper*, Vol. 14, No.724, , p. 03P–227.

Ross, P. J. and Ross, P. J. 1988, ‘*Taguchi techniques for quality engineering: loss function, orthogonal experiments, parameter and tolerance design*’. McGraw-Hill New York.

Roy, S.Das, A. K.and Banerjee, R. 2014, ‘‘Application of Grey–Taguchi based multi-objective optimization strategy to calibrate the PM–NHC–BSFC trade-off characteristics of a CRDI assisted CNG dual-fuel engine’’, *Journal of Natural Gas Science and Engineering*, . Elsevier Vol. 21, pp. 524–531.

Ryan, T. W. and Shahed, S. M. 1994, ‘*Injection pressure and intake air density effects on ignition and combustion in a 4-valve diesel engine*’. SAE Technical Paper.

Rychter, T. J. *et al.* 1992, ‘‘A Theoretical Study of a Variable Compression Ratio Turbocharged Diesel Engine’’, *Proc. Inst. Mech. Eng. A: J. Power Energy*, Vol. 206, No.4, , pp. 227–238.

Saaty TL 2000, ‘*Fundamentals of decision making and priority theory with the AHP*’. Pittsburg: RWS Publications.

Sahoo, P. K. and Das, L. M. 2009, ‘‘Combustion analysis of Jatropha, Karanja and

Polanga based biodiesel as fuel in a diesel engine'', *Fuel*, . Elsevier Ltd. Vol. 88, No.6, , pp. 994–999.

Sahu, P. K. and Pal, S. 2015, ''Multi-response optimization of process parameters in friction stir welded AM20 magnesium alloy by Taguchi grey relational analysis'', *Journal of Magnesium and Alloys*, . Elsevier Ltd. Vol. 3, No.1, , pp. 36–46.

Saito, T. *et al.* 1984, '*Intercooling effects of methanol on turbocharged diesel engine performance and exhaust emissions*'. SAE Technical Paper.

Sakthivel, G. *et al.* 2014, ''Multi-criteria decision modelling approach for biodiesel blend selection based on GRA–TOPSIS analysis'', *International Journal of Ambient Energy*, . Taylor & Francis, Vol. 35, No.3, , pp. 139–154.

Sakthivel, G. and Ilangkumaran, M. 2017, ''Optimisation of compression ignition engine performance with fishoil biodiesel using Taguchi-Fuzzy approach'', *International Journal of Ambient Energy*, Vol. 38, No.2, , pp. 146–160.

Sakthivel, G.Nagarajan, G.Ilangkumaran, M.and Gaikwad, A. B. 2014, ''Comparative analysis of performance, emission and combustion parameters of diesel engine fuelled with ethyl ester of fish oil and its diesel blends'', *Fuel*, . Elsevier Ltd. Vol. 132, pp. 116–124.

Sakthivel, G.Nagarajan, G.Ilangkumaran, M.and Gaikwad, A. B. 2014, ''Comparative analysis of performance, emission and combustion parameters of diesel engine fuelled with ethyl ester of fish oil and its diesel blends'', *Fuel*, . Elsevier Ltd. Vol. 132, pp. 116–124.

Sanayei, A.Mousavi, S. F.and Yazdankhah, A. 2010, ''Group decision making process for supplier selection with VIKOR under fuzzy environment'', *Expert Systems with Applications*, . Elsevier Vol. 37, No.1, , pp. 24–30.

Schwitzer 1991, '*Introduction To Turbochargers*'. Indianapolis, Indiana.

Selvan, V. A. M.Anand, R. B.and Udayakumar, M. 2009, ''Combustion characteristics of diesohol using biodiesel as an additive in a direct injection compression ignition engine under various compression ratios'', *Energy and Fuels*, Vol. 23, No.11, , pp. 5413–5422.

Senthilkumar, N.Tamizharasan, T.and Anandakrishnan, V. 2014, ‘‘An hybrid Taguchi-grey relational technique and cuckoo search algorithm for multi-criteria optimization in hard turning of AISI D3 steel’’, *Journal of Advanced Engineering Research*, Vol. 1, No.1, , pp. 16–31.

Shahid, E. M. and Jamal, Y. 2011, ‘‘Production of biodiesel: A technical review’’, *Renewable and Sustainable Energy Reviews*, . Elsevier Ltd. Vol. 15, No.9, , pp. 4732–4745.

Shaik, A.Moorthi, N. S. V.and Rudramoorthy, R. 2007, ‘‘Variable compression ratio engine: A future power plant for automobiles - an overview’’, *Proceedings of the Institution of Mechanical Engineers, Part D: Journal of Automobile Engineering*, Vol. 221, pp. 1159–1168.

Sharma, A. and Murugan, S. 2015, ‘‘Potential for using a tyre pyrolysis oil-biodiesel blend in a diesel engine at different compression ratios’’, *Energy Conversion and Management*, . Elsevier LtdVol. 93, pp. 289–297.

Silitonga, A. S.Hassan, M. H.Ong, H. C.and Kusumo, F. 2017, ‘‘Analysis of the performance, emission and combustion characteristics of a turbocharged diesel engine fuelled with Jatropha curcas biodiesel-diesel blends using kernel-based extreme learning machine’’, *Environmental Science and Pollution Research*, . Environmental Science and Pollution Research Vol. 24, No.32, , pp. 25383–25405.

Singh, B. and Shukla, S. K. 2016, ‘‘Experimental analysis of combustion characteristics on a variable compression ratio engine fuelled with biodiesel (castor oil) and diesel blends’’, *Biofuels*, . Taylor & Francis, Vol. 7, No.5, , pp. 471–477.

Singh, B. and Shukla, S. K. 2016, ‘‘Experimental analysis of combustion characteristics on a variable compression ratio engine fuelled with biodiesel (castor oil) and diesel blends’’, *Biofuels*, . Taylor & Francis, Vol. 7, No.5, , pp. 471–477.

Sivaramakrishnan Kaliamoorthy, R. P. 2013, ‘‘Investigation on performance and emissions of a biodiesel engine through optimization techniques’’Vol. 17, No.1, , pp. 179–193.

Smith, A. 2008, ‘‘Stroke of genius for gasoline downsizing’’, *Ricardo Q Rev*, Vol. p.

Q3.

Solbrig, C. E. and Litzinger, T. A. 1990, '*The effect of intake charge temperature on combustion and emissions in an optically accessible DI diesel engine with and without swirl*'. SAE Technical Paper.

Stobart, R. and Weerasinghe, R. 2006, ''Heat Recovery and Bottoming Cycles for SI and CI Engines - A Perspective'', *SAE Technical Paper*, Vol. , No.Apr. 3.

Sutadian, A. D.Muttil, N.Yilmaz, A. G.and Perera, B. J. C. 2017, ''Using the Analytic Hierarchy Process to identify parameter weights for developing a water quality index'', *Ecological Indicators*, . Elsevier Vol. 75, pp. 220–233.

Taguchi, Genichi and Elsayed, Elsayed A and Hsiang, T. C. 1989, '*Quality engineering in production systems*. 173rd Edn'. New York: McGraw-Hill.

Talibi, M.Hellier, P.and Ladommatos, N. 2017, ''The effect of varying EGR and intake air boost on hydrogen-diesel co-combustion in CI engines'', *International Journal of Hydrogen Energy*, . Elsevier Ltd. Vol. 42, No.9, , pp. 6369–6383.

Tan, P.Hu, Z.Lou, D.and Li, Z. 2012, ''Exhaust emissions from a light-duty diesel engine with Jatropha biodiesel fuel'', *Energy*, . Elsevier LtdVol. 39, No.1, , pp. 356–362.

Tanin, K. V.Wickman, D. D.Montgomery, D. T.Das, S.and Reitz, R. D. 1999, ''The Influence of Boost Pressure on Emissions and Fuel Consumption of a Heavy-Duty Single-Cylinder D.I. Diesel Engine''Vol. , No.March.

Tarng, Y. S.Juang, S. C.and Chang, C. H. 2002, ''The use of grey-based Taguchi methods to determine submerged arc welding process parameters in hardfacing'', *Journal of Materials Processing Technology*, Vol. 128, No.1–3, , pp. 1–6.

Tesfa, B.Mishra, R.Zhang, C.Gu, F.and Ball, A. D. 2013, ''Combustion and performance characteristics of CI (compression ignition) engine running with biodiesel'', *Energy*, Vol. 51, pp. 101–115.

Thangaraja, J.Anand, K.and Mehta, P. S. 2012, ''Experimental investigations on combustion, performance and emission characteristics of neat jatropha biodiesel and

its methanol blend in a diesel engine'', in *Proceedings of the ASME*, . Vancouver, BC, Canada: 2012 Internal Combustion Engine Division Fall Technical Conference ICEF2012 September 23-26, 2012, Vancouver, BC, CanadaVol. pp. 7–8.

TL, S. 1980, '*The analytic hierarchy process*'. New York: McGraw Hill.

Tsao, C. C. 2009, ''Grey – Taguchi method to optimize the milling parameters of aluminum alloy''Vol. pp. 41–48.

Tzeng, G. H. and Tasur, S. H. 1994, ''The multiple criteria evaluation of grey relation model'', *The Journal of Grey System*, Vol. 6, No.2, , pp. 87–108.

United States Environmental Protection Agency 2016, '*EPA Emission Standards for Heavy-Duty Highway Engines and Vehicles*'. Available at: https://www.epa.gov/emission-standards-reference-guide/epa-emission-standards-heavy-duty-highway-engines-and-vehicles (Accessed: 13 April 2018).

Venkanna, B. K.Wadawadagi, S. B.and Reddy, C. V. 2009, ''Effect of Injection Pressure on Performance , Emission and Combustion Characteristics of Direct Injection Diesel Engine Running on Blends of Pongamia Pinnata Linn Oil (Honge oil) and Diesel Fuel'', *CIGR Ejournal*, Vol. XI, No.1316, , pp. 1–17.

Venkateswarlu, K.Kumar, K. V.Murthy, B. S. R.and Subbarao, V. V. 2012, ''Effect of exhaust gas recirculation and ethyl hexyl nitrate additive on biodiesel fuelled diesel engine for the reduction of NO x emissions'', *Frontiers in Energy*, Vol. 6, No.3, , pp. 304–310.

Verhelst, S.Maesschalck, P.Rombaut, N.and Sierens, R. 2009, ''Increasing the power output of hydrogen internal combustion engines by means of supercharging and exhaust gas recirculation'', *International Journal of Hydrogen Energy*, . Elsevier Vol. 34, No.10, , pp. 4406–4412.

Watson, N., J. M. S. 1982, '*Turbocharging the Internal Combustion Engine*'. London and Basingstoke: THE MACMILLAN PRESS LTD.

Wilson, V. H. 2012, ''Optimization of Diesel Engine Parameters Using Taguchi Method and Design of Evolution''Vol. XXXIV, No.4, , pp. 423–428.

Win, Z.Gakkhar, R. P.Jain, S. C.and Bhattacharya, M. 2005, ‘‘Parameter optimization of a diesel engine to reduce noise, fuel consumption, and exhaust emissions using response surface methodology’’, *Proceedings of the Institution of Mechanical Engineers, Part D: Journal of Automobile Engineering*, Vol. 219, No.10, , pp. 1181–1192.

Wind, Y. and Saaty, T. L. 1980, ‘‘Marketing applications of the analytic hierarchy process’’, *Management science*, . INFORMSVol. 26, No.7, , pp. 641–658.

Wu, D. and Gao, H. 2016, ‘‘An Adaptive Particle Swarm Optimization for Engine Parameter Optimization’’, *Proceedings of the National Academy of Sciences, India Section A: Physical Sciences*, . Springer India.

Wu, H. W. and Wu, Z. Y. 2012, ‘‘Combustion characteristics and optimal factors determination with Taguchi method for diesel engines port-injecting hydrogen’’, *Energy*, . Elsevier LtdVol. 47, No.1, , pp. 411–420.

Wu, H. W. and Wu, Z. Y. 2013, ‘‘Using Taguchi method on combustion performance of a diesel engine with diesel/biodiesel blend and port-inducting H2’’, *Applied Energy*, . Elsevier Ltd. Vol. 104, No.Apr. 1, , pp. 362–370.

Wu, J. *et al.* 2006, ‘‘Study of combustion and emission characteristics of a turbocharged diesel engine fuelled with dimethyl ether’’, *International Journal of Automotive Technology*, Vol. 7, No.6, , pp. 645–652.

Wu, Q.Sun, P.Mei, D.and Chen, Z. 2013, ‘‘Influence of Micro-emulsified Biodiesel on Combustion and Emission Characteristics of a Turbocharged Diesel Engine’’, *Progress in Renewable and Sustainable Energy, Pts 1 and 2*, Vol. 608–609, No.x, , pp. 269–274.

Wu, Z. Y.Wu, H. W.and Hung, C. H. 2014, ‘‘Applying Taguchi method to combustion characteristics and optimal factors determination in diesel/biodiesel engines with port-injecting LPG’’, *Fuel*, . Elsevier Ltd. Vol. 117, No.PART A, , pp. 8–14.

Yamin, J. A. A. and Dado, M. H. 2004, ‘‘Performance simulation of a four-stroke engine with variable stroke-length and compression ratio’’, *Applied Energy*, .

ElsevierVol. 77, No.4, , pp. 447–463.

Ye, P. 2010, ‘‘Investigation of the Impact of Engine Injection Strategy on the Biodiesel NOx Effect with a Common-Rail Turbocharged Direct Injection Diesel Engine’’Vol. 121, No.2009, , pp. 4215–4225.

Yoshimoto, Y. 2016, ‘‘Influence of Supercharging on Biodiesel Combustion in a Small Single Cylinder DI Diesel Engine’’, *SAE International*, .

Yusri, I. M. *et al.* 2017, ‘‘Application of response surface methodology in optimization of performance and exhaust emissions of secondary butyl alcohol-gasoline blends in SI engine’’, *Energy Conversion and Management*, . Elsevier Ltd. Vol. 133, pp. 178–195.

Zeyaeyan, S.Fattahi, E.Ranjbar, A.and Vazifedoust, M. 2017, ‘‘Classification of Rainfall Warnings Based on the TOPSIS Method’’, *Climate*, . Multidisciplinary Digital Publishing InstituteVol. 5, No.2, , p. 33.

Zhang, L.Takatsuki, T.and Yokota, K. 1994, ‘‘An Observation and Analysis of the Combustion Under Supercharging on a DI Diesel Engine’’Vol. , No.412, .

Zhen, D.Wang, T.Gu, F.Tesfa, B.and Ball, A. 2013, ‘‘Acoustic measurements for the combustion diagnosis of diesel engines fuelled with biodiesels’’, *Measurement Science and Technology*, Vol. 24, No.5, .

Zhu, Y.Stobart, R.and Deng, J. 2010, ‘‘Analysis of the Impact on Diesel Engine Fuel Economy and Emissions by Variable Compression Ratio Using GT-Power Simulation’’, *SAE*.

APPENDIX

ERROR / UNCERTAINTY ANALYSIS

Errors and uncertainties in the experiments can arise from instrument selection, condition, calibration, environment, observation, reading and test planning. Uncertainty analysis is needed to prove the accuracy of the experiments (Holman, J.B. 1988). The percentage uncertainties of various parameters like brake power and brake thermal efficiency were calculated using the percentage uncertainties of various instruments given in Table 1. An uncertainly analysis was performed using Eq. (1).

Table 1. Various used instruments and its range, accuracy and percentage uncertainties

S. N.	Instruments	Range	Accuracy	% uncertainties
1.	Smoke meter	BSU 0-10	± 0.1	± 0.1
2.	Speed measuring unit	0-5000 rpm	± 10 rpm	± 10
3.	Load indicator	0-50 kg	± 0.1 kg	±0.2
4.	Burette for fuel measurement		± 0.1 cc	± 1
5.	Digital stop watch		± 0.6 s	± 0.2
6.	Manometer		± 1 mm	± 1
7.	Pressure pickup	0-345 bar	± 0.1 kg	± 0.1
8.	Crank angle encoder		$\pm 1^0$	± 0.2
9.	Exhaust gas temperature ind.	$0\text{-}1200^0$ C	$\pm 1^0$ C	± 0.15
10.	Five Gas analyzer	CO, 0-15%	±0.001%	±0.06
		HC, 0-30000 ppm	± 1 ppm	± 0.2
		O_2, 0-25%	±0.01%	±0.01
		CO_2, 0-20%	±0.01%	±0.5
		NO, 0-5000 ppm	± 1 ppm	± 0.2

$$Percentage\_Error = \sqrt{X_1^2 + X_2^2} + ... \quad (1)$$

Percentage of uncertainty occurring in the experiments = square root of ((uncertainty of pressure transducer)^2 + (uncertainty of angle encoder)^2 + (uncertainty of NOx)^2 + (uncertainty of HC)^2 + (uncertainty of CO)^2 + (uncertainty of CO_2)^2 + (uncertainty OF O_2)^2 + (uncertainty of Smoke opacity)^2 + (uncertainty K-2 thermocouple)^2 + (uncertainty of stop watch)^2 + (uncertainty of manometer)^2 + (uncertainty of burette)^2)

% Error in experimental measurement =square root of ($(0.1)^2$ + $(0.2)^2$ + $(0.2)^2$ + $(0.2)^2$ + $(0.6)^2$ + $(0.5)^2$ + $(0.01)^2$ + $(0.01)^2$ + $(0.15)^2$ + $(0.2)^2$ + $(1)^2$ + $(1)^2$) = **1.674%**